CHARACTERISATION OF THE ROLE OF BIFOCAL AND ITS INTERACTING PARTNERS IN *DROSOPHILA* DEVELOPMENT

KAVITA BABU

A THESIS SUBMITTED FOR THE DEGREE OF DOCTOR OF PHILOSOPHY

INSTITUTE OF MOLECULAR AND CELL BIOLOGY

NATIONAL UNIVERSITY OF SINGAPORE

2004

ACKNOWLEDGEMENTS

This work was carried out in the Laboratories of Prof. William Chia, at the Institute of Molecular and Cell Biology, Singapore and the MRC Centre for Developmental Neurobiology at Kings College London, UK. I thank Bill for accepting me as his graduate student, being a brilliant supervisor and mentor and for giving me a lot of freedom to shape my projects. His insightful suggestions and critical comments have been invaluable in shaping this work and thesis to its present form.

I am extremely grateful to Dr. Sami Bahri for his help and guidance throughout this work. I also thank Dr. Yang Xiaohang for his help during my time at IMCB. This work would not have been possible without the collaborations I have had throughout the course of my PhD. I am grateful to Dr. Yu Cai for being a great collaborator and giving me the *homer* mutant line and the Anti-Homer antibody. I also thank Cai Yu for his assistance with the North-western analysis. My thanks also go to Drs. Nick Helps and Patricia Cohen for collaborating with me for the first part of my graduate work and for the reagents they gave me. I also thank Dr. Fengwei Yu for the Anti-Homer antibody and Dr. Richard Tuxworth for his help with image collections. Thanks go to Hing Fook Sion and Ong Chin Tong for their technical assistance. I thank Heinrich Horstmann and Ng Chee Peng for assistance with electron microscopy and Guo Ke for help with sectioning the fly brains.

I thank all the members of the Bill Chia Lab, Guy Tear Lab and Yang Xiaohang Lab. Thanks to Cathy, Cai Yu, Devi, Fengwei, Fitz, Greg, Marita, Martin, Mike Z, Murni, Paul, Priya, Rachna, Richard, Sami, Sergei, Xavier and Zalina for their help and suggestions on my work.

I am grateful to the members of my supervisory committee Drs. Ed Manser, Thomas Dick and Uttam Surana for their suggestions during the yearly committee meetings. I also thank Drs. Anne Ephrussi and Daniel St. Johnston for their comments and suggestions on my work.

Many thanks to a lot of other people, especially those at the Bloomington *Drosophila* centre and the many people from the fly community, who have generously given me reagents at various stages during this work. They are mentioned in the charts indicating sources of Antibodies or flies.

I am especially grateful to Rachna for being a great friend throughout the course of my PhD. Many thanks to a lot of my friends in and out of the labs for friendship and most importantly laughter. Lastly, I thank my family especially my parents and brother for all their encouragement and support.

TABLE OF CONTENTS

LIST OF FIGURES AND TABLES

FIGURES:

TABLES:

ABBREVIATIONS

aa	amino acid
Ab	Antibody
abl	*abelson tyrosine kinase*
Amp	Ampicillin
A/P	Anterior/Posterior
aPKC	atypical Protein Kinase C
APS	Ammonium Persulphate
ast	*asteroid*
ATP	Adenosine 5' Triphosphate
β-Gal	β-Galactosidase
baz	*bazooka*
bcd	*bicoid*
bif	*bifocal*
bp	basepairs
BSA	Bovine Serum Albumin
bw	*brown*
$CaCl_2$	Calcium Chloride
ca	*claret*
cAMP	cyclic Adenosine Monophosphate
capu	*cappuccino*
Cdc42	Cell division cycle 42
cDNA	complementary DNA
CD	Cytochalasin D
C. elegans	*Caenorhabditis elegans*
CIP	Calf Intestinal Phosphatase
cn	*cinnabar*
CNS	Central Nervous System
comm	*commissureless*
cp	*clipped*
CS	Canton-S (wild type fly strain)
C-terminal	Carboxy (COOH) terminal
cu	*curled*
cv-c	*crossveinless c*
Cy3	Cyanine 3 conjugated
Dac	Dachshund
DCC	Deleted in Colorectal Cancer
def	*deficiency*
Df	*Deficiency*
DEPC	Diethyl Pyrocarbonate
DIG	Digoxygenin
Dlar	Drosophila leukocyte antigen related like
DNA	Deoxyribonucleic acid
dNTP	deoxynucleotide triphosphate
D. melanogaster	*Drosophila melanogaster*

dmoe or *moe*	*Drosophila moesin*
dock	*dreadlocks*
DPTP	Drosophila Protein Tyrosine Phosphatase
DTT	1, 4-Dithio-DL-threitol
e	*ebony*
ECL	Enhanced Chemiluminescence
E. coli	*Escherichia coli*
EDTA	Ethylenediaminetetraacetic acid
EGTA	Ethylene glycol-bis(2-aminoethylether)-N,N,N',N'-tetraacetic acid
EGF	Epidermal Growth Factor
ena	*enabled*
Eph	Ephrin Receptors
ERM	Ezrin-Radixin-Moesin
eve	*even-skipped*
EVH	Ena/VASP Homology
F-actin	Filamentous actin
Fas II	Fasciclin II
FISH	Fluorescent *in situ* Hybridisation
FITC	Fluorescein isothiocyanate
FRT	FLP recombinase recombination target
g	Grams
G-actin	Globular actin
GTPase	Guanine 5'-Triphosphatase
GST	Glutathione-S-Transferase
HCl	Hydrochloric acid
HEPES	N-2-hydroxyethyl piperazine-N'-2-ethanesulphonic acid
hom	*homer*
H_2O	Water
hr	Hour
HRP	Horse Radish Peroxidase
hs	Heat shock
I-2PP1	Inhibitor-2 of PP1
IgG	Immunoglobulin
IP	Immunoprecipitation
in	*inturned*
IPTG	Isopropyl-β-thiogalactopyranoside
kb	Kilobase
KCl	Pottasium Chloride
khc	*kinesin heavy chain*
kni	*knirps*
kV	Kilovolts
L1	A Transmembrane Adhesion molecule
LacZ	Lactose converting reporter gene from *E. coli*
lar	*leukocyte antigen related like*
Lat A	Latrunculin A
LB	Luria Broth
LiCl	Lithium Chloride
LPC	Lamina Precursor Cell
M	Molar

mAb	monoclonal Antibody
Mef2	*Myocyte enhancing factor 2*
$MgCl_2$	Magnesium Chloride
µF	Microfarad
µg	Microgram
µl	Microlitre
µM	Micromolar
ml	Millilitre
mM	Millimolar
MOPS	4-Morpholinepropanesulphonic acid
mRNA	messenger RNA
mins	Minutes
mm	Millimetres
msec	milliseconds
msn	*misshapen*
MTOC	Microtubule Organising Centre
NaCl	Sodium Chloride
NB	Neuroblast
NCAM	Neural Cell Adhesion Molecule
Nck	Non-catalytic region of Tyrosine Kinase
NIPP1	Nuclear Inhibitor of PP1
nm	Nanometres
N-terminal	Amino (NH_2) terminal
OD	Optical Density
ORF	Open Reading Frame
Orb	Oo18 RNA-binding protein
Osk	Oskar
pak	*p-21 activated kinase*
Par	Partitioning defective
Pax6	*Paxillin 6*
pBS	plasmid BlueScript
PBS	Phosphate Buffered Saline
PCR	Polymerase Chain Reaction
PDZ domain	PSD-95, Dlg and ZO-1/2 domain
PFF	Paraformadehyde fixative
PFS	Paraformadehyde solution
pGMR	plasmid Glass Multimer Reporter
PKA	Protein Kinase A
PP1	Protein Phosphatase 1
PP1c	Catalytic subunit of PP1
Rac	Ras-related C3 botulinum toxin substrate
RbCl	Rubidium Chloride
R cells	Photoreceptor cells or neurons
red	*red malpighian tubules*
Repo	Reversed Polarity
RGC	Retinal Ganglion Cell
Rh	*Rhodopsin*
Rho	Ras homology gene family
RNA	Ribonucleic acid
RNAi	interfering RNA

Ro	*Rough*
Robo	Roundabout
rpm	Rotations per minute
RPTP	Receptor Protein Tyrosine Phosphatase
RT	Room Temperature
RTK	Receptor Tyrosine Kinase
ru	*roughoid*
Sb	*Stubble*
SDS-PAGE	Sodium Dodecyl Sulphate-Polyacrylamide Gel Electrophoresis
SEM	Scanning Electron Microscopy
Sema	Semaphorin
sens	*senseless*
Ser	Serine
sr	*stripe*
st	*scarlet*
Stau	Staufen
TE	Tris EDTA
TEMED	N, N, N', N' tetramethylethylene diamine
TGF-β	Transforming Growth Factor-β
th	*thread*
Thr	Threonine
Tris	Tris (hydroxymethyl) aminomethane
Tyr	Tyrosine
UAS	*Upstream Activator Sequence*
UNC-5	Uncoordinated-5
V	Volts
VNC	Ventral Nerve Chord
WT	Wild Type
Wnt	Mammalian Wingless

SUMMARY

Normal development of organisms and cell survival requires integration of a number of signalling pathways and regulatory molecules. Intracellular and extracellular molecules co-ordinate to regulate a number of cell functions including cell differentiation, proliferation and morphogenesis. Many of these molecules and signalling pathways are highly conserved throughout evolution. Hence, studies in model organisms have been critical in defining the basic concepts that govern all cell functions. This thesis focuses on using *Drosophila melanogaster* as a model system to study some of these developmental processes. *Drosophila* has been an effective model system for nearly one hundred years helping to define the components necessary for processes such as neural and embryonic development.

The work described in this thesis uses *Drosophila* as the model organism and deals with the characterisation of an actin binding protein, Bifocal (Bif), its interacting partners and their role in the developing cytoskeleton. The work in this thesis focuses on the developing fly eye, the targeting of axons from the eye to the brain and the anchoring of posterior determinants to the cortex during oogenesis in *Drosophila*. The results are described in three chapters.

Chapter 3 deals with the interaction between Bifocal and Protein Phosphatase 1 (PP1) and the *in vivo* requirement of this interaction for normal eye development. In the absence of *bif*, the actin rich rhabdomeres, of the fly eye, lose their star like appearance in the pupal stages and appear compressed, further the *bif* mutant eye shows split and elongated rhabdomeres as well as loss and multiplication of bristles on the surface of the eye. Wild type Bif driven in the eye can rescue these defects. However, when the PP1 binding region in Bif is mutated, the mutated form of Bif

cannot rescue these eye defects indicating that Bif interacts with PP1 *in vivo* and this interaction is required for the formation of a normal fly eye.

In chapter 4, I describe the photoreceptor axon guidance phenotype seen in *bif* mutants and present evidence to show that this phenotype can be uncoupled from the eye phenotype described in the previous paragraph. This function of Bif in photoreceptor axon guidance also requires the interaction between Bif and PP1. This chapter also describes the axon guidance defects seen in *pp1* mutants and the interaction between Bif and other phosphatases.

Chapter 5 describes the genetic interaction between *bif* and *homer* (*hom*) and the defects seen in oogenesis in *bif; hom* double mutants. The double mutant flies show defects in anchoring Osk to the posterior cortex of the oocyte. Further, although both Bif and Hom are actin binding proteins, the cortical localisation of Bif in the oocyte depends on F-actin while that of Hom does not depend on an intact F-actin cytoskeleton. Experiments using drugs to destabilise the F-actin cytoskeleton lead to the conclusion that there may be F-actin dependent and F-actin independent mechanisms required to anchor Osk to the posterior cortex of the oocyte and either of these mechanisms is sufficient for the anchoring of Osk to the posterior cortex.

Chapter 1

Introduction

1.1. *Drosophila melanogaster* as a model organism

It has been known for sometime now that differences between organisms are primarily due to differences in the genetic programming of the different organisms. The fruit fly, *Drosophila melanogaster* and the nematode *Caenorhabditis elegans* have been instrumental in this realisation.

The fruit fly has been used as a model system for the past century and has been recognised as an ideal model organism to elucidate many mechanisms involved in apoptosis, axon guidance, cell division and differentiation, cytoskeletal organisation, neurogenesis, pattern formation and other developmental processes. Whilst it is true that there are some differences between flies and vertebrates, it is clear that the similarities are far more overwhelming, and flies have taught us a great deal about many of these conserved mechanisms. Signalling pathways like Hedgehog, Wnt, Notch and TGF-β were first elucidated in flies, and are still producing important insights into their function and interactions. Some of the main advantages of using *Drosophila* as a model system are:

i. Short life cycle and easy to maintain

ii. Very genetically amenable with lots of tools for making mutations in the whole fly or mosaics with mutants in parts of the fly and balancers to keep mutant chromosomes intact. *Drosophila* also has a system to specifically express molecules in certain organs or tissues of the organism.

iii. The fly genome has been sequenced by the Berkeley *Drosophila* genome project led by G. Rubin and Celera genomics Inc. headed by C. Venter (Adams *et al.*, 2000).

iv. The entire life cycle as well as the anatomy of *Drosophila* have been well documented and hence make it relatively easy to study.

v. It has a basic cellular and molecular organisation, which is very similar to that of vertebrates.

This thesis looks at the function of *bif* and its interacting partners, Protein phosphatase 1 and Homer, in several different developmental contexts and focuses on Bif function in the eye, the larval visual system and the ovaries. The next few sections of this chapter will deal with introducing the various organs where the function of Bif is being studied as well as the molecules with which *bif* shows a genetic or physical interaction.

1.2. Eye development

1.2.1. Introduction to mammalian eye development

The eye is a very complex and fascinating organ that allows one to view the outside world. Evolution has generated at least three basically different types of eyes (reviewed in (Gehring, 2002), they are:

a. The camera type eye with a single lens projecting onto a retina that is found in vertebrates and cephalopods.

b. The compound eye with multiple ommatidia each consisting of a set of photoreceptor cells and a lens of its own, which are characteristic of insects and other arthropods.

c. The mirror eye that uses a lens for focussing the light onto a distal retina and a parabolic mirror for projecting the light onto a proximal retina as is seen in the case of scallop (Pecten).

Most of these eyes are positioned on the head of the animal and send signal to the brain, which processes the information and transmits the appropriate signal to the effector organs (reviewed in (Gehring, 2002).

Morphological development of the vertebrate eye begins with the formation of an outpouching of the diencephalon called the optic vesicle. The optic vesicle subsequently contacts the head ectoderm and signals the induction of a pseudostratified thickening of the ectoderm called the lens placode. The lens placode invaginates and separates from the surrounding ectoderm to form a lens vesicle. Eventually, the cells of the lens vesicle differentiate into fibre cells characteristic of the adult lens. Concomitantly, the optic vesicle folds inward on itself, surrounding the lens vesicle and forming the optic cup, which will eventually comprise the neural and pigmented layers of the adult retina. Although the early stages of vertebrate eye development have been the subject of numerous embryological experiments, until recently little was known about the molecular identities of the regulators involved. *Pax6*, a member of the vertebrate Paired box family of transcription factors provided an exception to this, as its expression pattern initially suggested a role in eye development (Walther and Gruss, 1991). Prior to lens induction, *Pax6* is expressed in a broad domain of head ectoderm and in the optic vesicle, and expression becomes restricted to the lens placode, lens vesicle and optic vesicle as development proceeds (reviewed in (Wawersik and Maas, 2000).

1.2.2. *Drosophila* as a model system to study eye development

The eye of *Drosophila* is a so-called compound eye, consisting of multiple facets with photoreceptors that detect light and transmit light images to the brain. Although its structure is very different from that of the human eye and from the simple photoreceptors in primitive worms, the eyes of *Drosophila* serve essentially the same function as they do in these other organisms.

Evidence of similarities between the fly and human eyes comes from studies of mutations in a gene called *eyeless* in *Drosophila.* These mutations can either cause eye deficiencies or eliminate the eyes altogether. Furthermore, ectopic expression of *eyeless* (i.e., expression of the gene in an abnormal location) can result in the formation of retinal tissue in those locations. Thus, expression of the wild-type allele of *eyeless* is necessary for eye development. This gene is at least one of the genes that are capable of triggering the events that result in the formation of eyes. Mutations that reduce or eliminate eyes have also been observed in mammals. These include *small eye* in mice and *aniridia* in humans. Molecular analyses have shown that these genes have substantial similarities in their nucleotide sequences to the *Drosophila eyeless* gene, hence making them homologues, which have probably derived from an ancestral gene. These genes that control eye development are members of a family of genes called *Pax-6*. *Pax-6* homologues have been discovered in organisms as diverse as mammals, squids, ascidians, insects, cephalopods, and nemerteans (Halder *et al.*, 1995; Tomarev *et al.*, 1997). The *Pax-6* genes in diverse organisms are so similar in their function that expression of the mouse *small eye* gene will cause the formation of ectopic eyes in *Drosophila*. Although the details of eye development differ dramatically from one species

to another, their specification was initially thought to be soleley dependent upon expression of the *Pax-6* gene. *Pax-6* genes are regulators of gene transcription. Thus, they must have target genes that mediate their role in eye development. In fact, a complex cascade of events that results in eye formation is triggered by *Pax-6* gene expression. Differences among these downstream events will result in different eye morphologies. One of those downstream genes in *Drosophila* is *eyes absent*, which also has homologues in vertebrates (Xu *et al.*, 1997).

Although *Pax-6* was initially thought to be the master control gene for production of eyes in animals of different phyla (Gehring and Ikeo, 1999), it is now known that *Pax-6* requires upstream signals to allow it to specify the eye (Pichaud *et al.,* 2001). It is now known that several additional genes can induce ectopic eye development in *Drosophila*. These include *sine oculus, dachshund* and *teashirt*, as well as a second *eyeless* gene in Drosophila called *twin of eyeless.* A similar complete suite of homologous genes has also been reported in mouse. It is also known that many animals with no eyes still express *Pax-6* or its homologs (eg. *C. elegans* and cnidarian corals). Further Pax-6 has also been shown to be involved in other developmental processes like anterior body determination in *Xenopus*. These results indicate that there probably is no conserved 'Master Regulator' gene in eye development although the process of eye development involving molecules acting both upstream and downstream of *Pax-6* is conserved (reviewed in (Fernald, 2000).

Besides the functional conservation of the Pax-6 signalling pathway the mechanism of differentiation of zebrafish and fly retina seems to be conserved. the photoreceptor clusters are specified during the third instar larval stages in a

posterior to anterior wave of differentiation led by an indentation called the morphogenetic furrow. Propagation of this wave, initiated at the posterior tip of the eye disc, requires the two diffusible molecules Hedgehog (hh) and Decapentaplegic (dpp), a *Drosophila* BMP homolog. *hh* is initially expressed at the posterior margin, and then turns on in the differentiating photoreceptors; hh activates *dpp* expression in a stripe just anterior to its own expression domain. Thus, cells that receive the hh signal themselves turn on *hh* expression, allowing the domains of *hh* and *dpp* to progress dynamically across the eye disc. Differentiation of the zebrafish retina uses the same strategy as the fly retina. A wave of differentiation marked by Sonic hedgehog (Shh) sweeps through the fish retina, leaving behind differentiated retinal cells. Shh expression is first detected in a single patch of newly formed retinal ganglion cells (RGCs) close to the optic stalk, and then progresses circumferentially within the RGC layer as a wave that follows the ontogenesis of RGCs. (reviewed in (Pichaud *et al.,* 2001).

It is also known now that in mice as in insects the first retinal neurons (R8 in flies and Retinal ganglion cells in mice) require the basic-helix-loop-helix gene *atonal,* in *Drosophila,* or its homolog *math5,* in mice. In *Drosophila*, the manner of *atonal* regulation determines initial pattern formation. The *atonal* gene is not activated independently in each cell of the R8 grids. Instead, a stripe of *atonal* expression coincides with a morphogenetic furrow. The stripe of expression signifies R8 competence at the furrow, and it becomes refined by lateral inhibitory signalling to successive rows of evenly spaced R8 cells. This progression of *atonal* activation allows self-organisation of the R8 grid, as the spacing of one row of R8 cells helps to template the

spacing of the next row. Highly regular spacing of R8 cells within the epithelium is crucial, as deviations can result in lattice packing defects of the ommatidia, which in turn will impair visual function. In vertebrates, the retinal ganglion cells are somewhat overdispersed in the retina, possibly pointing to lateral inhibition among proneural-gene-expressing cells. Moreover, neurogenesis has been found to occur in a wave in the vertebrate retina. Most intriguingly, neurogenesis also begins in the optic cup epithelium closest to the optic stalk, and then spreads outwards from there (from nasal to temporal in zebrafish, for example). It has now been shown that this wave is associated with expression of the zebrafish *atonal* homologue *ath5*. These findings suggest a conserved mechanism of fly eye and vertebrate eye development (reviewed in (Jarman, 2000). Another molecule conserved in eye development is Opsin. Opsins are light-collecting visual pigments that are denseley arranged in the apical outer membrane of photoreceptors and have also been shown to be required for photoreceptors to acquire their final morphological features. These molecules are known to be conserved across the various phyla (Cook and Desplan, 2001; Fernald, 2000; Land and Fernald, 1992). One of the areas of dissimilarity among eyes are proteins required to make lens tissue which vary across the phylogenetic tree (Fernald, 2000). Another point of difference among eyes is seen in the light sensitive apical membrane of photoreceptors in the eye. These membranes are called outer segments in vertebrates and rhabdomeres in flies. They originate from different apical extensions, from cilia in the case of vertebrates and microvilli in the case of invertebrates, they also have different mechanisms of transducing light. However the final morphology of both structures is quite similar and in both cases consists of a packed apical

membrane with high concentrations of opsins. The rhabdomere is connected by a specialised membrane the stalk and the vertebrate outer segment is similarly supported by the inner segment (Pichaud and Desplan, 2002). Thus one can see that although one part of the eye does not rely on homologous proteins there is a large amount of similarity in the core mechanisms underlying eye development, making *Drosophila* a good model organism to study this process.

1.2.3. Brief outline of *Drosophila* eye development

The *Drosophila* adult eye (Fig. 1.1A) is made up of regular hexagonal arrays of approximately 750 facets called the ommatidia. A single ommatidium is made up of 8 photoreceptors and 11 accessory cells (illustrated in Fig. 1.1B). Briefly, the **photoreceptors** (**R cells**) comprise of 8 cells R1-R8. The outer photoreceptor cells, R1-R6, are present in a ring surrounding two central photoreceptors. The 2 central photoreceptors are R7, which is the outer cell and R8, or inner, central cell. Each of these photoreceptors has a distinct circular shape and a specific position in the ommatidium. The 6 outer cells give rise to an irregular trapezoidal shape with R7 and R8 at the centre of the trapezoid (illustrated in Fig. 1.1 B, note that in any given section only one of either the R7 or the R8 cell is visible). Overlying the photoreceptors is a quartet of **cone cells**, which are the lens secreting cells in the ommatidium.

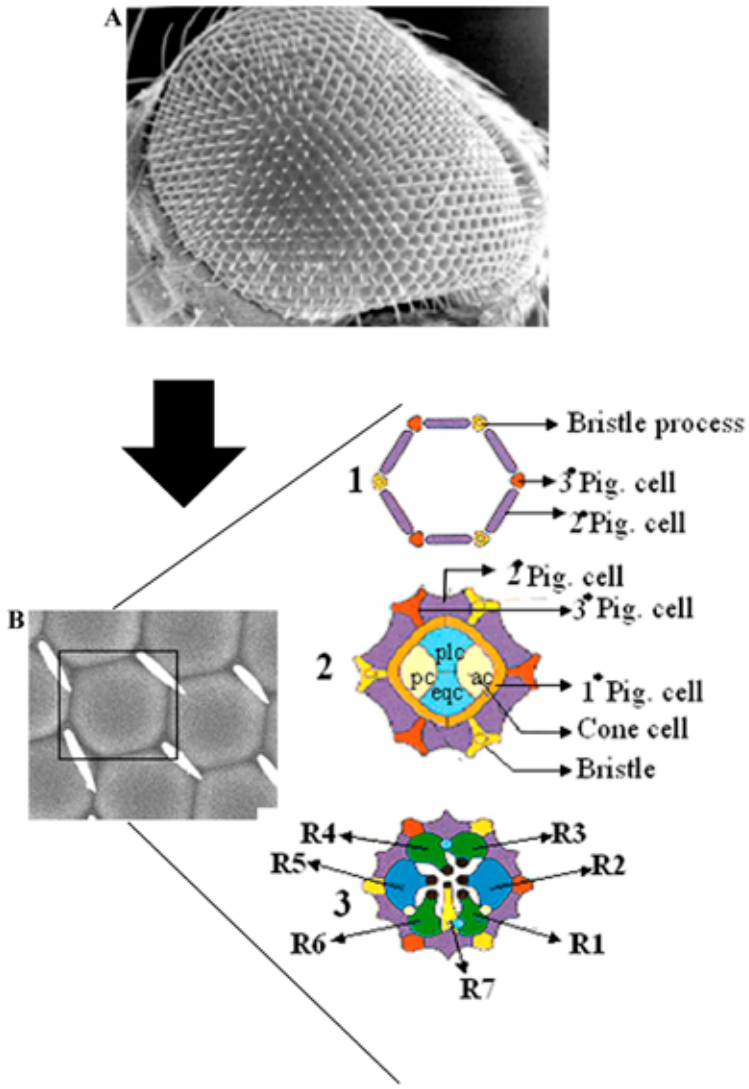

Fig. 1.1: The adult fly eye (adapted from Wolff and Ready, 1993)
Panel A shows a scanning electron micrograph of an adult compound eye with a regular hexagonal array of approximately 750 facets called ommatidia.
Panel B shows a larger magnification of a single ommatidium that is made up of an assembly of 8 photoreceptors and 11 accessory cells. B also shows a schematic of three sections of a single ommatidium. The outermost section 1 shows six secondary pigment cells, which form 6 sides of a hexagon. The vertices of the hexagon alternate with bristle cells and tertiary pigment cells. The middle section 2 shows four cone cells termed polar cone cell (plc), equatorial cone cell (eqc), anterior cone cell (ac) and posterior cone cell (pc) based on their position within the ommatidium. 2 primary pigment cells completely encompass the cone cells. The secondary and tertiary pigment cells as well as the bristle cells are also seen in this section. Section 3 shows R1-R7 rhabdomeres as well as the secondary and tertiary pigment cells and the bristle cells. In any given section where the rhabdomeres are observable, R1-R6 rhabdomeres can always be seen and either the upper R7 or the lower R8 rhabdomere is visible.

Two **primary pigment cells** surround the cone cells and **secondary pigment cells** lie between two ommatidia. The **tertiary pigment** cells are shared among three ommatidia at a vertex. Rhabdomeres of the eye are the rhodopsin-rich apical surfaces of a photoreceptor, accommodating more than 90% of the photoreceptor's plasma membrane in a closely packed stack of about 60,000 microvilli. Every alternate corner of the hexagonal ommatidium has a bristle projecting above the surface of the ommatidia (Fig. 1.1B). Each **mechanosensory bristles** is made up of a four cell complement of neuron, glia and two support cells which are the shaft and the socket cells (Dietrich, 1909; Ready *et al.,* 1976; Waddington, 1960; Wolff and Ready, 1991; Wolff, 1993).

1.2.4. Introduction to Bifocal and its role in eye development

Mutations in *bifocal* (*bif*) were isolated in a P-element transposition screen. Bif is required for the development of normal rhabdomeres. The morphological defects seen in *bif* mutant animals, in which the distinct contact domains established by the newly formed rhabdomeres, are abnormal, first become apparent during midpupal development. The later defects seen in the mutant adult R cells are more dramatic, with the rhabdomeres enlarged, elongated, and frequently split (Fig. 3.4 B and 3.6 B in chapter 3) (Bahri *et al.*, 1997).

The Bif coding sequence is made up of 5 exons. So far, two isoforms of Bif have been found. One of which encodes a 1063 amino acid protein and the other encodes a 1196 amino acid protein. Both these isoforms differ in their splice sites in the 4^{th} exon (depicted in Fig. 4.5 in chapter 4) (Bahri et al., 1997; Helps et al., 2001). *bif* encodes a novel protein that is expressed in the embryo

and the larval eye imaginal disc in a pattern identical to that of F-actin. During pupal development, Bif localises to the base of the filamentous actin associated with the forming rhabdomeres along one side of the differentiating R cells. Its subcellular localisation and loss-of-function phenotype suggest that Bif plays a role in photoreceptor morphogenesis (Bahri *et al.*, 1997).

Various mutant alleles of *bif* are known to exist to date, during the course of this thesis I will discuss the phenotypes associated with the *bif* mutant allele bif^{R47} which has been previously described to be a protein null. This allele of *bif* shows deletion of exon 3 and 6 and affects both the isoforms of Bif. Further the phenotype seen using the bif^{R47} allele has been reported to be identical to the phenotype seen using a deletion of the *bif* gene (Bahri *et al.*, 1997).

1.3. Protein phosphatase 1

1.3.1. General introduction to kinases and phosphatases

Reversible protein phosphorylation is an important process used by eukaryotic cells to regulate many biological functions, including cell growth and differentiation, cell cycle progression, DNA replication and energy metabolism. Protein kinases and phosphatases modulate levels of cellular protein phosphorylation.

Many extracellular molecules that trigger various reactions within a cell exert their effect by activating or inhibiting transmembrane proteins that in turn control the production or activation of second messengers. Transmembrane proteins often mediate downstream events by modulating the activities of protein kinases and protein phosphatases. Phosphorylation (or

dephosphorylation) of Serine, Threonine and Tyrosine residues triggers conformational changes in the regulated proteins which alter their properties, leading to physiological responses in the cell. Extensive biochemical and genetic analysis have revealed that the balance of phosphorylated and non-phosphorylated forms of proteins is critical for the cell. Kinases and phosphatases, may work together to modulate a signal and they function in signalling networks with multiple kinases and phosphatases (Cohen, 1992; Morrison *et al.*, 2000).

1.3.2. Function of protein phosphatases

The *Drosophila* genome encodes 217 putative protein kinases, and 28 putative Ser/Thr phosphatases (Morrison *et al.*, 2000). The human genome encodes around 500 protein kinases (of which two thirds are putative Ser/Thr kinases) and less then 40 Ser/Thr phosphatases (International Human genome sequencing consortium). The past decade has seen the emerging of the molecular mechanism of how a small number of phosphatases dephosphorylate thousands of proteins while allowing the level of phosphorylation of each protein to be regulated independently. The molecule on which a lot of studies have been done is Protein Phosphatase 1 (PP1). The PP1 catalytic subunit (PP1c) can complex with more then 50 regulatory subunits in a mutually exclusive manner. The formation of these complexes converts PP1c into many different forms, each of which have distinct substrate specificities, restricted subcellular locations and diverse regulation. This allows numerous cellular functions that rely on PP1 to be controlled by independent mechanisms (reviewed in (Cohen, 2002).

1.3.3. *Drosophila* protein phosphatases and their functions

The *Drosophila melanogaster* genome encodes for 6 isoforms of Protein Phosphatase 1 (PP1). These molecules map to different regions in the genome and are: PP1β–9C (termed *flapwing*), PP1-13C, PP1-87B, PP1α-96A, PP1-Y1 and PP1-Y2. These protein phosphatases are named based on their approximate cytological locations on the *Drosophila* polytene chromosome (Carvalho et al., 2001; Dombradi et al., 1990b; Dombradi et al., 1993).

Although the function of these various phosphatases has not yet been well characterised, there are some ideas on what the function of some of the PP1's may be. It has been shown that PP1β–9C is required for the maintenance of muscle attachments, where mutants show muscles which break away from their attachment sites and degenerate (Raghavan et al., 2000). It has also been shown that PP1c acts as a regulator of Trithorax (a homeotic gene) function in *Drosophila* (Rudenko *et al.*, 2003).

The best studied PP1 is PP1-87B and this has been implicated in various functions in the fly. Null mutants at *pp1-87B* exhibit a lethal phenotype at the larval stage, failing to exit mitosis and show excessively condensed chromosomes (Axton et al., 1990; Dombradi et al., 1990a). *pp1-87B* mutants with some residual activity are viable and exhibit dominant suppression of position effect variegation indicating that *PP1-87B* also modulates chromosome condensation in interphase (Baksa et al., 1993; Dombradi and Cohen, 1992).

1.3.4. Role of Protein Phosphatase 1 in eye development and its interaction with Bif

It has been shown using biochemistry and crystallography that interaction of regulatory subunits with PP1c is mutually exclusive. This observation was explained by the discovery that a short motif -(R/K)(V/I) X-(F/W)- present in the majority of these subunits is sufficient for binding to PP1c (Egloff *et al.*, 1997; Johnson *et al.*, 1996; Zhao and Lee, 1997).

In this thesis I discuss the interaction between Bif and PP1 via a RVQF motif present in the C-terminal region of Bif. I further show that this interaction is required for the normal function of Bif in the *Drosophila* eye.

1.4. Axonal connectivity

1.4.1. Introduction to axon guidance and axonal connectivity

Wiring the human brain is one of nature's greatest feats, and one of its most daunting tasks. Neurons numbering in the billions must be specifically connected to one another to assemble functioning neural circuits. The basic framework of neuronal connectivity is built during foetal development in a process called axon pathfinding. During pathfinding, the axons of developing neurons navigate long distances along specific pathways to reach their appropriate targets. The characterisation of the molecules that guides axons in the developing brain environment, as well as the receptors and signalling cascades through which guidance molecules exert their influence, form the central areas of investigation in the field of axon guidance.

During pathfinding, axons elaborate specialised structures at their tips called growth cones through which they sense and respond to the environment

(see Fig. 1.2). The growth cone is a fan-shaped motile structure with finger-like filopodia, and is constructed of actin filaments extending from a central microtubule core (Suter and Forscher, 1998). As a growth cone extends in the embryonic environment, receptor molecules on its surface interact with guidance molecules displayed in the extracellular matrix or on the surfaces of surrounding cells. Upon activation of these receptors by guidance molecules, intracellular signalling cascades are triggered which eventually feed into pathways altering the assembly of cytoskeletal components such as actin and tubulin. Signalling cascades causing a net addition of cytoskeletal components are thought to lead to growth cone advance, while net disassembly may lead to axon retraction. Asymmetric signalling on one side of the growth cone is thought to lead to turning and change in the direction of growth (Song *et al.*, 1998; Song and Poo, 1999; Suter and Forscher, 1998). In the past several years, researchers have identified significant numbers of guidance molecules and begun to understand how particular combinations are used for specific pathfinding tasks.

Among the earliest axon guidance molecules identified were extracellular matrix molecules such as laminin and fibronectin that promote axon growth. Analysis of the protein domain structure of these and other subsequently identified families of guidance molecules showed that guidance molecules in general all contain a number of common domain motifs such as immunoglobulin-like repeats, EGF repeats, and fibronectin type III domains. Each family of guidance molecules is, however, also defined by its own distinctive domain (reviewed in (Tessier-Lavigne and Goodman, 1996; Yu and Bargmann, 2001).

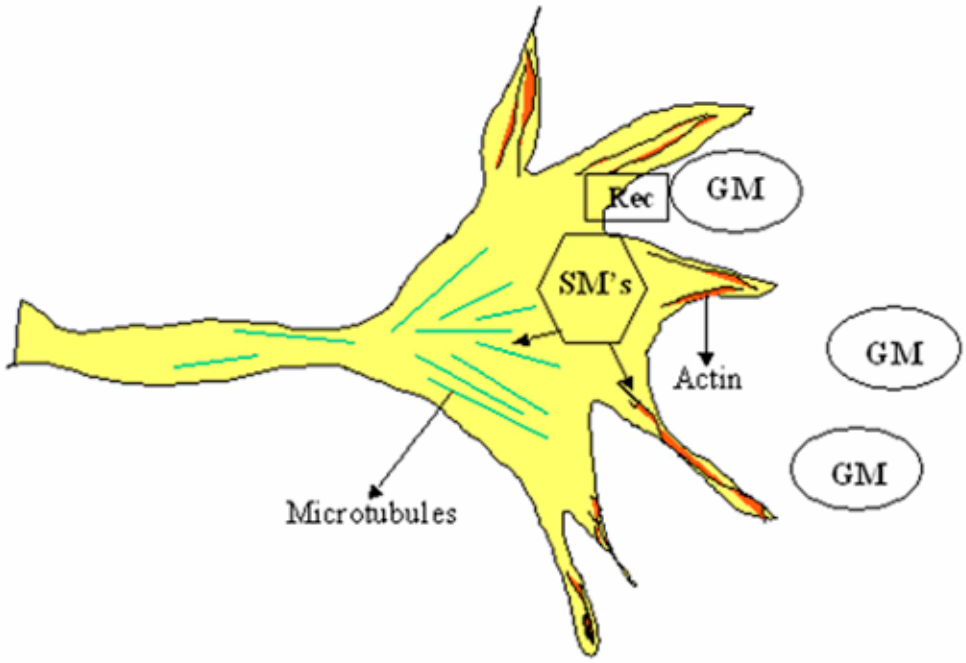

Fig. 1.2: A growth cone (adapted from Oster and Sretavan, 2003)
The growth cone is a fan-shaped motile structure with finger-like filopodia, and is constructed of actin filaments extending from a central microtubule core. Extracellular guidance molecules (GM) bind transmembrane receptors (Rec), which are present on the surface of the growth cone. These receptors then activate signalling cascades that ultimately influence growth cone cytoskeletal components, that control the morphology and the motility of the growth cones. These signalling cascades affect the actin cytoskeleton. SM indicates signalling molecules.

In addition to guidance molecules that promote axon outgrowth, an important contribution to our understanding of axon pathfinding was the discovery that a substantial number of guidance proteins control axons by inhibiting their ability to extend. Given that the nervous system is able to both encourage and inhibit axon growth, it would seem that one simple strategy for axon guidance is to use arrays of attractive and inhibitory guidance cues to steer developing axons along specific pathways to their targets (reviewed in (Oster and Sretavan, 2003).

During vertebrate embryonic and postnatal development of the nervous system, neuronal precursor cells have to migrate to their final destinations and axons have to navigate to the correct targets to establish normal connectivity. Neuronal migration and axon pathfinding are guided by extracellular cues, which initially include netrins, semaphorins, ephrins and Slits.

Netrins are secreted proteins that direct axon extension and cell migration during neural development. They are bifunctional cues that act as an attractant for some cell types and as a repellent for others. Several lines of evidence suggest that two classes of receptors, the deleted in colorectal cancer (DCC) family and the UNC-5 family that mediate the attractant and repellent response to netrins. Netrins function as both long- range and short-range cues close to the surface of the cells that produce them and contribute to guiding neurite outgrowth and mediating cell-cell interactions during development (Kennedy, 2000). The semaphorins belong to a family of phylogenetically conserved proteins, several members of which can act as repulsive cues for specific populations of neurons during development. The semaphorin family is very large and includes both secreted and transmembrane glycoproteins. This

suggests that some semaphorins influence growth cone guidance at a distance, while others act locally. A conserved extracellular semaphorin (sema) domain defines Semaphorins. Semaphorins are expressed in a wide variety of neuronal and nonneuronal tissues (reviewed in (Kolodkin and Ginty, 1997). Ephrin receptors (Eph) are members of the Receptor Tyrosine Kinase (RTK) family of genes. These transmembrane receptors typically bind Ephrins that are expressed by neighbouring cells and mediate short-range cell-to-cell communication. The influence of Ephrin–Eph interaction on cell behaviour depends on the cell type (reviewed in (Palmer and Klein, 2003). The Slit family of secreted proteins are important players in axon guidance and cell migration. Slit functions through its receptor, Roundabout, and an intracellular signal transduction pathway that includes the Abelson kinase, the Enabled protein, GTPase activating proteins and the Rho family of small GTPases. It has been shown that Slit functions as an extracellular cue to guide axon pathfinding, promote axon branching and to control neuronal migration (reviewed in (Wong *et al.,* 2002).

The molecules described above form some of the essential players in axon pathfinding in many different organisms and show a largely conserved mode of action during axon guidance. These and other molecules are involved in various aspects of axon guidance in *Drosophila* as will be described below.

1.4.2. Axon guidance at the midline of *Drosophila* embryonic CNS

The central nervous system (CNS) of higher organisms is bilaterally symmetric. The transfer of information between the two sides of the nervous system occurs through commissures formed by neurons that project axons across the midline to the contralateral side of the CNS. Interestingly, these

axons cross the midline only once. Other neurons extend axons that never cross the midline; they project exclusively on their own (ipsilateral) side of the CNS. Thus, the midline is an important choice point for several classes of pathfinding axons. Recent studies demonstrate that specialised midline cells play critical roles in regulating the guidance of both crossing and non-crossing axons at the ventral midline of the developing vertebrate spinal cord and the *Drosophila* ventral nerve cord. For example, these cells secrete attractive cues that guide commissural axons over long distances to the midline of the CNS. Furthermore, short-range interactions between guidance cues present on the surfaces of midline cells, and their receptors expressed on the surfaces of pathfinding axons, allow commissural axons to cross the midline only once and prevent ipsilaterally projecting axons from entering the midline. Remarkably, the molecular composition of commissural axon surfaces is dynamically altered as they cross the midline. Consequently, commissural axons become responsive to repulsive midline guidance cues that they had previously ignored on the ipsilateral side of the midline. Concomitantly, commissural axons lose responsiveness to attractive guidance cues that had initially attracted them to the midline. Thus, these exquisitely regulated guidance systems prevent commissural axons from lingering within the confines of the midline and allow them to pioneer an appropriate pathway on the contralateral side of the CNS. Many aspects of midline guidance are controlled by mechanistically and evolutionarily conserved ligand-receptor systems. Strikingly, recent studies demonstrate that these receptors are modular; the ectodomains determine ligand recognition and the cytoplasmic domains specify the response of an axon to a given guidance cue (reviewed in (Kaprielian *et al.*, 2001).

Molecular genetic studies performed in *Drosophila* provide support for an altered-responsiveness guidance system operating at the midline of the developing CNS. Large-scale screens for *Drosophila* mutants in which too many or too few axons cross the midline have resulted in the isolation of genes that collectively control midline crossing. In *commissureless (comm)* mutants, the CNS is devoid of essentially all commissural tracts and contains only the two longitudinal connectives located on either side of the midline. Consistent with this phenotype, commissural growth cones/axons properly orient to, but never cross the midline in this mutant. The *comm* gene product, Comm, is likely to be directly required for midline crossing since the differentiation of midline-associated glia and neurons are normal in these embryos (Seeger *et al.*, 1993; Tear *et al.*, 1996).

Another molecule essential for normal midline axon guidance in *Drosophila* is Roundabout (Robo). In *robo* mutants, the ventral nerve cord contains thickened commissures that reflect excessive midline crossing events. Antibody labelling demonstrates that axons that normally pioneer ipsilateral projections now cross the midline, while contralaterally projecting axons re-cross the midline multiple times. Interestingly, only those axons that project within the innermost longitudinal connectives aberrantly cross and re-cross the midline in *robo* mutants. It is also known that Comm and Robo act in concert to control midline crossing (Kidd *et al.*, 1998a; Kidd *et al.*, 1998b; Seeger *et al.*, 1993).

Studies have now provided genetic evidence supporting a role for Slit as the repulsive Robo ligand. The key result, which suggested this possibility, was the finding that the strongest gain-of-function Comm phenotype resembles

the collapsed-midline phenotype exhibited by *slit* mutants. It was also shown that flies which carry a single mutant copy of *robo* and *slit* display a *robo*-like phenotype. This observation supports a receptor-ligand relationship between Robo and Slit (Kidd *et al.*, 1999). Consistent with this notion, Robo and Slit proteins serve as binding partners for each other. Taken together, these data suggest that Slit is the Robo ligand (Brose *et al.*, 1999).

Receptor-linked tyrosine phosphatases (RPTPs) also regulate midline crossing in the *Drosophila* ventral nerve cord. RPTPs regulate tyrosine dephosphorylation in growth cones and thus reverse reactions catalysed by tyrosine kinases. Consistent with potential roles as repellent receptors, it has been demonstrated that the *Drosophila* RPTPs, Dlar and Dptp10D are, like Robo, selectively localised to longitudinal axonal tracts in the embryonic ventral nerve cord. Further, many longitudinally growing axons are re-routed across the midline in flies lacking Dptp10D and another neural RPTP, Rptp69D. It has also been found that *dptp10d* and *rptp69d* genetically interact with *robo, slit* and *comm.* This provides support for the possibility that these two RPTPs regulate Robo/Slit repulsive signalling at the midline, possibly by modulating tyrosine phosphorylation events mediated by repulsive Robo/Slit interactions (Sun et al., 2000).

Netrins are also required for commissural axon guidance in the developing *Drosophila* CNS. Midline cells express Netrin-A and Netrin-B during the initial stages of commissure formation in the ventral nerve cord. Deletion of both genes results in thinner than normal commissures (an indication that fewer than normal axons have crossed the midline), as well as occasional breaks in the longitudinal connectives. Genetic analyses

demonstrate that *netrin-A* and *netrin-B* presumably play redundant roles at the midline. Further, ectopic expression of either Netrin-A or Netrin-B leads to defects in commissural and longitudinal axonal tracts that resemble those seen in the double mutants. This result demonstrates that the precise spatial distribution of Netrin-A and Netrin-B, and not simply their presence, is required for the proper formation of commissural tracts. Taken together, these data provide additional support for the evolutionarily conserved role of Netrins in commissural axon guidance (Harris *et al.*, 1996; Mitchell *et al.*, 1996).

The observation that the *Drosophila* DCC ortholog, Frazzled, is expressed at high levels on commissural and longitudinal axon tracts in the ventral nerve cord provides additional support for an evolutionarily conserved role for Netrins in midline guidance. Reminiscent of the CNS phenotype detected in the absence of both netrin genes, thin or missing commissures characterise the ventral nerve cord of *frazzled* null mutants. These findings suggest that Frazzled functions as a putative Netrin receptor in flies (Kolodziej *et al.*, 1996). However, there is also some data that suggests that Frazzled may indirectly regulate the guidance of specific axons by capturing and localising Netrins at specific sites within the CNS. This capture/relocation mechanism elucidated in these studies could facilitate the efficient and widespread use of guidance cues, some of which may be selectively synthesised by midline cells, in the developing CNS (Hiramoto *et al.*, 2000; Kaprielian *et al.*, 2001).

1.4.3. Axon guidance in the visual system

One of the best-studied models of axon guidance is the developing Retinal Ganglion Cell (RGC) and its axon. Recent work has begun to shed light

on the molecular mechanisms that govern RGC axon guidance during optic nerve development, the formation of the optic chiasm and the establishment of retinotopic maps in visual targets such as the superior colliculus.

The first major pathfinding task for a newly born RGC is to extend an axon towards the optic nerve head. During development, ganglion cells are born in a central to peripheral gradient such that the oldest RGCs are closest to the optic disc and the younger RGCs are in the more peripheral retina. Newly formed RGC axons are in contact with axons of older RGCs and travel along, or fasciculate with, these neighbouring axons to reach the optic nerve head. This fasciculation appears to be due to growth promoting molecules such as L1 on the RGC axons themselves. L1 is a member of the Immunoglobulin (Ig) family of cell adhesion molecules (Burden-Gulley *et al.*, 1997), and functions in a homophilic manner. Homophilic binding means that an L1 molecule on a given axon binds an L1 molecule on an adjacent axon. It is thought that such L1 homophilic interactions encourage retinal axons to grow in bundles, or fascicles, within the retina on their way to the optic disc. This model is supported by the finding that experimental blockade of L1 function, or the function of related Ig guidance molecules, causes RGC axons to wander in the retina instead of growing directly to the optic disc (Brittis *et al.*, 1995; Ott *et al.*, 1998). Thus, RGC axon pathfinding to the optic disc appears to involve the ability of retinal growth cones to follow a trail of attractive axon guidance molecules.

Some insight can be obtained by considering the fact that the molecular basis of growth cone guidance is highly conserved throughout evolution. For example, homologues of many of the axon guidance molecules, such as netrins,

slit, and semaphorins, have been identified in invertebrates such as the fruit fly, *Drosophilia* and the nematode, *C. elegans,* where they also participate in axon pathfinding during neural development (Hedgecock *et al.*, 1990; Kidd *et al.*, 1999; Kolodkin *et al.*, 1993; Kolodkin *et al.*, 1992; Mitchell *et al.*, 1996). Human homologues of netrins, slits, semaphorins, and ephrins have also been identified (Brose *et al.*, 1999; Kolodkin *et al.*, 1993), but as yet, little is known about their patterns of expression or function during human development. However, it seems highly likely that these same gene families, and similar axon guidance principles, contribute to patterning the human visual system.

1.4.4. Axon guidance in the *Drosophila* visual system

For the visual system, the synaptic circuitry of the *Drosophila* brain is organised into three distinct ganglia: the lamina, the medulla and the lobula. This structure and quite possibly the function of the axons innervating the optic lobe of the brain has been shown to be conserved between insects and crustaceans, indicating a degree of similarity between these two apparently diverse groups of organisms (Osorio and Bacon, 1994). The compound eye, known for its precise ommatidial architecture, establishes equally precise patterns of axonal connections within the lamina and medulla ganglia of the optic lobe. Of the eight, photoreceptor neurons in an ommatidium, six (the R1–R6 photoreceptors) establish synaptic connections in repeating lamina target cell ensembles known as `cartridges'. The two remaining photoreceptor axons (R7 and R8) project beyond the lamina to establish connections within the columnar units of the medulla (illustrated in Fig. 1.3). An amazingly complex pattern of local circuitry within the lamina distributes the six R1–R6 axon

terminals of each ommatidial unit to six adjacent cartridges. This elaborate circuitry improves the optical performance of the compound eye by `focusing' each cartridge on one point in the visual field (reviewed in (Kunes, 2000) .

A constant feature of this complex circuitry is an exact numerical match of ommatidia, lamina cartridges and medulla columns. This match is achieved by regulating the size of the optic ganglia in relation to the eye. At the outset, the axons from an ommatidium grow together as a fascicle into the lamina target field. Because eye development is a temporal affair, beginning at the posterior edge of the eye disk and progressing anteriorly, ommatidial fascicles arrive in the brain in a posterior-to-anterior temporal order. Their arrival in a retinotopic posterior-to-anterior order drives lamina development from the posterior to the anterior of the target field (Selleck and Steller, 1991). Retinal axons arrive at the anterior margin of the lamina target field and induce neuronal precursors (lamina precursor cells, or LPCs) to undergo a terminal cell division and assemble into a column sandwiched between adjacent retinal fascicles. In older (more posterior) cell columns, each ommatidial fascicle selects postmitotic LPCs to form a cartridge ensemble containing five lamina neurons. The arrival of retinal axon fascicles also elicits the differentiation of lamina glia (Winberg et al., 1992) and their migration into the lamina target field (Perez and Steller, 1996). The differentiation of lamina cartridge neurons is followed by ‘axon shuffling’; as the fascicle splits up to form its intricate pattern of connections in adjacent cartridges. A fascicle forms no (permanent) synaptic connections with the cartridge neuron ensemble that it has induced (reviewed in (Kunes, 2000).

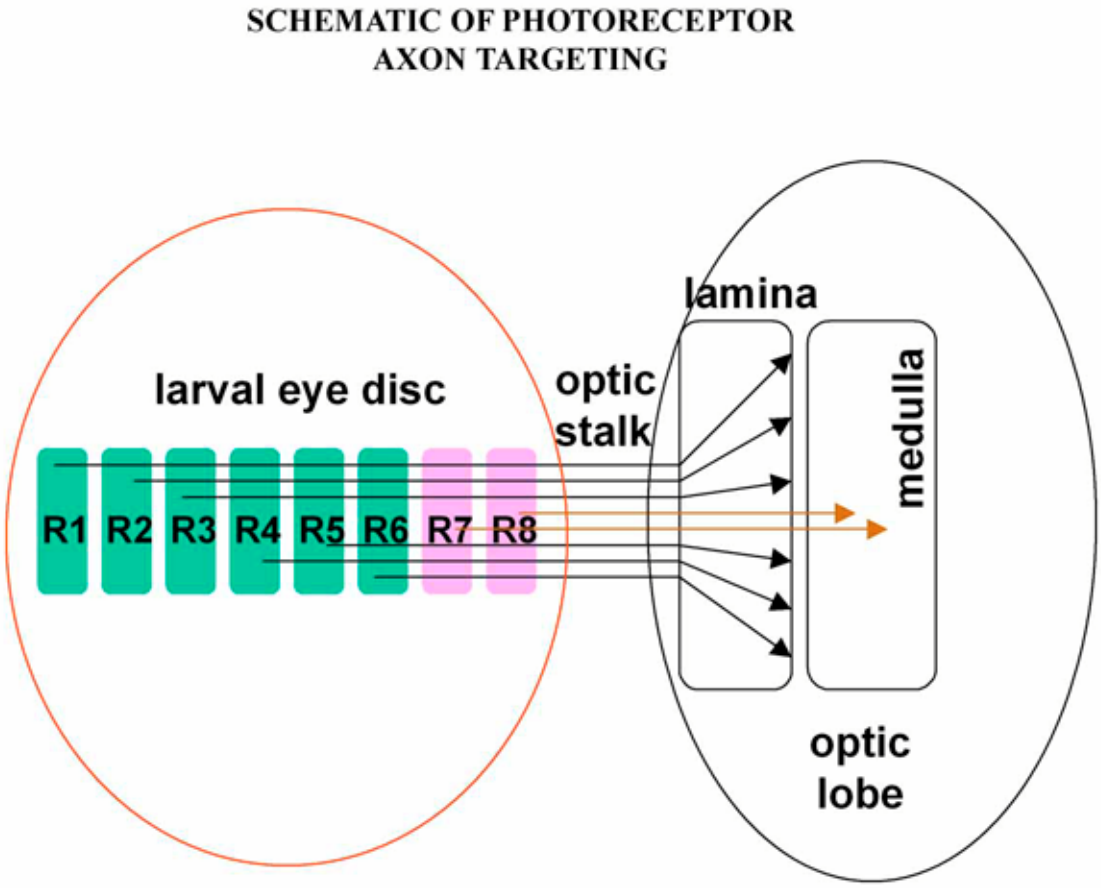

Fig. 1.3: Schematic of photoreceptor axons targeted from the eye disc to the optic lobe

The axons from the photoreceptors are targeted to the optic lobe. The above figure shows a cartoon of a third instar larval optic lobe with the eye disc attached to it. For simplicity only a single ommatidium is shown in the with eight photoreceptor neurons is shown in the eye disc. The outer six photoreceptors R1-R6 are shown in green, whereas the inner two photoreceptors R7 and R8 are in pink.
The outer six photoreceptor cells (R1-R6) send their axons through the optic stalk to the outer neuropile of the optic lobe, the lamina. While, the inner two photoreceptors (R7, R8) send their axons to the inner neuropile of the optic lobe, the medulla.

1.4.5. Molecules involved in photoreceptor axon guidance

Both histological and behavioural screens have identified many molecules involved in photoreceptor axon guidance. The photoreceptor cells are highly amenable to genetic manipulation. This is due to the intensive study of pattern formation and cell fate determination in the developing eye and the availability of an impressive battery of genetic techniques in *Drosophila*. These techniques allow one to specifically manipulate R cell genotypes through both gain and loss-of-function studies in an otherwise wild-type animal (Lee et al., 2001; Newsome et al., 2000). Markers for different classes of axons facilitate both genetic screening for targeting mutants and phenotypic analyses. That different R cells mediate different visual behaviours forms the basis of behavioural screens for mutations disrupting patterns of R cell connections.

Many genetic screens utilised histological methods in the third instar larval stage to assay R cell axons as they project to their targets. These screens focused on genes whose functions were required in R cells and whose mutant phenotypes did not affect R cell fate specification (Garrity *et al.*, 1996; Martin *et al.*, 1995). Later screens allowed for making mutant clones only in the eye and looking at their affect on the R cell axons (Newsome *et al.*, 2000b). Some of the genes identified in histological screens include the transcription factor *brakeless*, mutants of which give rise to strong targeting defects in R1-R6 neurons. Experiments on *brakeless* mutants suggest that *brakeless* and *runt* act in a pathway controlling genes regulating signalling systems in the growth cone that recognise targeting determinants produced by lamina glia (Rao *et al.*, 2000; Senti *et al.*, 2000). Most of the other molecules found in these screens are cell surface associated molecules like the receptor tyrosine phosphatase

PTP69D. These screens also identified mutations affecting an evolutionarily conserved signal transduction pathway in R cell growth cones. These include *dreadlocks* (*dock*), *p21 activated kinase* (*Pak*), and *Trio* (Garrity et al., 1996; Hing et al., 1999; Newsome et al., 2000). Mutations in these genes result in complex phenotypes with highly disorganised projections into the optic ganglia, including abnormalities in both local topographic mapping and in target specificity. *Dock* encodes the fly homologue of Nck, an SH3/SH2 adaptor protein. *Pak* encodes a kinase that binds to Dock and regulates the actin cytoskeleton downstream from the activated Rho family GTPases Cdc42 and Rac. *Trio* encodes a Rho family guanine nucleotide exchange factor that activates Rac.

Behavioural screens have also been applied to the isolation of R cell targeting mutants (Clandinin et al., 2001; Lee et al., 2001). These screens unearthed mutations affecting N-cadherin, which was identified in screens for R1-R6 and R7 mistargeting. N-cadherin is a classical cadherin, which possesses a cytoplasmic domain that physically interacts with β-catenin and, though its extracellular domain differs considerably from vertebrate N-cadherin, it too mediates homophilic cell adhesion. N-cadherin plays multiple roles in regulating axon guidance in the embryo (Iwai *et al.*, 1997). N-cadherin is widely expressed in R cell axons and their target neurons in the lamina and the medulla. Removal of N-cadherin from all R cells gives rise to a complex phenotype arguing for multiple roles in regulating R cell connectivity. Mutations in the gene encoding Lar (homologous to human leukocyte homology antigen-related receptor tyrosine phosphatase), were also identified in behavioural screens for defects in both the R1-R6 and R7 neurons and in

histological screens for defects in R7 connectivity. The phenotypes of *lar* mutant R1-R6 neurons and R7 neurons projecting into a wild-type target are largely indistinguishable from *N-cadherin* mutants. It is suggested that Lar could regulate N-cadherin interactions, or alternatively, it could act in a pathway parallel to it (Clandinin et al., 2001; Maurel-Zaffran et al., 2001).

1.4.6. Role of Bif and PP1 in photoreceptor axon guidance

Chapter 4 in this thesis deals with the elucidation of the functional significance of the interaction between PP1 and Bif in photoreceptor axon guidance. I show here that Both Bif and PP1 have a photoreceptor axon guidance phenotype and the interaction between Bif and PP1 is required for normal guidance in the larval optic lobe.

1.5. Process of anchoring and maintaining molecules to the cortex of a cell

1.5.1. Process of anchoring molecules

Cytoskeletal anchoring of proteins regulates cell shape and restricts the activity of ion transport proteins to specialised membrane domains. The association of actin filaments with the plasma membrane provides stability and maintains cell shape and adhesion. A number of integral membrane proteins anchor actin filaments and the cortical cytoskeletal network to the plasma membrane (Sastry and Burridge, 2000). The F-actin cytoskeleton in turn is required for anchoring molecules to the cortex as is seen in the case of asymmetrically localised proteins in *Drosophila* neuroblasts (Broadus and Doe,

1997). This anchoring of molecules as a means to generate asymmetry is an integral part of the development of the organism right from very early stages.

1.5.2. *Drosophila* as a system used for studying this process

Various cell biological systems are used to look at the cytoskeleton and its associated proteins. The *Drosophila* neuroblasts and oocytes are two very well studied cell biological systems. It has been well documented that the asymmetric localisation of molecules in neuroblasts is required for the normal formation of the neurons (progeny of the NB) (Knoblich, 2001; Kraut *et al.*, 1996). It has been shown that disruption of the F-actin cytoskeleton using drugs like cytochalasin D and Latrunculin A, causes the disruption of cortically localised proteins like Staufen, Inscuteable and Prospero (Broadus and Doe, 1997). Although it has been thought that F-actin may be one of the most important anchoring proteins required for normal anchoring of asymmetrically localised molecules at the cortex of the *Drosophila* oocyte (Cha *et al.*, 2002), this has not yet been clearly demonstrated. The process of cortical anchoring of molecules is essential for normal development, however there are not many anchors as yet known which are required to attach various cortical proteins to the cortex. In the fly, anchoring of Oskar (Osk) to the posterior cortex of oocyte, although an essential process is not very well understood. Recent data suggests that the ERM protein *Dmoesin* which is an actin binding protein is required for normal Osk anchoring to the posterior cortex of the oocyte (Baum, 2002; Jankovics *et al.*, 2002; Polesello *et al.*, 2002). One reason that the process of anchoring of molecules to the oocyte is not well understood could be because the molecules required for the anchoring process are required for other

processes earlier in oocyte development. My work sheds some light on the process of anchoring of Osk to the posterior of the oocyte and the role of Bif, Homer (Hom) and F-actin in this process.

1.6. *Drosophila* oogenesis

1.6.1. Introduction to *Drosophila* oogenesis

Female flies have an ovary that is made up of smaller units called ovarioles that are present from stage 2 through to stage 14 (schematised in Fig. 1.4A). Each ovariole is made up of an oocyte and 15 nurse cells, two stages are illustrated in Fig. 1.4B and C (Spradling, 1993). The entire process of oogenesis is essential to give rise to a normal embryo. *Drosophila* oogenesis begins with the division of a germline stem cell to form a 16-cell cyst, where ring canals interconnect the cells. One of the 16 cells becomes the oocyte and the others become polyploid nurse cells. Proteins are processed in the nurse cells and enter the anterior region of the oocyte (eg. Staufen). Similarly RNA like *bcd, osk* and *grk* RNA enter the anterior of the oocyte and some of them move towards the posterior of the oocyte or towards the dorsal region of the oocyte. These molecules are essential to give rise to the normal polarity of the oocyte and later on the anterior/posterior and dorsal/ventral patterning of the embryo. Many of the RNA and proteins required for the normal polarity of the oocyte are deposited into the embryo as maternal effect genes hence making them very essential for normal fly development. Therefore, the process of oogenesis is very important for normal fly development (Spradling, 1993).

Oogenesis is also a good system to study cell biology as the oocyte is relatively thin, stains easily and can be easily viewed under the microscope. It

is also relatively large and shows very distinct protein localisation patterns, which are easily seen on staining with proteins and RNA, localising to the anterior or posterior of the oocyte cortex.

1.6.2. Establishment of anterior/posterior polarity in the *Drosophila* oocyte

Polarisation of the *Drosophila* egg begins during oogenesis and is completed before fertilisation. Asymmetries along the Anterior/Posterior (A/P) axis are established during two distinct stages of oocyte development. The first polarisation phase occurs early in oogenesis, during the process of oocyte specification. Later in oogenesis, the egg is repolarised, and it is during this second polarisation that A/P determinants assume their final positions along the A/P axis (Riechmann and Ephrussi, 2001).

One of the 16 cells of the early 16-cell cyst stage adopts the fate of the oocyte. It has been hypothesised that this process occurs due the asymmetric distribution of a membranous organelle called the fusome. The cell that inherits the most fusome material is thought to become the oocyte (de Cuevas and Spradling, 1998; Lin and Spradling, 1995). Differentiation of the oocyte is a gradual process that depends on the accumulation of several determinants, such as Oo18 RNA-binding protein (Orb) (Lantz *et al.*, 1994), which travel to the oocyte on a polarised microtubule network that forms in a fusome-dependent manner throughout the cyst. The determinants initially accumulate at the anterior side of the oocyte and later shift to the posterior, coincident with relocalisation of the oocyte microtubule organising centre (MTOC) to the posterior. This redistribution marks the first polarisation phase of the oocyte

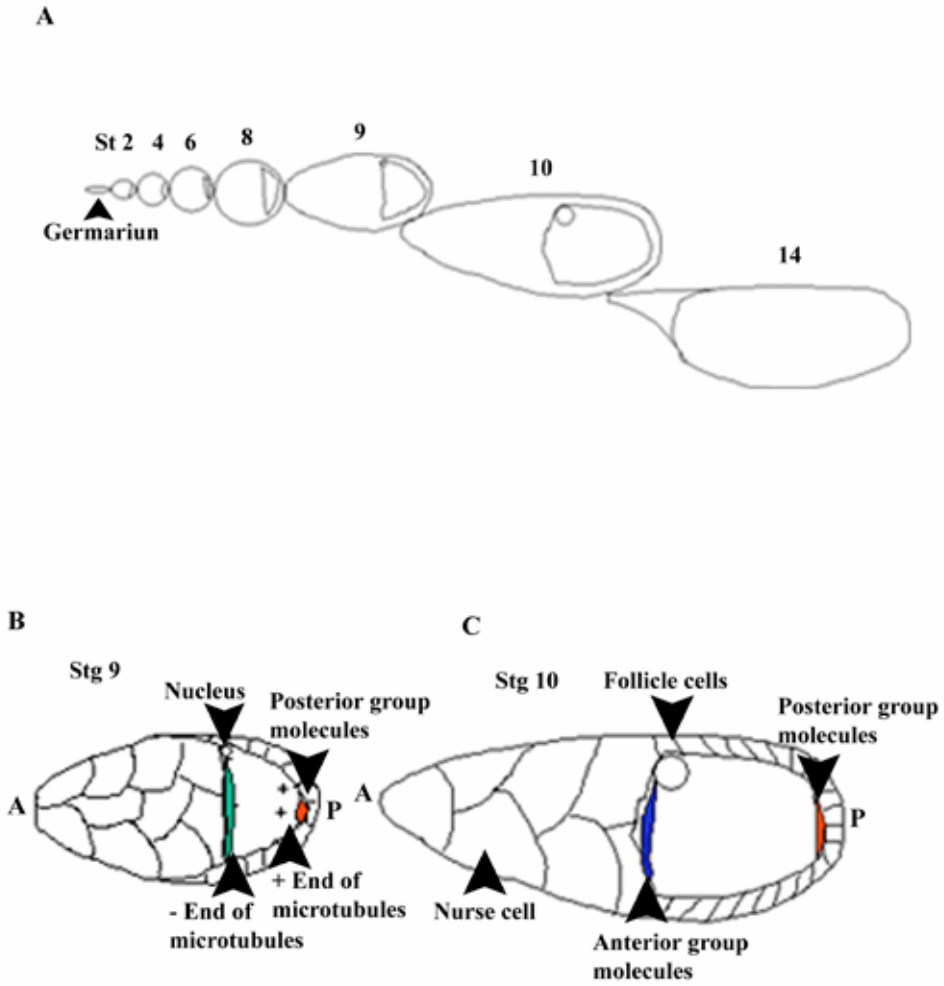

Fig. 1.4: Cartoon of *Drosophila* oogenesis

Panel A shows a cartoon of the stages of *Drosophila* oogenesis. The egg chamber is assembled in the germarium and emerges as a stage 2 egg chamber. It then grows and matures until stage 9 and 10 when the nurse cells rapidly transport their cytoplasmic contents into the oocyte. Finally, by stage 14, the fully developed egg is ready for fertilisation.

Panel B shows a stage 9 ovariole with a nucleus on the anterior dorsal margin, posterior group genes are towards the posterior cortex, the '+' end of the microtubules is towards the posterior and the '-' end of the microtubules is towards the anterior side. The follicle cells surrounding the oocyte and the nurse cells are also seen. Panel C shows a stage 10 ovariole. At this stage the oocyte is bigger and the follicle cells and nurse cells are larger and more prominent. In both B and C- A denotes the anterior side of the oocyte and P the posterior side of the oocyte.

and appears to be coupled to stable establishment of oocyte fate (reviewed in (Navarro *et al.*, 2001).

Drosophila Partitioning defective-1 (Par-1) localises to the fusome and becomes restricted to the future oocyte in a microtubule dependent manner. In *par-1* null mutants, oocyte selection is delayed or does not occur at all, suggesting that Par-1 may be one of the fusome-associated factors that participates in oocyte selection. Par-1 is also required for polarisation of the new oocyte: in the absence of Par-1, the Microtubule Organisation Centre (MTOC) and Orb never relocalise to the posterior, Orb eventually disappears, and the oocyte reverts back to the nurse cell fate. The *Drosophila* homologues of *par-3* (*bazooka*, *baz*), *par-4*, *par-5*, *par-6*, and *Atypical Protein Kinase C* (*aPKC*) are also required for anterior-to-posterior translocation of oocyte markers and for maintenance of oocyte fate. In *Drosophila*, localisation of Par-1 to the fusome is independent of Baz, Par-6, and Par-5. In the oocyte, Par-1 initially accumulates in the anterior and relocates to the posterior during polarisation. In *baz* mutants, Par-1 is present early in the anterior but is lost after polarisation and never appears in the posterior, suggesting that Baz may regulate Par-1 localisation at this stage. The reverse, however, is also true: Baz disappears from oocytes in *par-1* mutants. In established oocytes, Baz and Par-1 occupy complementary cortical domains, but the importance of this localisation, which is observed after oocyte polarisation, is not yet known. Hence the *par* genes in *Drosophila* function together to create a polarised axis (Cox et al., 2001a; Cox et al., 2001b; Huynh et al., 2001a; Huynh et al., 2001b; Pellettieri and Seydoux, 2002).

After oocyte specification, somatic follicle cells surround the 16-cell cyst. The oocyte is positioned at the posterior end of the cyst, in direct contact with follicle cells on all sides except at its anterior end, where it remains connected to the nurse cells via ring canals. This arrangement permits two essential processes. First, messenger RNA's (mRNAs) encoding determinants important for embryonic development (e.g., *bicoid* and *oskar*) are transcribed in the nurse cells and transported into the oocyte via the ring canals. Second, the oocyte and the follicle cells exchange signals that define both the A/P and dorsal/ventral (D/V) axes. In particular, follicle cells at the posterior end of the cyst send a signal that repolarise the oocyte and a new microtubule network at the posterior is formed to localise *bicoid* and *oskar* RNA's to opposite poles of the oocyte (Riechmann and Ephrussi, 2001).

1.6.3. Osk localisation during *Drosophila* oogenesis

There are many molecules including the cytoskeletal molecules like F-actin and microtubules, which are required for normal oocyte development. The process of Osk localisation at the posterior of the oocyte is very important for normal oogenesis. Briefly, Stau and *Osk* RNA bind at the anterior region of stage 9 oocyte and they move towards the posterior region of the oocyte. This process is a microtubule dependent process and the plus end directed microtubule motor, Kinesin is required to move *Osk* RNA from the microtubule rich anterior and lateral regions to the posterior cortex. The decreased density of microtubules at the posterior subsequently allows *oskar* access to the cortical actin network specifically in this region, thereby promoting its posterior localisation (Cha *et al.*, 2002). This process is thought

to be regulated by Par-1 (Huynh et al., 2001a; Tomancak et al., 2000). Once at the posterior cortex, *Osk* RNA gets tethered to the posterior cortex where it gets translated to give rise to Osk protein. This occurs because translational inhibitors like Bruno are removed from the *Osk* RNA, Stau complex allowing for the translation of *Osk*, at the posterior cortex. Osk has two isoforms the long and the short Osk isoforms. The process of movement of *Osk* RNA and Stau complex is preceded by the change in polarity of the microtubules from positive end at the anterior in stage 8 oocytes to positive end at the posterior in late stage 8 early stage 9 oocytes. Recent studies suggest that once Osk protein is tethered to the posterior cortex of the oocyte, the kinase Par1 phosphorylates it. The phosphorylated Osk isoforms are then stabilised and anchored to the cortex; the longer isoform is required for the normal anchoring of Osk to the cortex. Once Osk is normally anchored to the posterior cortex, it allows for more *Osk* RNA and Stau get to the posterior cortex. Hence allowing for this process to be an effective feedback mechanism (Kim-Ha *et al.*, 1995; Riechmann *et al.*, 2002; Rongo *et al.*, 1995; St Johnston *et al.*, 1991; Vanzo and Ephrussi, 2002).

1.6.4. Introduction to Homer

Homer (Hom) is an Ena Vasp homology (EVH) protein that has been shown to interact with F-actin in *in vitro* assays (Cai, 2002; Shiraishi *et al.*, 1999). The protein has an EVH domain at the N-terminal and a coiled- coil domain at the C terminal. Homer in mice has 2 isoforms (the longer b-Homer and the shorter a-Homer isoforms which bind each other *in vitro*) that have been shown to be required for normal glutamate receptor clustering at the

synapses (Brakeman *et al.*, 1997). It has also been shown to be required for normal retinotopic axon targeting in *Xenopus*. However, in *Drosophila* there is just one isoform of Homer (equivalent of the Homer b isoform) present and null mutations in *hom* appear not to show any obvious defects. The mutants however show defects in mating behaviours and movement. *Drosophila hom* mutants show hyperactive movement and mating activity (Diagana *et al.*, 2002; Foa *et al.*, 2001).

1.6.5. Role of Bif and Homer during oogenesis in flies

In Chapter 5 of this thesis, I show that although *bif* and *hom* mutants by themselves are viable and fertile, the *bif; hom* double mutants are largely sterile and show defects in anchoring posterior molecules to the cortex of the oocyte. In this chapter I further show that when F-actin is disrupted in a *hom* mutant background it gives rise to more severe defects in anchoring of molecules to the oocyte cortex as opposed to the defects seen in the absence of just an intact F-actin cytoskeleton.

The work in this thesis focuses on the function of Bif and its interacting partners in three different developmental contexts in the fly. These are –

i. Interaction between Bif and PP1 during adult eye development.
ii. Interaction between Bif and PP1 in the larval stages and the requirement of this interaction for normal photoreceptor axon guidance.
iii. Interaction between *bif* and *hom* during fly oogenesis.

Chapter 2

Materials and Methods

All chemicals and reagents were obtained from BDH Laboratory supplies (UK) and Sigma Chemical Company (USA) unless otherwise stated. Restriction enzymes and DNA modifying enzymes were purchased from New England Biolabs and Roche

2.1. Molecular work

2.1.1. Recombinant DNA methods

General recombinant DNA methods were performed essentially as previously described (Sambrook and Russell). Polymerase Chain Reaction (PCR) was done with Taq DNA polymerase. Restriction enzyme digestions were performed using appropriate buffers supplied by the manufacturers. Blunt ending of DNA fragments was carried out using Klenow DNA polymerase (large fragment). Dephosphorylation of DNA fragment was done using calf intestinal phosphatase (CIP). T4 DNA ligase was used for ligation of DNA fragments. Double-stranded DNA sequencing was performed with automatic PCR-based Big-Dye sequencing method.

2.1.2. Strains and growth conditions

The *E. coli* strain DH5α (GIBCO BRL, USA) was used throughout this study for all cloning procedures. *E. coli* cells were either cultured in LB broth (1% bacto-tryptone, 0.5% bacto-yeast extract. 1% NaCl pH 7.0) or maintained or LB agar plates (LB containing 1.5% bacto-agar) at 37^{o}C. When recombinant

plasmid-containing cells were cultured, the media was supplemented with 100µl/ml of Ampicillin.

2.1.3. Cloning strategies and constructs used in this study

In most cases, when the cDNA molecules were obtained by PCR amplification, they were first cloned into cloning vector pBlueScript (pBS from Stratagene), before being cloned into other vector such as expression vectors and transgenic vectors. A brief summary of PCR cloning is as follows:

The PCR product was first separated on an appropriate agarose gel. The product was then recovered from the agarose gel using Qiaquick gel extraction kit according to the manufacturers instructions (Qiagen, Germany). The DNA was then dissolved in 26µl elution buffer. The PCR product was then digested with required enzymes (most of the constructs made in this study had EcoRI and Xho I sited engineered in the PCR products). At the same time the vector (initially pBS and later the required vector) was cut with the same enzymes and treated with Calf intestinal phosphatase. The vector was recovered after CIP treatment using Qiaquick gel extraction kit. This was the protocol used to make most of the constructs used in the F-actin binding assay, they were then cloned into the *pGADT7* vector. The only exception was the 1st 500 amino acids of Bif cloned into the *pGADT7* vector. In this case both the vector and insert from the *pUAST-bif* vector were both cut with EcoRI and ClaI and the 500bp insert was ligated into the *pGADT7* vector.

Ligation of the insert with vector was s*et al*ong with ligase buffer and ligase enzyme. This reaction was done overnight at 16^{o}C. Transformation of

the ligation mixture was then done using heat shock transformation or electroporation transformation method.

List of DNA constructs used in this study:

DNA Constructs	Source	Reference
UAS-*bif*$^{+}$	N. Helps	(Helps et al., 2001)
UAS-*bif*^{F995A}	N. Helps	(Helps et al., 2001)
UAS-*bif*^{10Da}	N. Helps	(Helps et al., 2001)
pGADT7-bif (amino acids 1-1196-Full length)	K. Babu	Unpublished
pGADT7-bif (amino acids 1-500)	K. Babu	Unpublished
pGADT7-bif (amino acids 400-1196)	K. Babu	Unpublished
pGADT7-bif (amino acids 800-1196)	K. Babu	Unpublished
pGADT7-bif (amino acids 800-950)	K. Babu	Unpublished
pGADT7-bif (amino acids 900-1050)	K. Babu	Unpublished
pGADT7-bif (amino acids 800-900)	K. Babu	Unpublished
pGADT7-bif (amino acids 950-1050)	K. Babu	Unpublished
pGADT7-bif (amino acids 1000-1196)	K. Babu	Unpublished
pGADT7-bif (amino acids 1000-1063)	K. Babu	Unpublished
pNB-oskar7	W. Saxton	(Brendza *et al.*, 2000)
pBS-bicoid	W. Saxton	(Brendza *et al.*, 2000)
GST-Homer	Y. Cai	(Cai, 2002)
GST-Staufen S3	Y. Cai	(Li *et al.*, 1997)
GST-Staufen S1	Y. Cai	(Li *et al.*, 1997)

2.1.4. Transformation of *E. coli* cells

2.1.4.1. Preparation of competent cell for heat shock transformation

400ml of LB was inoculated with 10ml DH5α culture (that was grown overnight). The cells were shaken vigorously at 37°C until the OD_{600} was about 0.5 (approximately 2 hours). The cells were then harvested by centrifugation in 50ml falcon tubes at 4°C and spinning at 3,500 rpm for 5 minutes. The cell pellet was then resuspended in 20ml of ice-cold Buffer A (10 mM MOPS, 10 mM RbCl, pH7.0) and centrifuged as before. The cell pellet was then gently resuspended in 20ml of Buffer B (100 mM MOPS, 50 mM $CaCl_2$, 10 mM RbCl, pH 6.5) by inverting each tube. The cells were chilled on ice for 15 minutes and the pellet was resuspended in 5ml of ice-cold Buffer B containing 10% volume of glycerol. These cells were then snap-frozen in aliquots of 200µl and stored at –80°C.

2.1.4.2. Heat shock transformation of *E. coli*

The competent cells were thawed on ice, and 10 µl of the ligation reaction mix was added and the cells kept on ice for 30-45 minutes. The cells were then heat shocked at 42 °C for 60 seconds in a water bath. And then chilled on ice for 1 minute. The cells were then recovered in 1ml of LB lacking antibiotic at 37°C for 1 hour. They were then briefly spun and resuspended in 100µl of LB. The cells were then spread on LB agar plate containing the appropriate antibiotic.

2.1.4.3. Preparation of competent cells for electroporation

A litre of LB was inoculated with 10 ml DH5α culture that was grown overnight. The cells were shaken vigorously at 37°C until the OD_{600} reached about 0.9-1 (about 4 hours). The cells were chilled on ice for 30

minutes, and centrifuged in a cold SS34 rotor for 15 minutes at 3000 rpm at 4°C. The supernatant was then removed and the pellet resuspended in 1:l cold deionised water. This was followed by another round of centrifugation as was done previously and the pellet was resuspended in 500ml of cold water and centrifuged again. The supernatant was then removed and the pellet resuspended in 20-30 ml of cold 10% glycerol. Another round of centrifugation followed this step. The supernatant was then removed and the pellet was resuspended in 2-3 ml of cold 10% glycerol. Aliquots of 50µl were made and snap-freezed and stored at –80°C.

2.1.4.4. Electroporation transformation of *E. coli*

The electrocompetent cells were allowed to thaw on ice. 1-2µl of ligation reaction was added to the cells and mixed gently. The mixture was then kept on ice for 1 minute and then transferred to a cold, 0.2 cm electroporation cuvette. The Gene Pulser Apparatus (Biorad) was set to 25µF and 2.5 kV. and the Pulse Controller set to 200 Ω. The cell suspension was knocked to the bottom of a cuvette and a pulse applied with a time constant of 4 to 5 msec and field strength of 12.5 kV/cm. 1 ml of LB was added to the cells immediately after electroporation and this was followed by transfer of the suspension to a 1.5 ml eppendorf tube. The cells were then incubated at 37°C for 1 hr, with occasional shaking and plated on selective medium.

2.1.5. Plasmid DNA preparation

2.1.5.1. Plasmid Miniprep

A 3ml LB culture was set up and the cells were shaken vigorously for 8-12 hours at 37°C. The cells were then collected in 1.5 ml eppendorf tubes and spun at maximum speed (14,000 rpm) in microfuge for 30 sec. The cells were resuspended in 350 µl of STET buffer (8% Sucrose. 50mM Tris pH 8.0, 50mM EDTA, 0.5% triton X-100) and boiled for 2-4 minutes on a heat block. This is followed by centrifugation of the cell lysate at 14,000 rpm for 10 minutes. The pellet was then removed with a sterile toothpick and the supernatant was retained. An equal volume of isopropanol (350 µl) was added to each tube prior to mixing by vortexing. Each tube was then centrifuged at 14,000 rpm for 5 minutes at room temperature. The supernatant was then discarded and the pellet air-dried. The DNA pellet was then dissolved in 50µl of TE-RNAse and used for restriction enzyme digestion or double-stranded DNA sequencing.

Alternatively, plasmid minipreps of bacterial cultures (1-3ml) were also carried out using the QIAprep Miniprep kit from QIAGEN according to manufacturer's instructions. This system is based on alkaline lysis. DNA purity with this method is higher than that in STET boiling method, however, STET boiling method is more rapidly manipulated.

2.1.5.2. Plasmid Midi/Maxiprep

Plasmid midi/maxipreps of bacterial cultures (500 ml) were performed with the Qiagen Plasmid Midi/ Maxi Kit using Qiagen-tip 100/500 resin columns. These plasmid purifications that are based on alkaline lysis procedure, were carried out according to the manufacturer's protocol.

2.1.6. PCR reactions and Primers used in this study

PCR was performed using a reaction mixture containing 1µl of template DNA (50ng), 1µl of thr N-terminal primer (100ng/µl), 1µl of the C-terminal primer (100ng/µl), 10ml of dNTPs (2.5mM each), 10 µl of PCR buffer, 76 µl of double distilled water and 1 µl of Taq polymerase enzyme mix. The reaction cycles carried out using a thermocycler (Perkin Elmer) were 25 cycles of 94^{o}C for 30s, 60^{o}C for 30s and 72^{o}C for 1 min/1kb of DNA. The DNA bands required were isolated on standard DNA gels.

List of primers used in this study:

DNA Constructs	5' and 3' Primer sequences (read 5'-3' direction)
pGADT7-bif (amino acids 1-1196-Full length)	5'- CGGAATTCATGGAGTCACAGAAGCGGC 3'- CCGCTCGAGATATAGCAAATCCGTTTTCTGTGTA
pGADT7-bif (amino acids 400-1196)	5'- CGGAATTCATGAACAGCCAGGTGCGTG 3'- CCGCTCGAGATATAGCAAATCCGTTTTCTGTGTA
pGADT7-bif (amino acids 800-1196)	5'- CGGAATTCATGAGCCAGGGAGCCGGG 3'- CCGCTCGAGATATAGCAAATCCGTTTTCTGTGTA
pGADT7-bif (amino acids 800-950)	5'- CGGAATTCATGAGCCAGGGAGCCGGG 3'- CCGCTCGAGCGACGTCTCCACGGAGAGA
pGADT7-bif (amino acids 900-1050)	5'- CGGAATTCATGAACACCTCGATGGTGTTCAAC 3'- CCGCTCGAGCTGCTCCAGCTCCAGCTG
pGADT7-bif (amino acids 800-900)	5'- CGGAATTCATGAGCCAGGGAGCCGGG 3'- CCGCTCGAGCTCTGTGGAATGAAGGCT
pGADT7-bif (amino acids 950-1050)	5'- CGGAATTCATGACGGACACGGACTACGACG 3'- CCGCTCGAGCTGCTCCAGCTCCAGCTG
pGADT7-bif (amino acids 1000-1196)	5'- CGGAATTCATGACGCTGACGTCGACGTTTGAA 3'- CCGCTCGAGATATAGCAAATCCGTTTTCTGTGTA
pGADT7-bif (amino acids 1000-1063)	5'- CGGAATTCATGACGCTGACGTCGACGTTTGAA 3'- CCGCTCGAGCAACGGTAAATTCCCCAGCCATC
Homer primers (used to check for *hom^{LL17}* mutant)	5'- ATGGAATTCTTCAGCAACAGGGG 3'- CTGCTTTTAATTAAATAAACCGAATTC

2.2. Biochemistry

Frequently used buffers and solutions

2x SDS gel-loading buffer	100 mM Tris HCl pH 6.8, 200 mM dithiothreitol (DTT), 4% SDS, 0.2% bromophenol blue, 20% glycerol. Add DTT (1 M stock) before use.
10x Tris-glycine electrophoresis (PAGE) buffer, pH 8.3	30.2 g Tris, 188 g glycine, 50 ml 20% SDS, add distilled water to 1000 ml.
Resolving Gels for Tris-glycine SDS-Polyacrylamide Gel Electrophoresis (PAGE)	Required amounts of 30% acrylamide mix and deionised water, ¼ vol. 1.5 M Tris (pH 8.8), 0.01 vol. 10% SDS, 0.01 vol. 10% ammonium persulphate (APS), 0.0008 vol. TEMED.
Stacking gels for PAGE	0.68 vol. H_2O (deionised), 0.17 vol. 30% acrylamide, 0.125 vol. 1.0 M Tris (pH 6.8), 0.01 vol. 10% SDS, 0.01 vol. 10% APS, 0.001 vol. TEMED.
Western transfer buffer, pH 8.3	3.03 g Tris, 14.4 g glycine, 200 ml methanol, add distilled water to 1000 ml (do not adjust pH).
Blocking solution	PBS, 3% skimmed milk powder, 0.05% Triton X-100.

2.2.1. PAGE and western blotting of protein samples

10-20μg of protein extracts were mixed with equal volume of 2X SDS loading buffer and boiled for 6 minutes, after which the sample was loaded on the gel. Electrophoresis was carried out in a minigel apparatus (Biorad) at 50 V for 20 minutes and subsequently at 100 V for 1.5-2 hours. Transfer onto a Hybond C-extra nitrocellulose (Amersham) membrane was carried out in a Trans-Blot Electrophoretic transfer cell from Biorad. The transfer was performed at 100 V for 1.5 hr in the cold room. A magnetic stirrer was used to recirculate the transfer buffer.

2.2.2. Immunological detection of proteins

The membrane was blocked overnight at 4°C in blocking solution. It was then incubated in primary antibody diluted in blocking solution for 3 hours at RT. This incubation is followed by 7 washes in PBT (PBS, 0.1% Triton) for 5-7 minutes per wash. The membrane was then incubated in secondary anti-mouse and anti-rabbit IgG antibodies coupled with HRP (Immuno Jackson), at a dilution of 1:2000 in blocking solution, for 1 hour. The membrane was then washed as before and the antibodies bound to the membrane were detected by chemiluminescence using the ECL system from Amersham

2.2.3. Immunoprecipitation experiments

Ovaries were dissected and stored on ice before lysis in a buffer consisting of: 20mM Tris-HCl (pH 7.4), 150mM NaCl, 1mM EDTA, 1mM EGTA, 1% Triton X-100, 2.5mM sodium pyrophosphate and protease inhibitors (Sigma). These ovaries were then treated by grinding and passing through 21G needles. The lysates were then centrifuged at 4^{o}C for 15 minutes. The supernatant was used for co-IP (this involves treating lysate with the Ab used in the immunoprecipitation for 2 hours followed by treating with sepharose G beads for 3 hours, all at 4^{o}C).

The IP's were then subject to western blotting using standard protocols described above. The blot was then probed with Antibodies to see if two or more proteins are present in the same complex *in vivo*. Equal numbers of ovaries were taken for IP's in the presence and absence of Lat A and were stained in a normal coomasie gel to check for similar protein concentrations in the presence and absence of Lat A treatment.

2.2.4. *In vitro* actin binding assay

G-actin (Sigma) solution was first made in sterile water (approx. 0.1mg per experiment). 50µl of this solution was taken and 6µl of 10X buffer (2mM Tris-Cl pH=8.0, 0.2mM of $CaCl_2$, 0.2 mM ATP, 50mM KCl, 2mM $MgCl_2$ and 0.5mM mercaptoethanol, volume was made up to 1ml with sterile water) was added to the G-actin. This was left for 90 mins at room temperature with rolling and 24µl of 2M KCl was then added to this solution with mixing. The solution was then left standing at 4^oC for 60 minutes.

The required concentration of *in vitro* translated product (product was obtained using the *in vitro* translation kit from Promega, as per manufacturers instructions) was added to 30µl of the above mixture to make up the volume to 50µl. The proteins and actin were allowed to mix at room temp for 60 minutes, and spun in an airfuge for 40 minutes.

Equal volumes of the supernatant and pellet (dissolved in 50µl of water) were run on a SDS protein gel after adding the loading dye. The gel was then dried and exposed to an X-ray film to see bands where F-actin interacted with the *in vitro* translated protein. Controls were done with no actin, using water in place of actin solution.

2.2.5. GST-fusion protein expression

A single clone was picked and inoculated in 2ml culture media (LB + Amp) and allowed to grow over night. 50ul of this culture was then inoculated into 1ml LB+ Ampicillin. The culture was then grown till it reached an OD_{600} of 0.6-0.8 (2-3 hours). IPTG was added to induce protein expression and culture was grown for a further 3-4 hours at 37degree. The entire culture was

then spun down and resuspended in 250µl of 2XSDS buffer and boiled for 10 minutes. This was then run on a SDS-Page gel to normalise protein loading amounts.

2.2.6. RNA probe labelling

About 4-10µg of the required construct was digested with enzyme for 2-4 hours to get complete digestion. A gel was then run to recover the digested fragment in RNAse-free water. The labelled anti-sense RNA probe was then synthesised using Promega Riboprobe *in vitro* transcription system for T3 and T7 RNA polymerase, according to the manufacturers instructions. The reaction was then allowed to incubate at 37^{o}C for 90-120 minutes. RNAse free RQ1 was added for 15 minutes to remove any DNA template. This was followed by addition of 2µl 4M LiCl and100ul Ethanol, followed by precipitation at –20^{o}C for at least 30 minutes and then spinning the reaction mixture at 12K rpm for 15 minutes. Remove the supernatant and dissolve the pellet in 100-200 µl RNAse-free H_2O and store at –20 degrees.

2.2.7. North-western blotting

Two identical SDS-PAGE gels were run (one for loading control for coomasie staining). One of the gels was Electro-transferred on to a membrane. The proteins on the membrane were then denatured by treating the membrane with 8M Urea for 15 minutes. The proteins were then allowed to slowly renature by incubation in stepwise dilution of 8 M Urea in Tris-buffered saline (TBS: 10 mM Tris PH8.0, 150 mM NaCl) 2:3 vol/vol for 15 minutes each incubation. The membrane was then rinsed in TBS. This was followed by

blocking in 25 mM NaCl/ 10 mM $MgCl_2$/ 10mM Hepes, pH8.0/ 0.1mM EDTA/ 1mM DTT/ 5% skim non-fat milk for 1 hr at 4 degrees, and hybridisation in 50 mM NaCl/ 10mM $MgCl_2$ 10 mM Hepes, pH8.0/ 0.1 mM EDTA/ 1 mM DTT/ 2.5% skim non-fat milk (solution A) with labelled the RNA probe ($1X10^6$ cpm/ml). After hybridisation the membrane was washed thrice with solution A, 15 minutes per wash. The blot was then exposed to an X-ray at –70 degree overnight. And the film was then developed.

2.3. Immunohistochemistry and microscopy

Frequently used reagents and buffers for immunohistochemistry

PBS (Phosphate Buffer Saline)	130mM NaCl, 7mM Na_2HPO_4, 3mM NaH_2PO_4, pH 7.5
PBT	PBS, 0.1% Triton X-100 unless otherwise specified
20 % paraformaldehyde solution (PFS)	Add 20 g paraformaldehyde into 100 ml PBS, neutralise with 200 µl 10 M NaOH and dissolve at 65°C (keep for about 2 weeks at 4°C).
4% paraformaldehyde fixative (PFF)	Mix 0.8 ml 20% PFS with 3.2 ml 0.1 M HEPES pH 7.4 or PBS. Prepare fresh fixative each time.
HRP staining solution	1 ml 0.1 M Na acetate pH 6.0 (optional 2.5% $NiNH_4SO_4$), 50 µl DAB (5 mg/ml), 10 µl glucose (0.2 g/ml), 2 µl NH_4Cl (0.2 g/ml), 1-2 µl glucose oxidase (2 mg/ml)
TO-Pro3 DNA dye	1:5000-7000 (Molecular probes)

2.3.1. Fixing of eye discs and larval brains

Eye discs and brains of crawling 3rd instar larvae as well as 55 hour pupal eye discs were dissected in PBS on a petridish and fixed in 4% PFF or methanol free formaldehyde (from Polysciences Inc.) on ice for 30 minutes.

Fixation was performed in 1.5 ml Eppendorf tubes. After fixing these tissues were washed in 5 changes of PBT.

2.3.2. Fixing *Drosophila* ovaries

Ovaries were dissected in PBS and fixed for 30 mins at RT in 4% methanol free formaldehyde or 4% freshly made PFF. They were then washed 5 times in PBT (PBS and 0.1% Tween-20). These fixed ovaries were then separated into ovarioles and could then be stained as desired.

2.3.3. Fixing of embryos

Embryos were first rinsed in PBT and dechorionated with 50% bleach/50% PBT for 2-3 minutes, and then washed in PBT. The embryos were then transferred to scintillation vials containing 5ml 4% PFF and 5ml heptane, and were fixed by shaking vigorously for 15 minutes. The lower fixative phase was then removed and 5ml methanol added. The vials were shaken vigorously for 30-60 seconds to devitellinise the embryos. The devitellinised embryos sank to the bottom. Embryos were then collected and washed in 3 changes of ethanol. Embryos in ethanol were stored at –20°C. Prior to immunostaining, the embryos were rehydrated by giving them 3 washes in PBT for 10 min/wash.

2.3.4. Antibody staining of fixed tissues

The tissues were first blocked in PBT, 3% BSA or goat serum for at least 30 minutes. They were then incubated with primary antibody in PBT, 3% BSA or goat serum for 2 hr at RT or overnight at 4°C. In case of phalloidin staining, TRITC labelled phalloidin (Sigma) was added to the blocking solution

or after blocking at 1:200 dilution in PBT for 2 hours at RT or Alexa-488 or 568 phalloidin (Molecular Probes) was used at 1:250 dilution in PBT at RT. Phalloidin was also added again with the secondary antibody. The tissue was washed thrice in PBT for 10 minutes/wash. And then incubated in secondary antibody (HRP (1:150), FITC labelled secondary antibody (1:150) or Cy3 labelled secondary (1:750) from Jackson Laboratory or Alexa fluor secondary antibodies at light wavelengths 488, 543 and 633 (from Molecular Probes) in PBT, 3% BSA or goat serum for 2 hr at RT. The washing procedure was repeated after the secondary antibody incubation. In some cases the DNA staining dye To-Pro3 was added at 1:5000 to 1:7000 dilution to the last wash. Fluorescently labelled samples were mounted in Vectashield (Vector Laboratories).

2.3.5. Microtubule staining in oocytes

The ovaries were dissected in 1X Ringers solution (130mM NaCl, 4.7mM KCl, 1.9mM $CaCl_2$ and 10mM Hepes pH 6.9) and then fixed with 100µl fixing buffer (1ml MSB (100mM KH_2PO_4/K_2HPO_4 pH 6.9, 450mM KCl, 150mM NaCl, 5mM $MgCl_2$ and 10mM EGTA), 2.8ml 10% formaldehyde (methanol free) and distilled water to make the final volume 6ml) and 600µl heptane. The fixing was done for 5 minutes with gentle rocking. The fixative was then removed and the ovaries were washed thrice with PBS and thrice with PBT, with each wash lasting for 5 to 10 minutes. The ovaries were then incubated for 2 hours at room temperature in PBT. The ovaries were then teased apart into ovarioles and incubated with PBS and 1% triton-X 100 for 2 hours at room temperature. The tissues were then blocked with PBT-BSA (1%

BSA in PBT) for 2 hours at room temperature. The blocking solution was then removed and the ovarioles were incubated with FITC conjugated anti tubulin antibody (anti-α tubulin monoclonal DM1A-FITC conjugate from Sigma) in PBT-BSA. The Antibody was used at 1:10 dilution and the incubation was done overnight at 4^{o}C. The tissues were then washed with PBT-BSA for 2-3 hours at room temperature with changes in the wash solution every 15-20 minutes. This was followed by washing with PBT, twice for 15 minutes/wash and then with PBS for 10 minutes. The PBS was then removed and the sample mounted in Vectasheild and viewed under the confocal.

2.3.6. Antibodies used in this study

Antibody	Dilution	Source	Reference
Sheep Anti-Bifocal	1:1000	P. Cohen	(Helps et al., 2001)
mAb 24B10	1:3	Developmental Hybridoma	(Fujita *et al.*, 1982)
Anti α-tubulin (FITC Conjugate)	1:10	Sigma	
Mouse Anti β-Galactosidase	1:300	Promega	
Rabbit Anti β-Galactosidase	1:3000	Cappel	
mAb Dachshund	1:1000	G. Mardon	(Mardon et al., 1994)
Rabbit Anti-Reverse Polarity	1:500	G. Technau	(Halter *et al.*, 1995)
Rabbit Anti-Protein Phosphatase-1	1:1500	P. Cohen	(Helps et al., 2001)
mAb 22C10	1:4	Developmental Hybridoma	(Zipursky *et al.*, 1984)
Mouse Anti-Homer	1:2000	Y. Cai and F.Yu	(Babu *et al.*, 2004)
mAb Drop 1.1	1:500	T. Karr	(Karr, 1991)
Rabbit Anti-Vasa	1:2000	P. Lasko	(Lasko and Ashburner, 1990)
Rabbit Anti-Staufen	1:2000	D. St Johnston	(St Johnston *et al.*, 1991)
Rabbit Anti-Oskar	1:3000	A. Ephrussi	(Markussen *et al.*, 1995)
mAb Gurken	1:10	T. Schupbach	(Queenan *et al.*, 1999)

2.3.7. Scanning electron microscopy of the *Drosophila* eye

For scanning of adult eyes, the heads were fixed, washed, dehydrated with ethanol in accordance with the protocol described in (Kimmel *et al.*, 1990). Briefly the protocol is as follows:

Whole adult flies were anaesthetised with CO_2 and then dehydrated through a graded ethanol series with a 24 hour incubation in each step. The heads of the flies were then separated from the rest of the body. The fly heads were then equilibrated with the low surface tension solvent Freon 113 (Ted Pella, Inc.) by passing the sample through a graded Freon 113 series in 100% ethanol, with a 24 hour incubation in each step. After the last incubation the fly heads were air-dried and mounted onto SEM stubs. They were then sputter coated with platinum coat. The samples were then visualised under a scanning electron microscope-Jeol JSM 5600 LV

2.3.8. Transmission electron microscopy of the *Drosophila* eye

For transmission electron microscopy, adult heads were embedded in eponresin and processed in accordance with published protocols (Tomlinson and Ready, 1987) with minor modifications. The protocol is as follows:

Fly heads were fixed for 1 hour in 1% Glutaraldehyde in 250mM Hepes buffer pH 7.4. After a 3, 5 minute buffer washes, tissues were postfixed in 2% Osmium tetraoxide and 1.5% Potassiumferricyanide in distilled water for 1 hour at room temperature. After 4, 10 minute washes in distilled water the heads were dehydrated through a graded alcohol series. After 100% alcohol the tissues were treated with 50% propylene oxide, twice for 10 minutes. The

heads were then transferred to 50% propylene oxide and 50% eponresin. This mixture was left overnight at 4^{o}C. The fly heads were then embedded in pure eponresin for 48 hours at 56^{o}C and polymerised. Ultrathin sections were then made and collected on Formvar-coated slot grids.

The ultrathin sections were counterstained with lead citrate and uranyl acetate (briefly- The grid was treated with uranyl acetate for 5-8 minutes and then washed 5 times with distilled water. Lead citrate was then added to the grid for 1 minute and this was washed with distilled water as below. The water was then removed using a whatman filter paper). The sections were then visualised under a Transmission electron microscope- Jeol JEM 1220.

2.3.9. Sectioning and staining of the *Drosophila* brain

Fly heads were fixed in 2.0% formaldehyde and 0.05% Triton X-100 in PBS at 4^{o}C for 60-90 minutes. Before fixing the proboscis was removed. The tissues were washed in PBS and transferred to 12% sucrose in PBS at 4C for 16 hours. This allowed for the sucrose solution to infiltrate the tissue. The fly heads were then removed from the sucrose solution and submerged in a drop of O.C.T. Tissue Tek Compound (Miles Scientific). The O.C.T. compound was allowed to permeate the tissue for 10-30 minutes at room temperature. The heads were then embedded in frozen O.C.T. compound using an ethanol-dry ice bath. The heads were oriented upright in the block, so that the ocelli were pointing towards the microscope objective. Slow freezing by periodic immersion of the block support in a dry ice/ethanol bath allowed several heads to be precisely positioned in a single block with fine forceps.

The frozen block containing the tissue to be sectioned was placed in a cryostat chamber for at least 20 minutes to equilibrate it to the cryostat temperature (-14^{o}C to –18^{o}C). 10 μm sections of the fly head were cut on the cryostat and loaded onto freshly gelatinised slides. The slides were dried for 5 minutes at RT.

The sections were immediately fixed in 0.5% formaldehyde in PBS for 20-60 minutes at room temperature. Slides could be stored in this fixative at 4C for a few days if necessary. The slides were washed two or three times for 5 minutes/wash in PBS. They were then blocked for 30 minutes in 1% BSA and 0.3% triton X-100 in 1X PBS (PBT-X). The slides were then washed through several changes of PBS/0.3% triton X-100 in 1X PBS. 75-150 μl of the primary antibody at the appropriate dilution in blocking solution was added to each slide, which were then incubate in the primary antibody overnight at 4^{o}C in a moist, airtight chamber. The slides were then washed through several changes of PBT-X and incubated with the secondary antibody at the appropriate dilution in blocking solution as was done previously for the primary antibody. For a HRP-conjugated secondary antibody, the slides were again washed through several changes of PBT-X and then incubated in 0.5ml of staining solution per slide. For the 24B10 Antibody the Vector Antibody amplification kit was used as per manufacturers instructions. After staining, the sections were mounted in glycerol and viewed. In case of fluorescent secondary antibodies the sections were mounted in Vectashield after washing after secondary antibody incubation.

2.3.10. *in situ* hybridisation on *Drosophila* oocytes

2.3.10.1. Making the probe for *in situ* hybridisation

The two constructs, pNB-*osk* and pBS-*bcd* (3-5µg each), were linearised using Hind III and Kpn I respectively. The digested templates were purified by phenol-chloroform method (this involves treating the digested DNA with phenol-chloroform, mixing and giving a 2 minute spin and removing the DNA layer, this process is repeated thrice, the DNA is then precipitated with $1/10^{th}$ the volume of NaCl and 2.5 times the volume of 100% ethanol and spun at high speed for 10 minutes and the supernatant removed and pellet air died) and the pellet was dissolved in 30µl RNAse free (DEPC treated) water. The labelling reaction was then carried out using the Roche DIG RNA labelling kit according to the manufacturers instructions. Of the 15µl of probe obtained at the end, 3-5µl of the probe was used per RNA *in situ* reaction.

2.3.10.2. *In situ* hybridisation

The ovaries were fixed in 4% formaldehyde (methanol free) for 30 minutes at room temperature and then washed 5 times in PBT (0.1% Tween 20), for 5 minutes each wash. They were then washed for 5 minutes in 1:1 PBT/hybridisation solution. This was followed by a 5 minutes wash in Hybridisation Solution. (50% formamide, 5x SSC, 0.1% Tween 20, 50 µg/ml heparin, 100 µg/ml salmon sperm DNA). The ovaries were then pre-hybridised in 700µl Hybridisation Solution at 70°C for at 1-2 hours, after which they were hybridised overnight in 100µl hybridisation Solution + Digoxygenin labelled probe (around 0.5ng/ml depending on the probe) at 70°C. The ovaries were then washed in hybridisation Solution for 20

minutes at 70°C. This wash was followed by a wash in PBT/hybridisation Solution 1:1 for 20 minutes at 70°C, and by 3, 20 minute washes in PBT at 70°C (last wash was done at room temperature). The ovaries were then incubated overnight at room temperature in HRP-conjugated Anti-Dig IgG (Roche) at 1:200 dilution. They were then washed thrice for 10 minutes/wash in PBT. This was followed by tyramide staining.

Tyramide staining: The tyramide reagent was diluted 1:30 in the amplification diluent provided with the TSA Fluorescein System kit (PerkinElmer Life Sciences, Inc.). The ovaries were then stained for 25 minutes in the dark. They were then washed thrice for 10 minutes/wash in PBT. The PBT was then removed, vectashield added and the samples were mounted.

For *in situ* Hybridisation coupled with Immuno Fluorescent staining the sample were processed as above but at 65°C instead of 70°C. After the washes after overnight hybridisation, the ovaries were incubated in HRP-conjugated Anti-Dig IgG at 1:200 dilutions in PBT (at room temperature) together with primary antibody, overnight. They were then washed twice for 20 minutes/wash in PBT. This was followed by incubation with secondary antibody in PBT for 1.5h (in dark). The ovaries were washed again followed by the tyramide staining step.

2.3.11. Cytoplasmic streaming assays on the oocyte

4-6 day old female ovaries were dissected in halocarbon oil and the ovarioles separated. The separated ovarioles were then transferred onto a slide with a drop of halocarbon oil and a cover slip places over the oocytes. This

preparation was immediately taken to the confocal microscope and the cytoplasmic granules were viewed under 488nm light. Their movement is recorder by doing a time series at the confocal microscope.

2.3.12. Confocal analysis and image processing

Stained and mounted tissue samples were analysed with a Zeiss Axiophot microscope. Photographs were taken with an attached 35 mm camera or using a Kontron Prog Res 3012 digital camera (Kontron Elektronik) connected to a Personal Computer. The fluorescently labelled tissue samples were visualised using confocal microscopy using the MRC1024 laser scanning microscopes from Biorad or the Zeiss LSM510 confocal. All digital images were processed using Adobe Photoshop.

2.4. Drug Treatments

Dissected ovaries were rinsed with 0.9% NaCl and treated with Latrunculin A (Molecular probes) at a final concentration of 20-100μM in NaCl and 50% octane (v/v) for 30 mins, and then rinsed with heptane. Cytochalasin D (Sigma) was used at a concentration of 20μg/ml for 15 mins. Treatments involving Latrunculin A and cytochalasin D were done consecutively with 40μM Lat A for 30 mins followed 20μg/ml CD for 15 mins or vice versa. Following treatment, ovaries were fixed and stained as above. For the FISH hybridisation experiments after Latrunculin A treatment, some ovaries in the treated and untreated experiments were stained with phalloidin after fixing while the rest of the ovaries were processed for FISH.

2.5. Fly genetics

2.5.1. Fly stocks used in this study

Fly stocks	Source	Reference
bif ^{R47} homozygous viable mutation in the X chromosome	S. Bahri	(Bahri *et al.*, 1997)
UAS-bif $^{+}$ on the 2nd chromosome	K. Babu	(Helps et al., 2001)
UAS-bif ^{F995A} on the 3rd chromosome	K. Babu	(Helps et al., 2001)
pGMR-GAL4 on the 2nd chromosome	M. Freeman	(Hay *et al.*, 1997)
24B-GAL4 on the 3rd chromosome	Bloomington (BL-1767)	(Brand and Perrimon, 1993)
bif ^{LH114} homozygous viable mutation in the X chromosome	S. Bahri	(Bahri *et al.*, 1997)
Ro^{tau} *lacZ/cyo*	U. Gaul	(Garrity et al., 1999)
UAS-bif ^{10Ba} on the 3rd chromosome	K. Babu	Unpublished
Rh1-τlacZ on the 2nd chromosome	B. Dickson	(Newsome et al., 2000b)
Rh4-τlacZ on the 2nd chromosome	B. Dickson	(Newsome et al., 2000b)
pp1 ^{e211}*/TM6*	P. Cohen and L. Alphey	(Axton et al., 1990)
pp1 ^{e078}*/TM6*	P. Cohen and L. Alphey	(Axton et al., 1990)
pp1 ^{hs46}*/TM6*	P. Cohen and L. Alphey	(Axton et al., 1990)
UAS-PP1-87B/TM6	L. Alphey	(Parker et al., 2002)
UAS-NIPP1/TM6	L. Alphey	(Parker et al., 2002)
UAS-I-2PP1 or *UASI2Dm* on the 2nd chromosome	L. Alphey	(Bennett *et al.*, 2003)
FRT-pp1 ^{e211}*/TM6*	K. Babu	Unpublished
FRT-pp1 ^{e078}*/TM6*	K. Babu	Unpublished
FRT-pp1 ^{hs46}*/TM6*	K. Babu	Unpublished
ptp10d^{1} homozygous viable mutation in the X chromosome	K. Zinn	(Sun et al., 2000)
pak6/TM6	N. Harden	(Hing et al., 1999)
ptp69d^{1}*/TM3*	Bloomington (BL-5088)	(Desai et al., 1999)
ptp69d/TM3	Bloomington (BL-5090) Deficiency uncovering *ptp69d*	(Desai et al., 1999)

hom^{LL17} homozygous on the 2nd chromosome	Y. Cai	(Babu *et al.*, 2004)
Osk-βGal on the 2nd chromosome	A. Ephrussi	(Vanzo and Ephrussi, 2002)
khc β-Gal on the 3rd chromosome	W. Saxton	(Brendza *et al.*, 2000)
moe^{G0415} on the X chromosome (deficiency)	Bloomington (BL-12015)	(Jankovics *et al.*, 2002)
moe^{EP1652} on the X chromosome	Bloomington (BL-11272)	(Jankovics *et al.*, 2002)
moe^{PL106}*-FRT101* on the X chromosome	F. Payre	(Polesello *et al.*, 2002)
ovo^{D2} *v*^{24} *P{w*$^{+mW.hs}$*=FRT(w*^{hs}*)}9-2/C(1)DX, y*^{1} *f*^{1}*/Y;hs-FLP*	Bloomington (BL-1843)	(Chou and Perrimon, 1996)

2.5.2. Germ line clones

To generate germline mutant clones the following protocol was used: Female virgin flies with mutations that were recombined with the FRT101 element were crossed with *ovo*^{D1}, FRT101; hs-FLP males. The flies were allowed to lay eggs for 24 hours at 25°C. A first heat shock was given at 72 hours of development for 1 hour at 37°C. A similar second heat shock was given at 96 hours of development and a similar third heat shock was given at 120 hours of development. The ovaries of the flies were dissected and stained 3 to 5 days after hatching of the fly during which time the females are mated.

2.5.3. Single fly PCR'S

A single fly was placed in a 0.5 ml tube and mashed for 5 - 10 seconds with a pipette tip containing 50µl of buffer (10 mM Tris-Cl pH 8.2, 1 mM EDTA, 25 mM NaCl, and 200 µg/ml Proteinase K, with the enzyme diluted fresh from a frozen stock each day) without expelling any liquid (sufficient liquid escapes from the tip). The remaining buffer was then expelled into the tube. This was then incubated at 25-37^{o}C for 20-30 minutes. This incubation

was then followed by heating the tube to 95°C for 1-2 minutes, which inactivates the Proteinase K. 0.5µl of the DNA from a single fly was then used for one PCR reaction.

In cases where *hom* mutants were recombined with markers, the recombinant events were scored by PCR. Single fly PCR's were performed with primers flanking the *hom* gene (in the list of primers section) and the mutant band was approximately 1.1kb where the wt band was approximately 3kb in size

2.5.4. Germ line transformation

For making transgenic flies, Full-length bif cDNAs were cloned into pUAST vector (Brand and Perrimon, 1993) and injected into embryos using standard procedures. F0 flies were crossed to *yw* flies and w^+ transformant progeny were collected and balanced. To ensure that these transgenes are capable of producing a Bif protein, several *bif* transformant lines were tested for expression by crossing to a mesodermal driver line, 24B-GAL4. 24B-GAL4 drives expression in the muscles where Bif it is not normally expressed. Bif expression in embryos was visualised using a primary anti-Bif antibody raised in sheep and HRP-conjugated secondary antibody.

For driving Bif expression in the eye, the pGMR-GAL4 driver, which allows Bif expression in many of the different cell types of the eye (Hay *et al.*, 1994) was used.

Chapter 3

Role of Bifocal in eye development and its interaction with Protein Phosphatase 1

3.1. Introduction:

The *D. melanogaster* eye is an excellent model system for the study of developmental processes at the cellular and subcellular levels. The adult compound eye comprises ~800 repeats of a basic unit referred to as an ommatidium, each of which contains eight photoreceptor neurons (R cells) and a fixed array of non-neuronal accessory cells. R cell development begins in the third instar larval eye disc and is completed by the end of the third instar larval stage (Dietrich, 1909; Ready *et al.,* 1976; Waddington, 1960). In the midpupal stage (~48h post puparium formation), each R cell projects to the centre of an ommatidium, a microvillar stack of membranes rich in rhodopsin, called the rhabdomere. The position of each rhabdomere depends on the class of R cell from which it is produced (Wolff, 1993). R7 cells project to the centre of the ommatidium and contact surrounding rhabdomeres of other R cells. R3 cells build their rhabdomere against the stalk of R2 and R4 cells, whereas R4 cells form contacts with rhabdomeres of R2 and R7 cells. Rhabdomere development is essentially completed at 110h of pupation (just prior to eclosion), by which stage they retract from the centre of the retina, leaving behind an interretinal space (Wolff, 1993). At the subcellular level, the rhabdomeral microvilli are supported by an axial actin cytoskeleton comprising of at least two actin filaments per microvillus (Arikawa *et al.*, 1990). The barbed ends of the actin filaments are located at the distal ends of the microvilli and the pointed ends project into the cytoplasm of the R cells.

The gene *bifocal* was previously identified in a P-element transposition screen; mutations in *bif* give rise to a rough eye phenotype (Bahri *et al.*, 1997). Externally, *bif* mutant eyes exhibit frequent fusion of adjacent ommatidia and loss or duplication of bristles. More detailed examination revealed alterations in normal rhabdomere development; they become enlarged and frequently split. At the subcellular level, disorganisation of the actin cytoskeleton is evident, actin staining becomes diffused and the interretinal space is absent.

Although the various defects seen in the *bif* mutant indicate that the molecule is required for the normal actin cytoskeleton in the eye, how Bif may function in the eye was largely unknown as were interacting partners of Bif. In this chapter I describe the *in vivo* interaction between Bif and a Protein phosphatase and elaborate on how this interaction is required for normal eye formation in *D. melanogaster*.

Reversible protein phosphorylation catalysed by protein kinases and protein phosphatases regulates the majority of cellular functions including many developmental processes. One of the most abundant eukaryotic protein phosphatases that dephosphorylate serine and threonine residues is Protein Phosphatase 1 (PP1), which exhibits pleiotropic functions (Bollen and Stalmans, 1992; Cohen, 1989; Shenolikar, 1994). The known diverse actions of PP1 reside in the ability of the catalytic subunit of PP1 (PP1c) to associate with different regulatory subunits *in vivo*, which may target the catalytic subunit to specific subcellular locations and often modify its substrate specificity. The activities of the various PP1 complexes may thus be regulated differentially by intra- and extracellular signals acting upon the different subunits. Over 25 different regulatory subunits of PP1c have now been identified. For example, in mammals glycogen binding subunits target PP1c to regulate the enzymes of glycogen metabolism and myosin subunits enable PP1c to regulate myosin

contractility (Hubbard and Cohen, 1993; Johnson et al., 1996; Tanaka et al., 1998). Binding of PP1c to scaffold proteins may modulate ion channel activity (Westphal *et al.*, 1999), while at neuronal synapses, neurabin I and II (also termed spinophilin) localise PP1c to the actin cytoskeleton at the plasma membrane (Allen et al., 1998; MacMillan et al., 1999; McAvoy et al., 1999; Satoh et al., 1998). Interaction of regulatory subunits with PP1c is mutually exclusive, an observation explained by the discovery that a short motif -(R/K)(V/I) X- (F/W)- present in the majority of these subunits is sufficient for binding to PP1c (Egloff *et al.*, 1997; Johnson *et al.*, 1996; Zhao and Lee, 1997). PP1c also binds to a number of small cytosolic inhibitor proteins including inhibitor-1 and inhibitor-2 (I-2), which inhibit PP1c activity at nanomolar concentrations (reviewed in (Cohen, 1989; Wera and Hemmings, 1995). In *Drosophila melanogaster,* widely distributed inhibitor-2 proteins as well as a testis specific inhibitor-2 like protein have been identified (Bennett et al., 1999; Helps and Cohen, 1999; Helps et al., 1998).

Of the six PP1 isoforms in *Drosophila,* the two genes on the X chromosome, share a lower degree of homology with the other four *PP1* genes, which are encoded at chromosomal loci 87B, 96A, 9C and 13C (Dombradi et al., 1990b; Dombradi et al., 1993). Null mutants at *pp1-87B* exhibit a lethal phenotype at the larval stage, failing to exit mitosis and showing over-condensed chromatin (Axton et al., 1990; Dombradi et al., 1990a). A yeast two-hybrid screen, conducted by Nick Helps and Patricia Cohen, for molecules interacting with PP1, identified Bifocal as one of the interacting partners of PP1-87B via the PP1 consensus-binding motif.

In this chapter, I show that an *in vivo* interaction between Bif and PP1 is probably essential for the role of Bif in normal ommatidia and bristle development in the *Drosophila* eye.

3.2. Results:

3.2.1. Bif interacts directly with Protein Phosphatase 1 (PP1)

Nick Helps and Patricia Cohen performed a yeast two hybrid screen using the mammalian PP1 as the bait and screening the *Drosophila* cDNA library. One of the interesting molecules they pulled out of this screen was Bif. Bif has a typical RVXF (RVQF) motif (residues Argenine, Valine, Glutamine and Phenyl alanine), that is present in more then 80% of PP1 interacting molecules (Egloff *et al.*, 1997) and when this motif is mutated to replace the F with an A, the strong interaction between Bif and PP1 no longer occurs (Helps et al., 2001). To see if this interaction is required *in vivo* I decided to see if the F to A mutated form of Bif could rescue the defects seen in the fly eye.

3.2.2. Interaction between PP1 and Bif is required for normal F-actin cytoskeleton during pupal stages

To elucidate the functional significance of this interaction *in vivo*, both wild type (wt) bif^{+} and a F995A mutated form of *bif* (bif^{F995A}), which does not bind PP1 *in vitro*, were introduced as transgenes in the pUAST vector (Brand and Perrimon, 1993) under the control of GAL4-*UAS* (Brand and Perrimon, 1993) into *bif* mutant flies.

To ensure that these transgenes are capable of producing a Bif protein, several *bif* transformant lines were tested for expression by crossing to a mesodermal driver line, 24B-GAL4. 24B-GAL4 drives expression in the muscles (Brand and Perrimon, 1993) where Bif it is not normally expressed (Fig. 3.1 A, B). A UAS-bif^{+} line expressing Bif in the muscles as well as a UAS-bif^{F995A} line that shows Bif expression in the muscles were selected for the rescue experiments.

These lines were further tested for expression of the transgene in the eye by driving the UAS-Bif transgenes using pGMR-GAL4, an eye specific driver (Hay *et al.*, 1994) in a *bif* mutant background and staining for Bif using an anti-Bif antibody that does not stain the mutant larval eye disc. Both the UAS-*bif* $^{+}$ and the UAS-*bif* ^{F995A} lines expressed the Bif protein in the larval eye disc, the expression of which is not seen in the *bif* ^{R47}mutants (Figs. 3.2 and 3.3), which deletes regions of exon 3 of *bif* (Bahri *et al.*, 1997).

At the subcellular level, *bif* mutations affect F-actin localisation, causing an abnormal pattern of F-actin distribution (Bahri *et al.*, 1997). In wt ommatidia from 55 hour pupal eye imaginal discs, F-actin is localised in a typical star-like pattern at the centre of each ommatidium with intense localisation at the microvillar tips of the rhabdomeres facing the central space (Longley and Ready, 1995) (Fig. 3.4 A). In *bif* null ommatidia of the same stage, the star like pattern of F-actin is no longer observable, and the F-actin staining shows an elongated and fused central region and decreased spacing in the centre of the eye (Fig. 3.4 B). The *pGMR-GAL4* mediated expression of *UAS-bif* $^{+}$ can rescue this defect whereas expression of *UAS-bif* ^{F995A} cannot (Fig. 3.4 C and D).

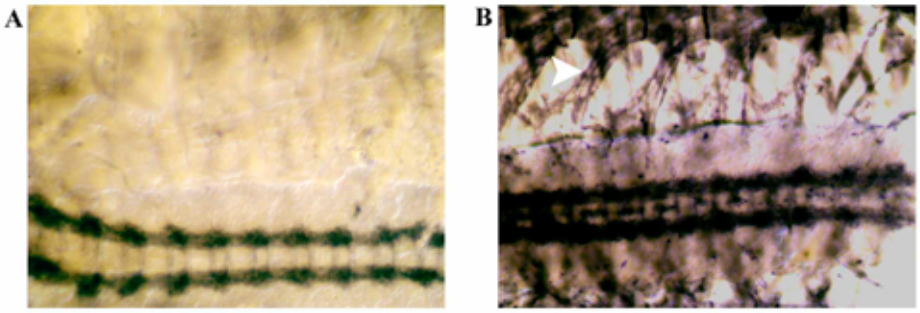

Fig. 3.1: Testing of *UAS-bif* expression in the *Drosophila* embryo using a muscle specific GAL4 driver
Anti-Bif staining of WT (A) and *UAS-bif,* overexpressed with the muscle driver *24B-GAL4* in WT background (B). Bif is expressed in the Ventral Nerve cord in WT embryos and no expression is seen in muscles. Overexpression of Bif in the muscles shows Bif expression in the muscles (arrowhead in B) as well as in the VNC as expected.

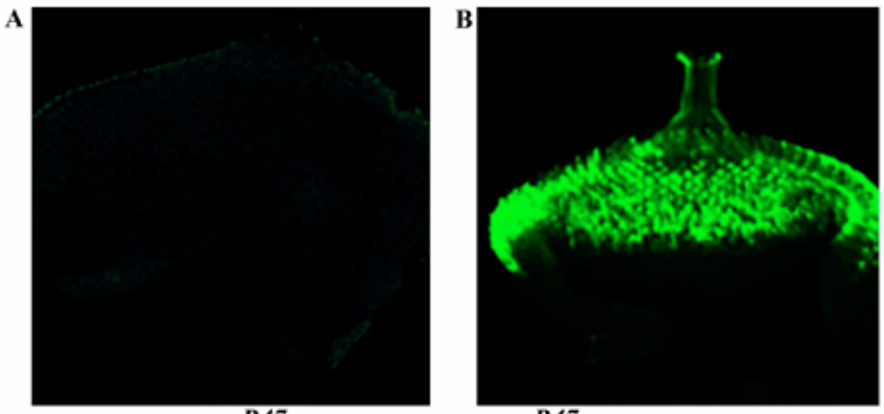

Fig. 3.2: Anti-Bif localisation in the larval eye discs of *bif* mutants and Bif overexpressed in the mutant background
Anti-Bif staining of *bif*^{R47} and *UAS-bif* driven by *pGMR-GAL4* in *bif* mutant background. *bif*^{R47} mutant eye discs do not stain with Anti-Bif antibody (A) indicating that the mutant line used is a protein null. The Bif overexpression lines expresses Bif in the mutant background (B) indicating that the *UAS-bif* construct expresses protein in the eye disc with a *pGMR-GAL4* driver.

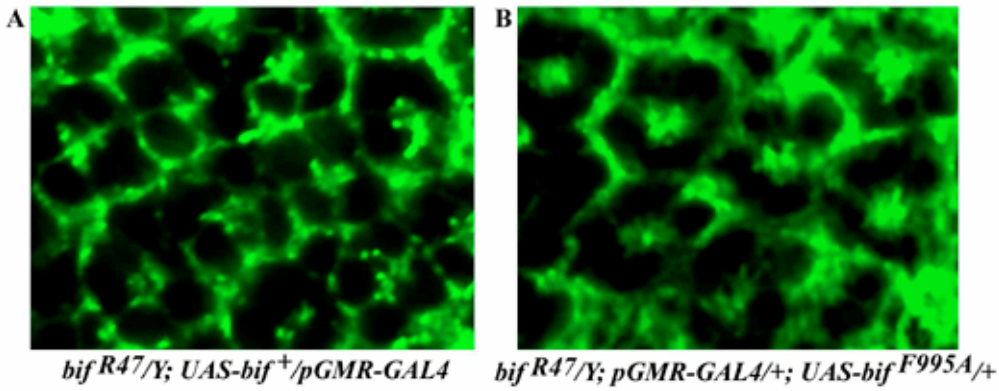

Fig. 3.3: Anti-Bif localisation in the *bif* mutant eye discs which have WT Bif or mutated Bif expressed under an eye specific promoter line
Anti-Bif staining of *UAS-bif*$^{+}$ (A) and *UAS-bif*^{F995A} (B) driven using *pGMR-GAL4* in the *bif* mutant background. Both the *UAS-bif* lines used in this study express Bif protein in the eye disc.

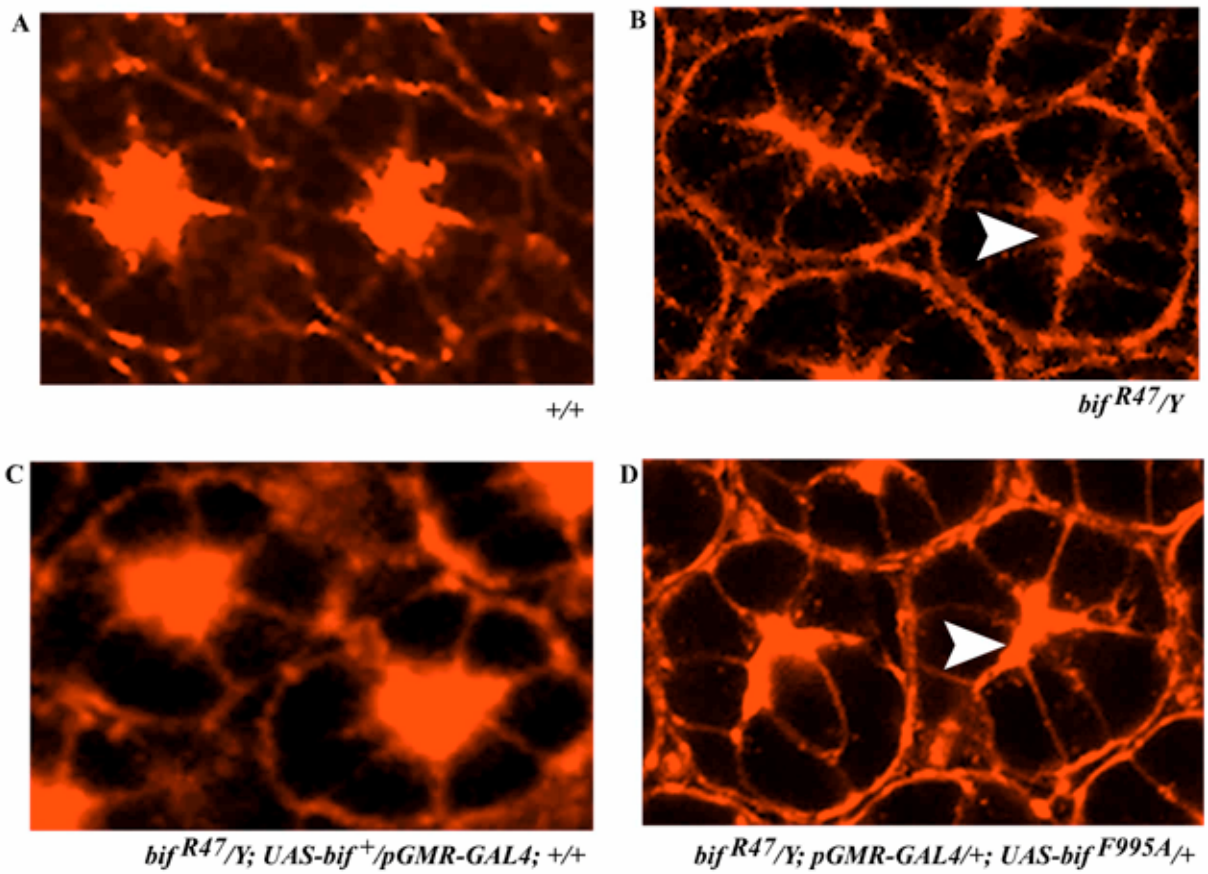

Fig. 3.4: Rescue of *bif* phenotypes seen in pupal eye discs
A-D are sections from 55 hour pupal eye discs stained with TRITC-labelled phalloidin. A shows a WT F-actin staining pattern revealing the organisation of rhabdomeres in the centre of the eye. B is a bif^{R47} mutant showing disorganised F-actin staining and merged rhabdomeres in the centre of the eye (arrowhead). C shows rescue of the *bif* pupal eye disc phenotype by ectopic overexpression of a WT *bif* transgene under control of the *pGMR* driver line. The expression of the bif^{+} transgene reverts the defective F-actin staining to an almost WT pattern. D shows ectopic expression of the F995A mutant form of the *bif* transgene under control of the *pGMR* driver line; The bif^{F995A} form of Bif fails to rescue the defective F-actin localisation pattern associated with bif^{R47} allele and shows a similar disorganised F-actin staining seen in bif mutants (arrowhead in D).

3.2.3. Interaction between PP1 and Bif is required for normal adult fly eye development

Homozygous and hemizygous deletions of the X-linked *bif* gene affect the morphology of the compound eye in *Drosophila* (Bahri *et al.*, 1997). Externally, the wt eye is comprised of ~800 ommatidia arranged in hexagonal shapes with bristles projecting from alternate ommatidial vertices (Wolff, 1993) (Fig. 3.5 A). In *bif* null adult eyes, adjacent ommatidia are often fused and bristles are short, missing or duplicated (Fig. 3.5 B). Expression of a wt *UAS-bif* $^{+}$ transgene in many of the cells of the ommatidia, using the *pGMR-GAL4* driver, rescues this *bif* mutant phenotype (Fig. 3.5 C), in contrast, expression of the *UAS-bif* ^{F995A} in a *bif* null mutant could not effect this rescue (Fig. 3.5 D).

Internally, the wt ommatidia contain eight photoreceptor cells (R1-R8), each of which projects into the centre a light gathering organelle called the rhabdomere. Rhabdomeres are round in shape and organised in an asymmetric pattern of seven with the R8 rhabdomere underlying the R7 rhabdomere so that the R8 rhabdomere is not visible at this plane of section (Wolff, 1993) (Fig. 3.6 A). In *bif* null mutants, the majority of rhabdomeres are enlarged, elongated and disrupted (Fig. 3.6 B). This phenotype could be partially rescued by pGMR-GAL4 driven expression of *UAS-bif* $^{+}$ (Fig. 3.6 C), however, pGMR-GAL4 mediated expression of *UAS-bif* ^{F995A} cannot rescue this defect (Fig. 3.6 D).

The observation that the rescue of the various *bif* mutant phenotypes by expression of *UAS-bif* $^{+}$ driven by pGMR-GAL4 is not always complete (see Table 3.1 for quantification of the rescue) could be attributed to several reasons. There are several alternatively spliced transcripts produced by the *bif* locus and more than one isoform could be required to show complete rescue; it could also be due to differences

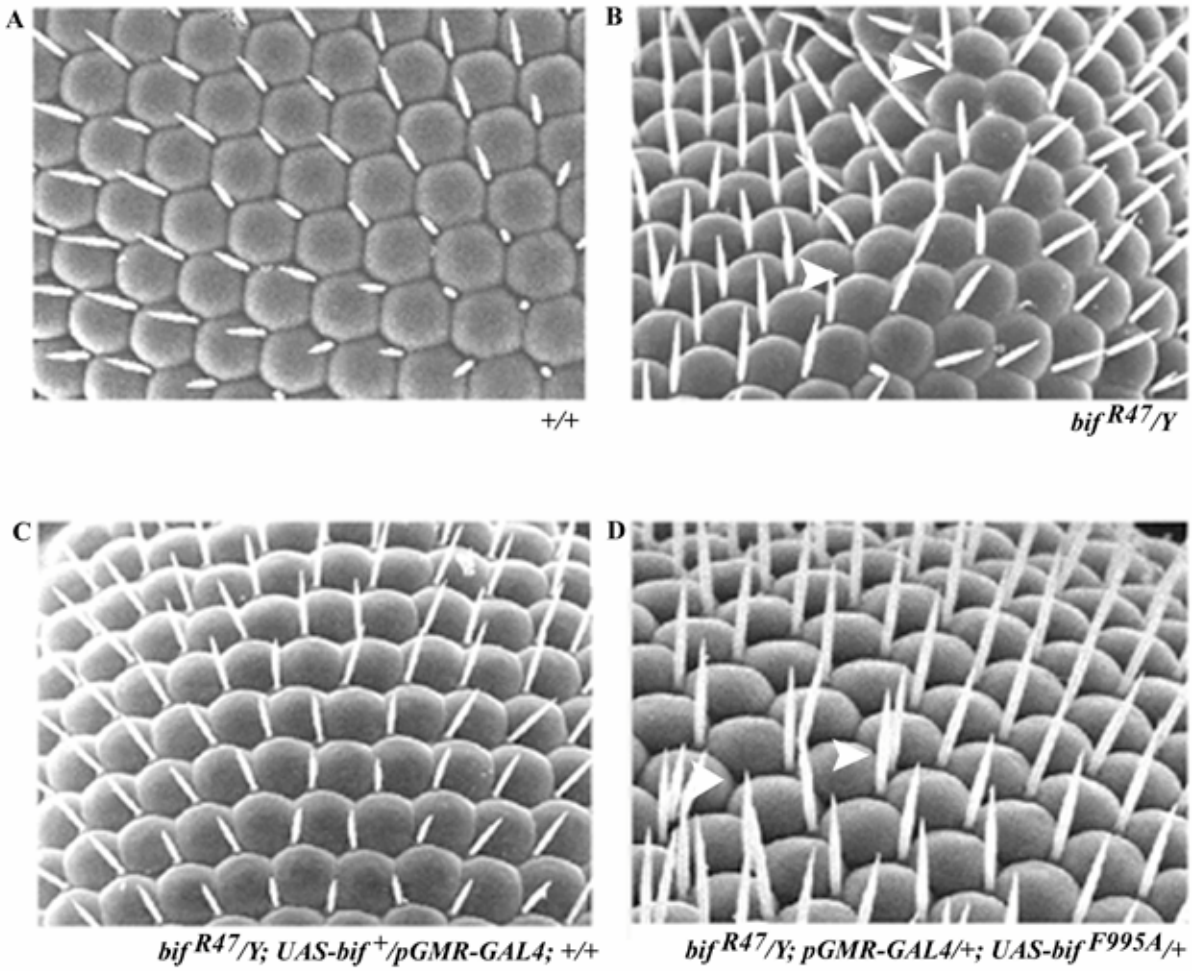

Fig. 3.5: Rescue of the bristle phenotype seen in *bif* mutants
A-D are scanning electron micrographs of adult eyes showing the organisation of ommatidia and bristles. A shows a region of a WT eye with its normal ommatidial and bristle organisation. B is a mutant bif^{R47} eye showing loss and multiplication of bristles phenotype (arrowheads). C shows rescue of the bif bristle phenotype by ectopic overexpression of a bif^{+} transgene under control of *pGMR* driver line; The expression of the WT *bif* transgene reverts the number and pattern of bristles in the mutant to almost WT. D shows ectopic expression of the F995A mutant form of the *bif* transgene under control of the *pGMR* driver line. The F995A mutant form fails to rescue any of the *bif* bristle phenotypes and shows missing and duplication of bristles similar to *bif* mutants (arrowheads in D).

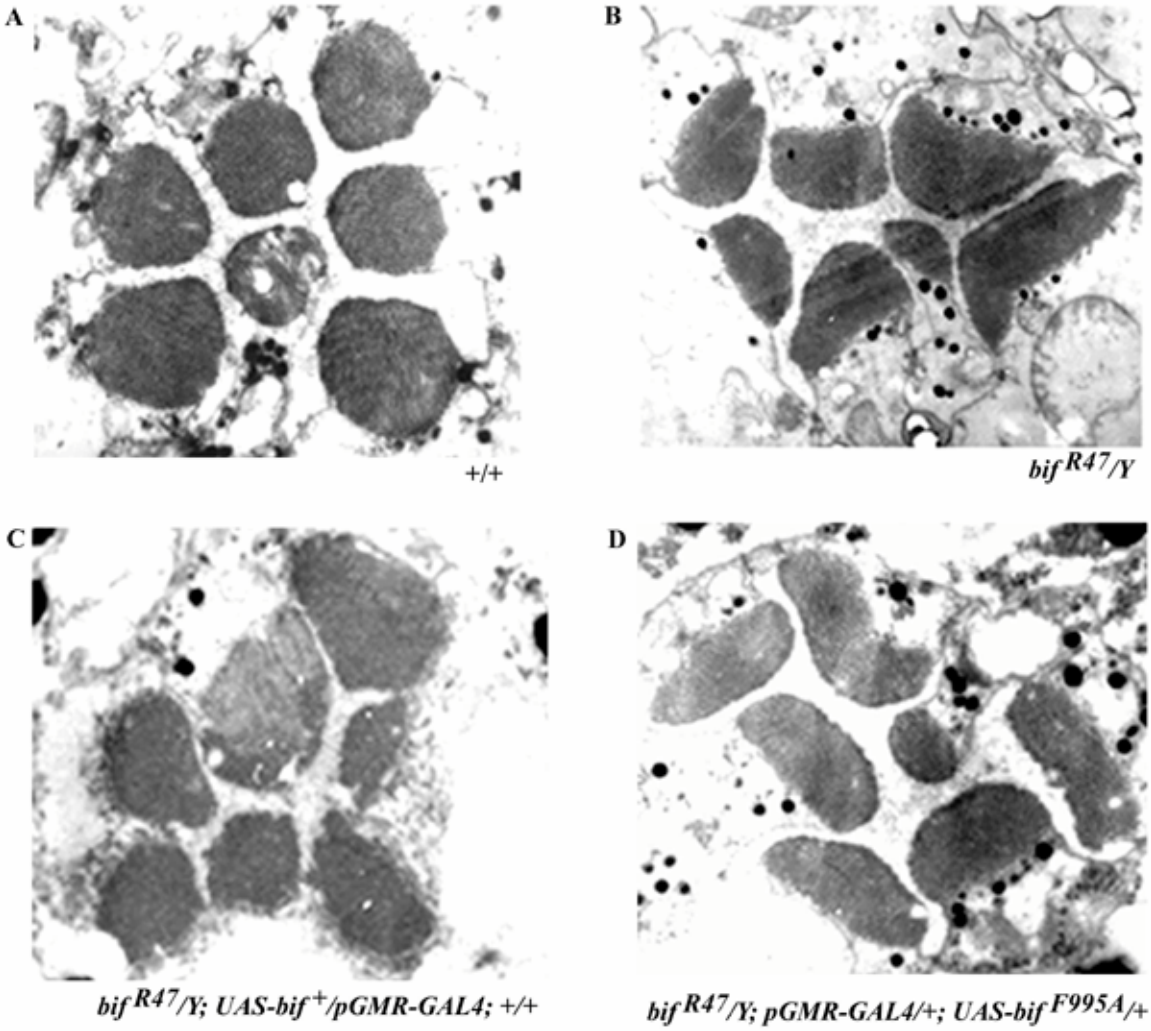

Fig. 3.6: Rescue of adult rhabdomere phenotypes associated with *bif* mutation
A-D are electron micrographs of dissected adult eyes. A shows 7 rhabdomeres of a WT ommatidium with their normal round shapes and ordered organisation. B shows a mutant ommatidium from the *bif*^{R47} allele; Note that the *bif* mutant rhabdomeres have abnormal shapes and irregular pattern of organisation. C shows rescue of the *bif* rhabdomere phenotype by ectopic overexpression of a WT *bif* transgene under control of *pGMR* driver line; The expression of the WT *bif* transgene reverted the shape and organisation of the mutant rhabdomeres to an almost WT pattern. D shows ectopic expression of the F995A mutant form of the *bif* transgene under control of the *pGMR* driver line; The *UAS-bif*^{F995A} mutant form fails to rescue any of the *bif* rhabdomere phenotypes.

between wt and *pGMR-GAL4*-driven levels and/or patterns of protein expression in the eye. Overall the levels of phenotypic rescue seen with the wt *bif* transgene are high whereas the *bif* ^{F995A} mutant transgene, which encodes a protein that cannot bind PP1 *in vitro* shows no obvious rescue.

Therefore, these *in vivo* results are consistent with the *in vitro* data and demonstrate that the PP1 binding motif present at the C-terminal of Bif, is required for the normal function of Bif in the fly eye.

Table 3.1: Rescue of the *bif* eye phenotypes

Phenotype	**CS**	***bif*** ^{R47}	***bif*** $^{+}$ **rescue**	***bif*** ^{F995A} **rescue**
Duplication of bristles n = 7 eyes	0	40	11	47
Multiplication of bristles n = 7 eyes	0	3	0	3
Abnormal pattern of rhabdomere arrangement n = 30 ommatidia	0	30	1	29
Abnormal rhabdomere shape n = 210 rhabdomeres	0	210	42	210
Abnormal F-actin in pupal eye discs n = 100 ommatidia	0	92	16	86

Numbers showing the various phenotypes seen in *bif* mutants and the rescue of the phenotypes using *UAS-bif* $^{+}$ and *UAS-bif* ^{F995A}.

3.3. Discussion:

A role for *bif* in the development of the eye was previously described through the isolation and examination of mutants of the *bif* locus (Bahri et al., 1997). Null *bif* mutants exhibited a rough eye phenotype at the morphological level, disorganised rhabdomeres in the ommatidia at the cellular level and alterations in actin cytoskeleton at the subcellular level. In order to see whether the binding of PP1 to Bif was important for its function, I decided to compare the affects of transforming a *bif* null mutant line with wt Bif and Bif mutated in the PP1 binding site at F995. Expression of wt *bif* transgenes resulted in significant rescue of the rough eye defects, rhabdomeral organisation and actin cytoskeleton abnormalities. The reason why rescue is not always complete may be because the level of Bif expression differs from the wild type level. Another possiblility that we cannot rule out is that the transgenes used for transformation do not contain sites that would allow alternative splicing and the production of transcripts that encode distinct Bif proteins. Nevertheless, clear restoration towards the wt morphology for all of the phenotype associated with *bif* loss of function is seen when the wt transgene is expressed in bif mutants.

In contrast, the expression of transgenes encoding the Bif F995A mutant protein, which disrupts binding to PP1, was unable to rescue any aspects of the mutant phenotype, even though the expression level of the transcript was similar to that in the wt rescue. These results indicate that the PP1-Bif interaction is critical for the rescue (and therefore function). Although it can be argued that the F995A mutant causes a conformational change in Bif, this is unlikely because some weak binding of BifF995A to PP1 is observed , consistent with residues surrounding the PP1 binding motif still being in the correct orientation to contribute their normal interactions. The latter in the presence of F995 are likely to account for the very tight binding of wt Bif

to PP1. Since the *in vitro* binding between Bif and PP1 has been well documented, with data indicating the fact that *in vitro* Bif binds PP1 and inhibits its phosphatase activity, while this interaction does not occur with the mutated Bif ^{F995A}. And Bif is also shown to be pulled down with an anti-PP1 antibody in IP's from drosophila extracts (Helps *et al.*, 2001). This data is consistant with the Bif/PP1 direct protein-protein interaction seen *in vitro.* However an absolute proof of Bif and PP1 having a function *in vivo* would require structural data to find how Bif and PP1 crystals actually bind and the exact residues required for Bif/PP1 binding. Experiments mutated forms of PP1 that can now bind Bif ^{F995A} and showing that this mutant PP1 can suppress the Bif ^{F995A} gene replacement in *bif* mutants *in vivo.*

These studies indicate that the normal morphology of the adult eye is probably dependent on the interaction of Bif with PP1 and suggest that a major function of Bif is to target PP1c to a specific subcellular location to regulate the normal developmental pattern of the eye. At the molecular level the organisation of the actin cytoskeleton is dependent on the Bif-PP1 interaction, suggesting that PP1 may influence actin movement or operate in a pathway that regulates actin distribution within the cell. Although the actin cytoskeleton is a highly ordered structure, it is very dynamic, undergoing changes that affect cell shape, motility and adhesion. Bif does not possess a known actin-binding motif, but its subcellular location within the eye is consistent with it playing a role in actin function and possibly binding to some component of the actin cytoskeleton (Bahri et al., 1997). Further in support of the fact that Bif could be associated with cytoskeletal elements is the fact that Bif has been shown to be associated in a complex with both actin and microtubules (Sisson et al., 2000). Further, my data in chapter 4 of this thesis shows that Bifocal binds F-actin directly in *in vitro*

actin co-sedimentation assays, supporting the possibility that Bifocal binding to F-actin is what is required for normal F-actin localisation in the fly eye.

It has been shown that two novel actin-binding proteins found in mammalian neurons, neurabin I and II, bind PP1c (Allen et al., 1998; MacMillan et al., 1999; McAvoy et al., 1999; Satoh et al., 1998). Neurabin I is highly concentrated at the synapse of mature neurons and in the lamellapodia of the growth cone during the development of neurons, suggesting that it is required in synapse function and formation (Nakanishi *et al.*, 1997). Suppression of the endogenous Neurabin I expression with antisense oligonucleotides in hippocampal neurons inhibits neurite outgrowth. Neurabin II is ubiquitously expressed, but is enriched in the postsynaptic density fraction of the brain (Satoh et al., 1998). The presence of a PDZ domain that might bind transmembrane proteins and effect their localisations makes it likely that neurabins II and I bind at the plasma membrane. The neurabins have therefore been suggested to serve as linkers between the actin cytoskeleton and the plasma membrane at cadherin based cell-cell adhesion sites (Satoh et al., 1998) and to localise PP1c to the plasma membrane in dendritic spines of neurons, where the complexes may modulate synaptic transmission (Allen *et al.*, 1998). Both neurabin II and I show F-actin crosslinking activity as do the α-actinin/spectrin family of actin binding proteins. However, the actin binding sites on the neurabins are distinct from other known actin binding sites. Although Bif has no homology to the neurabins, the Bif-PP1c complex may serve analogous functions in the photoreceptor cells of the eye, transmitting or modulating signals, possibly from cell-cell contacts, which cause a rearrangement of the actin cytoskeleton.

It has been shown by Helps and Cohen that Bif, inhibits the phosphatase activity of PP1c *in vitro***;** this is similar to a number of other PP1c binding proteins

such as the myosin binding subunits (Johnson *et al.*, 1996) and 53BP2 (Helps *et al.*, 1995) and Neurabins (Allen et al., 1998; MacMillan et al., 1999; McAvoy et al., 1999). Neurabin I has been shown to be phosphorylated in vitro by PKA, which decreases its binding to PP1c (McAvoy et al., 1999). In addition mutation of the phosphorylatable serine to glutamic acid reduces the inhibitory activity of neurabin, suggesting the complex participates in a cAMP/PKA signalling mechanism. Bif has several potential Ser/Thr phosphorylation sites; in the vicinity of the PP1 binding motif, the carboxy terminal sequence of Bif, -RRSSTIM, could serve as a potential phosphorylation site for PKA (as well as a number of other kinases). Phosphorylation of Bif could affect PP1c binding and/or activity, allowing the Bif-PP1c complex to modulate signalling processes. Alternately or in addition, the Bif-PP1c complex might be required to dephosphorylate proteins associated with actin. Actin-binding proteins can bind to actin monomers, cross-link actin filaments into bundles or gels, sever actin filaments or cap its growing ends. Some, such as myosin II (Tan et al., 1992) and cofilin (Lawler, 1999), are known to undergo phosphorylation. Dephosphorylation of such proteins, possibly by PP1c complexes, may effect a redistribution of the actin cytoskeleton

3.4. Future directions:

Future directions would involve finding the function of Bif in other tissues of the fruit fly and trying to elucidate if the interaction between PP1 and Bif is required for all aspects of Bif function. Another aspect of investigation would be to find other interacting partners of Bif and elucidate the genetic hierarchy of these molecules with respect to Bif and PP1.

Chapter 4
Role of Bifocal and Protein phosphatase1 in photoreceptor axon guidance

4.1. Introduction

Precise axon targeting is achieved by integrating signalling events involving guidance receptors and their downstream components (Tessier-Lavigne and Goodman, 1996). Some of the molecules involved in axonal guidance in the *Drosophila* embryo also play a role in retinotopic axonal targeting hence showing that a similar set of molecules govern axon guidance and normal topographic mapping of the axons in the embryo and the fly visual system. These include Dock, Trio, Lar, Cadherins, Ephrins, their receptors and Dptp69D (Awasaki et al., 2000; Bateman et al., 2000; Bossing and Brand, 2002; Clandinin et al., 2001; Dearborn et al., 2002; Desai et al., 1999; Garrity et al., 1999; Garrity et al., 1996; Hing et al., 1999; Iwai et al., 2002; Iwai et al., 1997; Krueger et al., 1996; Lee et al., 2001; Luo, 2000; Maurel-Zaffran et al., 2001; Newsome et al., 2000a; Newsome et al., 2000b; Rao and Zipursky, 1998; Schindelholz et al., 2001; Schmucker and Zipursky, 2001; Sun et al., 2000).

The fly eye has 750-800 repeats of a basic unit called an ommatidium, which comprises of 8 photoreceptor cells (R1-R8). Overlying the photoreceptor cells are four cone cells and two primary pigment cells surrounding the cone cells. Six secondary pigment cells lie between two ommatidia, and three tertiary pigment cells are shared among three ommatidia at a vertex. The mechanosensory bristles of the eye, which are products of a neuron, glia and shaft and socket cells, are also shared

among three ommatidia at a vertex (Wolff, 1993). The eight axons from the photoreceptors of an ommatidial unit in the eye travel via the optic stalk, that links the eye disc with the optic lobe, into the optic lobe region of the brain as part of an ommatidium specific fascicle with the axons of R1-R7 surrounding the R8 axon (Hanson, 1993). Incoming R cell axons induce the production and differentiation of lamina glia in the optic lobe (Huang and Kunes, 1998; Selleck and Steller, 1991; Winberg et al., 1992). Lamina differentiation by R cell-derived signals plays a crucial role in matching the number of afferents to their targets. Different R cells in the eye disc extend axons that terminate at different levels in the optic lobe. The 6 outer photoreceptors, R1-R6, of each ommatidium terminate their axons at the outer layer of the optic lobe or the lamina, while the inner two photoreceptors R7 and R8 send their axons beyond the lamina into the second optic ganglion the medulla (Hanson, 1993). The growth cone from an initial R8 neuron can be thought to pioneer the path to retinotopic target destination and enters the optic lobe first, while the growth cones of R2 and R5, R3 and R4, R1 and R6 and R7 follow in sequence along the expanding ommatidial fibre. This process of axonal targeting is apparent by the third instar larval stage of *Drosophila* development, such that at this stage a very precise pattern of connectivity is seen; with R1 to R6 axons ending at the lamina and R7 and R8 axons entering the medulla and sending their axons into two distinct neuropiles in the medulla (Kunes, 1999; Kunes et al., 1993a). This is schematised in figure 4.1.

Targeting errors for R cell axons have been described for several mutations including those for the receptor tyrosine phosphatases such as *lar* and *dptp69d* (Clandinin et al., 2001; Garrity et al., 1999). Downstream components of the phosphotyrosine signalling system, of which *dock* is a component, also play important roles in axon guidance in the visual system (Garrity et al., 1996). Targeting

defects in these mutant backgrounds include irregular and uneven lamina layer. In addition R1-R6 axons that normally synapse at the lamina, can bypass the lamina and enter the medulla, or stop at the wrong points in the lamina or medulla (Clandinin et al., 2001; Desai et al., 1999; Garrity et al., 1996). In this chapter I show that *bifocal* and *PP187B* are components of a genetic axon guidance pathway in the visual system involving the phosphatase receptors, *dptp69D* and *dptp10D*.

The Bifocal protein is expressed in neuronal cells in both the embryonic nervous system and the larval visual system of the fly (Bahri et al., 1997; Helps et al., 2001). Although Bif is expressed on embryonic CNS axons, *bif* mutants do not show any obvious defects in axon guidance during embryonic development. However, Bif is required for the normal shape of the R cell rhabdomeres in the fly eye (Bahri et al., 1997). Recent work has shown that Bif is one of the regulators of phosphatase activity by directly interacting with PP187B via its consensus phosphatase-binding motif, RVQF. A requirement for the Bif-PP1-87B complex in the normal photoreceptor rhabdomere development has also been shown (Helps et al., 2001). Loss of *bif* function has also been shown to give rise to axon guidance phenotypes in the larval optic lobe and *bif* mutants interact genetically with *misshapen* (*msn*), which encodes a protein kinase, to regulate normal photoreceptor axon targeting (Ruan *et al.*, 2002).

In this chapter, I demonstrate that both *bif* and *PP187B* are required for the formation of an even and regular lamina and the proper termination of R2 to R5 axons at the lamina during the larval stages. Further *bif* genetically interacts with the receptor tyrosine phosphatases *dptp10D* and *rptp69D* in the larval optic lobe. I also present evidence that Bif binds F-actin directly and propose that Bif may act as a linker between the RPTPs, PP187B, and the cytoskeleton.

4.2. Results

4.2.1. Mutations in *bif* show defects in larval photoreceptor axon guidance and the organisation of F-actin cytoskeleton in the larval brain

Bif is heavily expressed on embryonic CNS axons but *bif* mutants do not show any obvious axonal defects in this system (Bahri et al., 1997). In order to determine whether Bif plays a role in axonal projection, we examined axons of the third instar larval visual system in *bif* mutants using the monoclonal antibody 24B10 (Fujita *et al.*, 1982; Van Vactor *et al.*, 1988). In wild type (wt) larvae, R cell axon fascicles project through the optic stalk to appropriate topographic locations in the optic lobe (Hanson, 1993). R1-R6 axons normally stop in the lamina forming a dense layer of expanded growth cones, the lamina plexus, which falls between 2 layers of glial cells. R7 and R8 axons project through the lamina and terminate in the medulla where they elaborate an array of growth cones (Hanson, 1993; Kunes and Steller, 1993) (Schematic in Fig. 4.1). In homozygous bif^{R47} (an antigen minus allele) mutants, R cell axons formed a largely normal topographic array in both the lamina and the medulla. However in all cases n>50, the mutant lamina plexus was wavy, of varying thickness and discontinuous (Fig. 4.2 B). This phenotype is not seen in control bif^{R47}/+ (Fig. 4.2 A) or in the lamina of homozygous bif^{LH114} flies (inset in Fig. 4.2 A). bif^{LH114} is derived from the same parental chromosome used to generate bif^{R47} and does not affect *bif* ORF but deletes 3' sequences downstream of the *bif* gene (Bahri et al., 1997). This phenotype seen in the *bif* mutants has previously been described by Dr. Yang Rao's group (Ruan *et al.*, 2002). Similar discontinuity phenotypes in the mutant lamina were observed with phalloidin staining (Fig.4.2 D). This phenotype was seen in 100% of the

larval brains scored n=20. In wt larvae, phalloidin-stained axons normally reveal smooth lamina (Fig. 4.2 C).

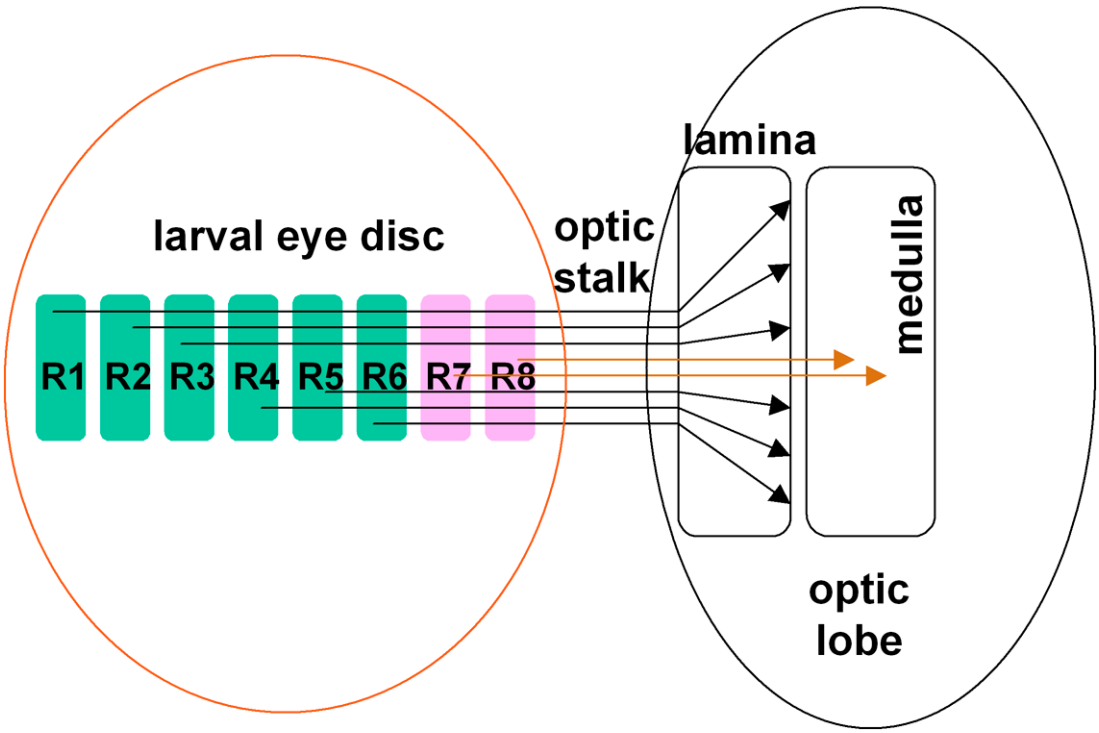

Fig. 4.1: Schematic of photoreceptor axons targeted from the eye disc to the optic lobe

The axons from the photoreceptors are targeted to the optic lobe. The schematic shows a third instar larval optic lobe with the eye disc attached to it. For simplicity only one ommatitium with R1-R8 neurons is shown in the eye disc. The outer six photoreceptor cells (R1-R6) send their axons through the optic stalk to the outer neuropile of the optic lobe, the lamina. While, the inner two photoreceptors (R7, 8) send their axons to the inner neuropile of the optic lobe, the medulla.

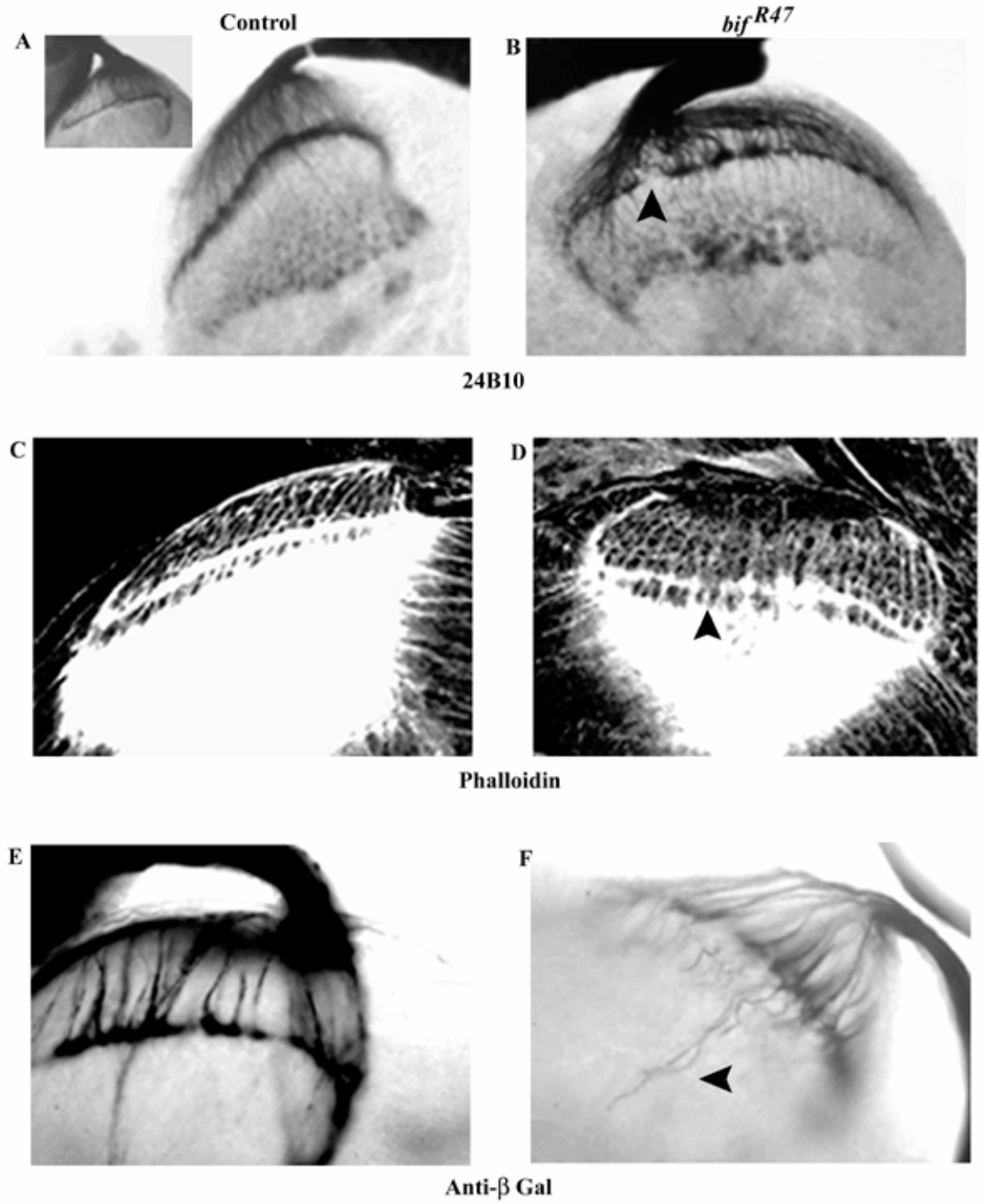

Fig. 4.2: Axon clumping and mistargeting phenotypes seen in bif mutants
Control brains and *bif*^{R47} mutant brains stained with the monoclonal anti-chaoptin antibody 24B10 (A, B). The mutant brain shows clumping of the axons at the lamina and the lamina shows breaks on the surface (arrowhead in B). This phenotype is not seen in the *bif*^{R47}/+ control brain (A) or the *bif*^{LH114} control brain (inset in A). Panels C and D show phalloidin staining in WT (C) and *bif* mutant brains (D). The lamina in this case also shows breaks (arrowhead in D) and clumping of the axons. The last two panels show targeting of the axons of photoreceptors R2-R5 as visualised using the *Ro*^{tau}*-LacZ* line. Panel E shows the targeting of some of the R2-R5 axons, which target to the lamina in WT optic lobes, most of the R2-R5 axons in *bif* mutant opic lobes bypass the lamina and terminate at the medulla (arrowhead in F).

Further characterisation of the axonal defects with the *Ro^{tau} lacZ* line (Garrity et al., 1999) which labels subsets of R cell axons, R2-R5, reveals additional axon targeting defects in *bif* mutants (Fig. 4.2 E). The mistargeting defect was seen in 65%-75% of the axons which entered into the medulla in all cases, n=17. Wild type R2-R5 axons normally terminate at the lamina and do not extend to the medulla (Fig. 4.2 E and schematic in 4.1). In contrast, mutant R2-R5 axons failed to stop at the lamina and extended further into the medulla (Fig. 4.2 F). In order to determine whether the axon guidance phenotypes of *bif* mutants are partly due to defects in the lamina or the adjacent glia cell layers in the third instar optic lobe, several markers were used to stain the larval brain. No obvious defects were detected with either Dachshund (Dac) (Mardon et al., 1994), which marks the proliferating cells of the lamina, or with Reversed polarity (Repo) (Halter *et al.*, 1995), which marks the glia, when compared to wt staining (Fig. 4.3 A-F). This indicated that the lamina and glia form normally in *bif* mutants. These results suggest that the axonal defects in *bif* mutants are due to a specific requirement for Bif function in R-cells and their axons and not in the target tissues.

4.2.2. Bif is expressed in the *Drosophila* optic lobe

Bif has been previously shown to be expressed in photoreceptor cells and to be localised in the rhabdomeres of larval and pupal eye discs (Bahri et al., 1997). In order to understand the basis of the R cell axonal phenotypes in *bif* mutants, the extent

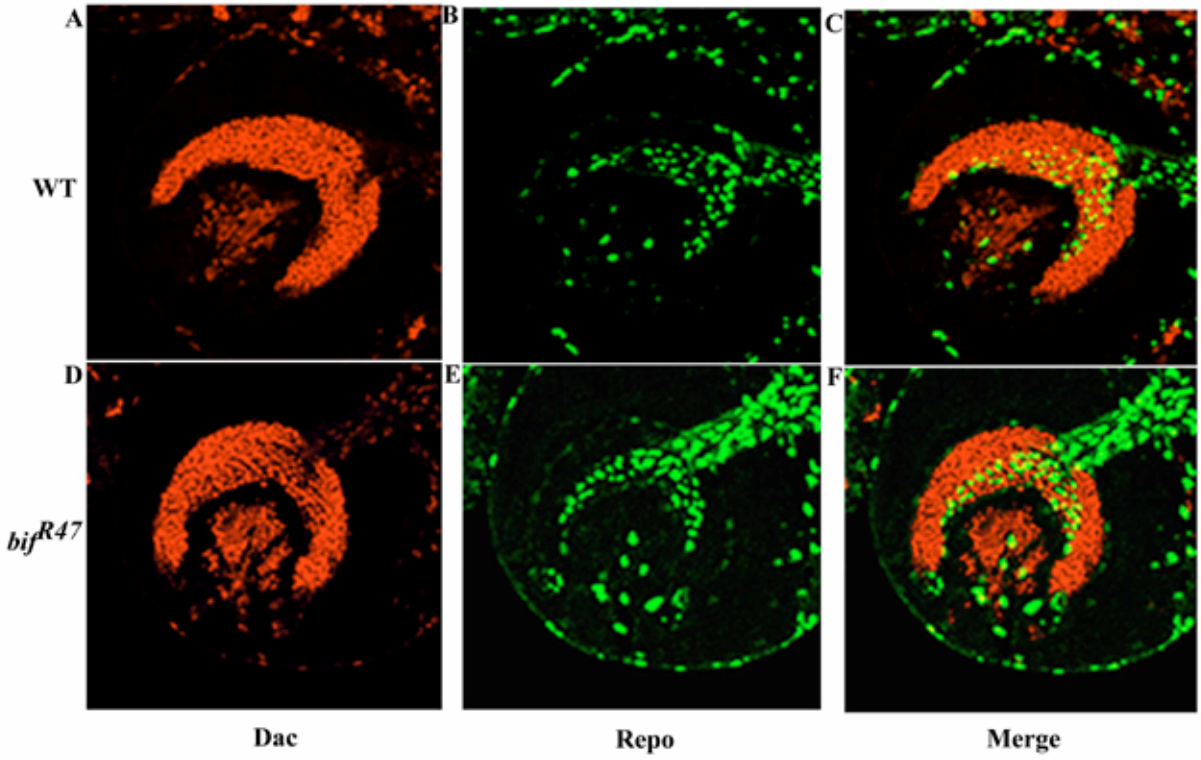

Fig. 4.3: Dac and Repo staining in WT and *bif* mutant optic lobes
WT (A-C) and *bif* mutant brains (D-F) were stained with anti-Dac (red) and anti-Repo (green) antibodies. There are no obvious defects seen in either Dac or Repo staining in the mutant optic lobe. C and F panels are a merge of the anti-Dac and anti-Repo staining.

of Bif expression in the third instar larval visual system and brain optic lobes was determined (Fig. 4.4). Double staining with anti-Bif and 24B10 showed stronger expression of Bif on R cell axons in the optic stalk and somewhat weaker staining on the axons as they enter the optic lobe (Fig. 4.4 D-I). Bif was also widely expressed in the optic lobe. Double labelling with anti-Bif and anti-Dachshund, where anti-Dac labels the cells of the lamina and medulla in the optic lobe (Garrity et al., 1999; Mardon et al., 1994) showed that Bif localises in the outer region of the lamina (Fig. 4.4 A-C), where the photoreceptor axons initially send their projections into the optic lobe (Kunes et al., 1993b). Similar to what has been reported in the eye disc (Bahri et al., 1997), Bif also showed co-expression with F-actin in the optic lobe (Fig. 4.4 J-L). In these experiments, Bif staining was stronger in the optic lobe cortex and weaker in the cortical axons (Fig. 4.4 M-O). The bif^{R47} mutants do not show any Bifocal staining in the eye disc or optic lobe, however F-actin is still visible in these mutants (Fig. 4.4 P-R).

4.2.3. Expression of Bif in the eye is sufficient to rescue its phenotype in the optic lobe

These observations indicate that Bif is expressed in both R cells and their axonal targets in the optic lobe. In order to determine in which tissue Bif function is required for proper axon projections, tissue-specific expression of *bif* in *bif* mutant backgrounds was carried out using the UAS/GAL4 system (Brand and Perrimon, 1993). GMR-Gal4 was used to drive the expression of UAS-bif^{+} transgene specifically in the eye disc (Hay et al., 1997) but not the optic lobe. Out of 36 larval preparations, 28 (78 %) showed complete rescue of the photoreceptor axon clumping phenotype as can be visualized with mAb 24B10 (Figs. 4.6 E and 4.8 A). The rescued lamina was

indistinguishable from the wt control. Partial rescue of the lamina phenotype was also observed in 6 of the remaining preparations. The extent of phenotypic rescue with the GMR-GAL4 driven *bif* transgene was also assessed with F-actin staining. Complete rescue of F-actin staining in the optic lobe was observed in 10 out of 12 preparations (Fig. 4.8 C). The remaining 2 preparations showed partial rescue. The R2-R5 mistargeting phenotype was also rescued when UAS-bif^{+} was driven in the eye. This was seen using Ro^{tau} *lacZ* (Fig. 4.8 E). These experiments demonstrate that the axonal defects observed in *bif* mutants are due to loss of Bif function in photoreceptor cells.

4.2.4. The axon guidance phenotype is uncoupled from the rhabdomere phenotype seen in *bif* mutants

The rescue experiment described above indicated a general requirement for Bif in R cells for normal axon projections but did not uncouple the function of Bif in axon guidance from its other requirements in maintaining normal cellular morphology of photoreceptors. *bif* mutants are known to affect not only axons but also the morphology of the rhabdomeres of R cells (Bahri et al., 1997). So far, two isoforms of Bif have been isolated (Bahri et al., 1997; Helps et al., 2001). These two isoforms differ in their splice sites, with the larger bif^{+} isoform having five exons and the smaller bif^{10Da} isoform having six exons (schematically represented in Fig. 4.5). The bif^{+} isoform encodes for a protein containing 1196 amino acids, whereas the bif^{10Da} isoform encodes a 1063 amino acid protein. Chapter 3 shows the use of the larger bif^{+} isoform, which was used to rescue the defects seen in *bif* mutant eyes. The defects in actin localization in the pupal eye disc and rhabdomere morphology observed in *bif* eyes were significantly rescued by driving either of the *bif* isoforms, with GMR-GAL4

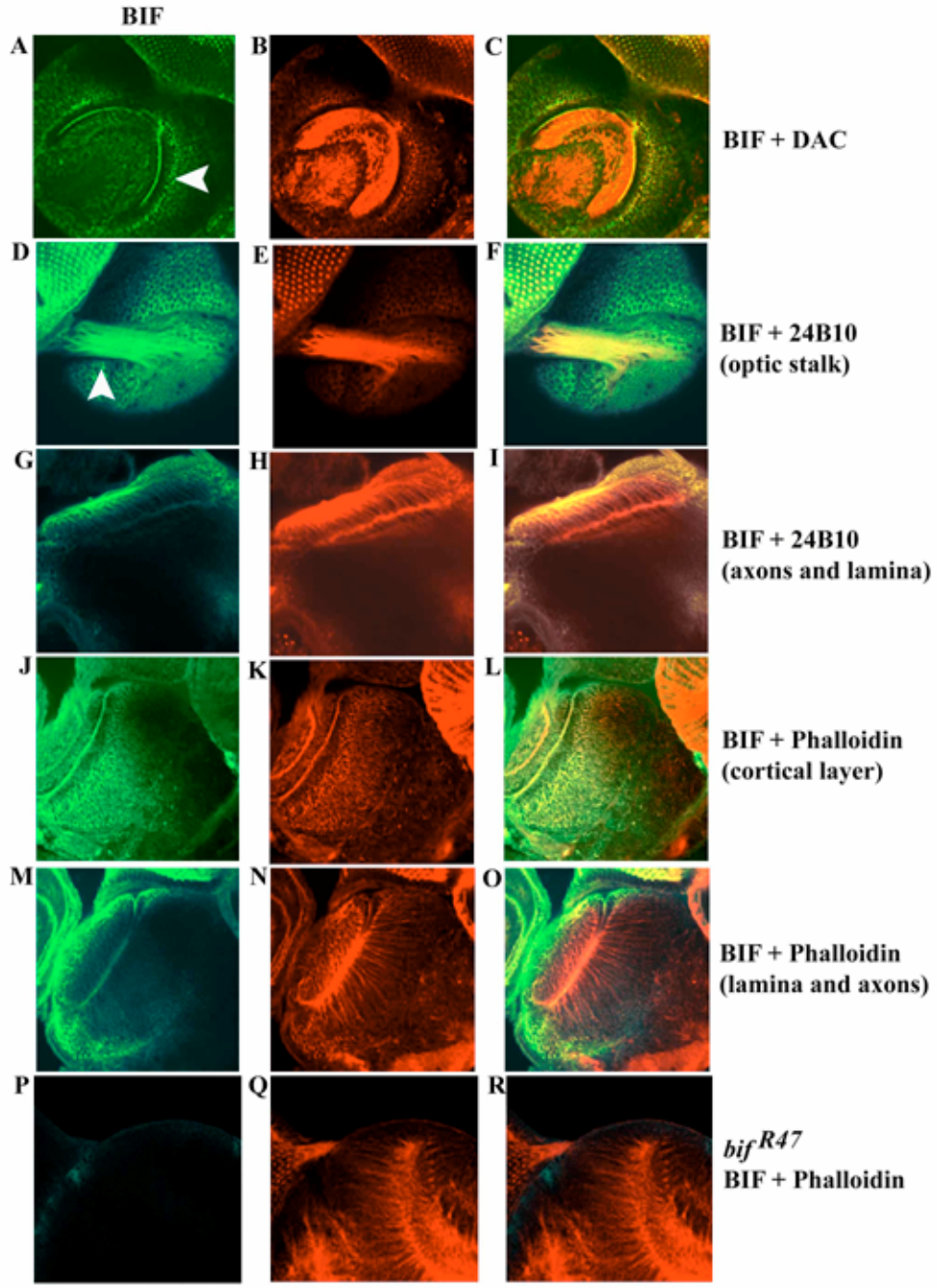

Fig. 4.4: Bif expression pattern in the optic lobe
The optic lobes of WT third instar larvae were stained with anti-Bif and anti-Dac (A-C). Bif is seen expressed in the cortex of the optic lobe and a high level of expression is seen on the outermost region of the lamina (arrowhead in A and merged panel C), where Dac is expressed (B). Double labelling with 24B10 (E and H) shows a high level of Bif expression in the axons that pass through the optic stalk (arrowhead in D and merged panel F). Bif expression in the axons when they enter the optic lobe becomes reduces when compared to its expression in the optic stalk (D and G). 24B10 expression is still seen at high levels in the optic lobe axons (H). Double labelling of anti-Bif with phalloidin (J-O) shows that Bif expression in the cortex is very high (J) and co-localises with F-actin in the cortex (K and L). Expression of Bif in a lower plane of the optic lobe is less then the cortical expression of Bif (M). No expression of Bif is seen in *bif*^{R47} mutant optic lobes used in this study (P), while phalloidin staining is still seen in these optic lobes (Q).

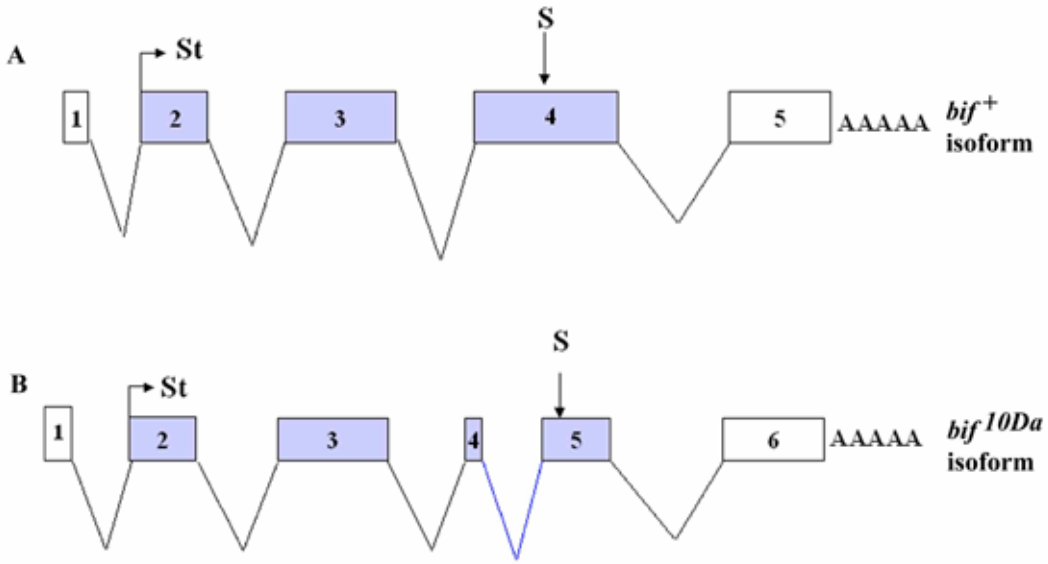

Fig. 4.5: Schematic of the two isoforms encoded by the *bif* gene
A indicates the larger *bif*$^{+}$ isoform which has five exons, the coding region comprises of four exons. B indicated the smaller *bif*^{10Da} isoform, which is made up of six exons with five exons giving rise to the coding region. Arrows with the 'St' symbol indicate the start of the coding region and arrows with the 'S' symbol indicate the end of the coding region. The exons in both A and B are connected with 'V' shapes which indicate the splice sited between the exons. The blue splice site in B shows the extra exon in the *bif*^{10Da} isoform (which is part of exon 4 being removed in this isoform of Bif) which is absent in the *bif*$^{+}$ isoform.

(Fig. 4.6 A-D) compared to *bif* mutant phenotypes in Fig. 4.7B, Fig. 3.4B from the previous chapter and (Helps et al., 2001). Details of bif^{+} rescue of the eye phenotypes is shown in Table 3.1 in the previous chapter. The rescue of the eye phenotype using the bif^{10Da} isoform of Bif is as follows:

1. For abnormal pattern of rhabdomere arrangement bif^{10Da} rescue is 90%, n = 30 ommatidia.
2. For abnormal rhabdomere shape bif^{10Da} rescue is 81% n = 210 rhabdomeres.
3. For abnormal F-actin organisation in pupal eye discs bif^{10Da} rescue is 92% n = 100 ommatidia.

However, the bif^{10Da} isoform was largely ineffective in rescuing the axonal defects. 88.6% showed no rescue of the axonal phenotype seen using the antibody 24B10, 9% showed partial rescue and 2.2% showed rescue of the axonal phenotype, n=44, 88.9% showed no rescue and 11.1% showed a partial rescue of the axon mistargeting phenotype using the Ro^{tau} *lacZ* marker n=9 (Fig. 4.6 F and H, control bif^{+} rescue are also shown here).

These experiments showed that only bif^{+} and not bif^{10Da} was able to effectively rescue the axonal defect of *bif* mutants (Fig. 4.6 F-H and Fig. 4.8 A and C). These experiments revealed dual requirements for the two *bif* isoforms, with bif^{10Da} being largely required for normal R-cell morphology but not having a predominant role in normal axonal projections onto the optic lobe, while bif^{+} is involved in both R-cell morphology and axon guidance. The uncoupling of Bif functions in axon guidance and cell body morphology suggested that the axon guidance phenotype of *bif* is not merely a secondary effect of the R cell morphological abnormalities, but rather a primary consequence of the loss of *bif* function required for axon guidance.

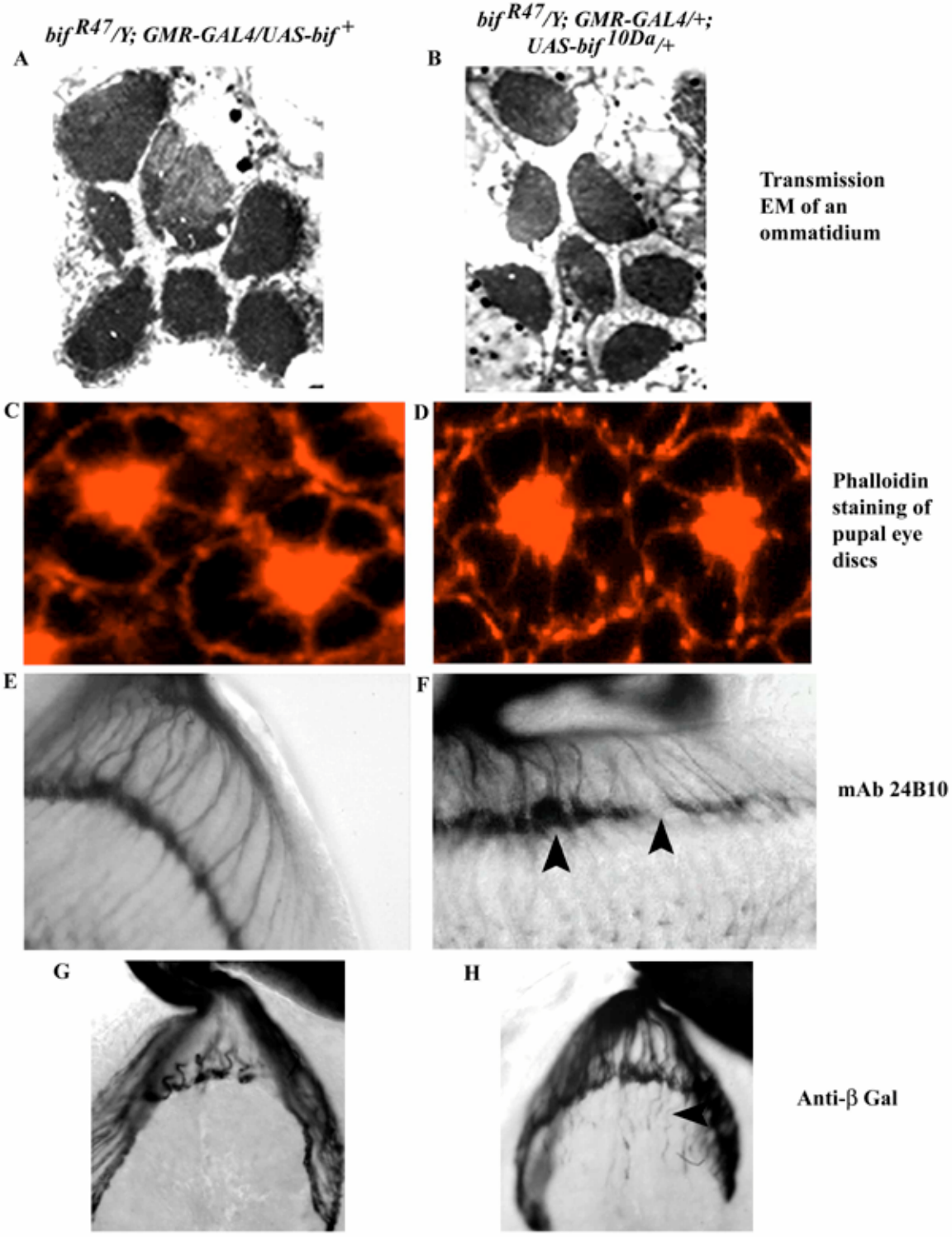

Fig. 4.6: Rescue of the eye phenotype seen in *bif* mutants using *bif*$^{+}$ and *bif*^{10Da} isoforms of bif

Panels A-D show rescue of the adult rhabdomere and pupal F-actin staining phenotypes of *bif* mutants using *bif*$^{+}$ (A and C) and *bif*^{10Da} (B and D) isoforms of *bif*. Compare the rescue using both isoforms of bif with the phenotype seen in *bif* mutants, which is shown in Fig. 4.7B. Panel E shows rescue of the bif mutant axon clumping phenotype using *bif*$^{+}$ which shows a high degree of rescue of this phenotype, while *bif*^{10Da} does not rescue the phenotype (F). The clumps and breaks and the R2-R5 mistargeting seen in *bif* mutants are not rescued using the *bif*^{10Da} isoform of *bif* (arrowheads in F and H).

Adult brains of *bif* mutants were also examined to see if the guidance defects seen in the larval brains are also seen in the adults. Staining of wt and *bif* mutant brains were performed with 24B10 (Fig. 4.7 C and D) and markers specific for either R1-R6 projections, *Rh1-τlacZ* (Fig. 4.7 E and F) or R7 projections, *Rh4-τlacZ* (Newsome *et al.*, 2000b) (Fig. 4.7 G and H). These stainings showed a largely normal array of axons even though the rhabdomeres of the mutant adult retina have defective morphology (Fig. 4.7 A and B.; (Bahri et al., 1997). These results show that the axonal phenotypes observed in the larval optic lobe is largely corrected in the adult brain of *bif* mutants and further demonstrates that axon guidance phenotypes and morphological defects of R cells can be uncoupled in *bif* mutants.

4.2.5. Interaction between Bif and PP1 is required for normal photoreceptor axon guidance

It has been previously shown that Bif can act to inhibit PP1-87B activity in vitro and that a single amino acid mutation in the PP1-binding motif of Bif can abolish its ability to bind and to inhibit PP1 activity in vitro. In addition this mutant form of Bif cannot rescue the *bif* R cell morphological defects in vivo (Helps et al., 2001) and Previous chapter). To test whether this site is also required for proper axon guidance in the larval optic lobe, the mutant UAS-*bif* ^{F995A} was driven by GMR-GAL4 in a bif mutant background. Very little rescue of the axonal defects was observed with this construct as can be visualized with mAb 24B10, 41/43 (95.3%) preparations showed a mutant phenotype, and 2/43 (4.7%) showed partial rescue, phalloidin staining indicated that 15/17 (88.2%) brains showed a phenotype while 2/17 (11.7%) showed partial rescue and the 6/7 (85.4%) showed no rescue and 1/7 (14.6%) showed a partial rescue of the axon

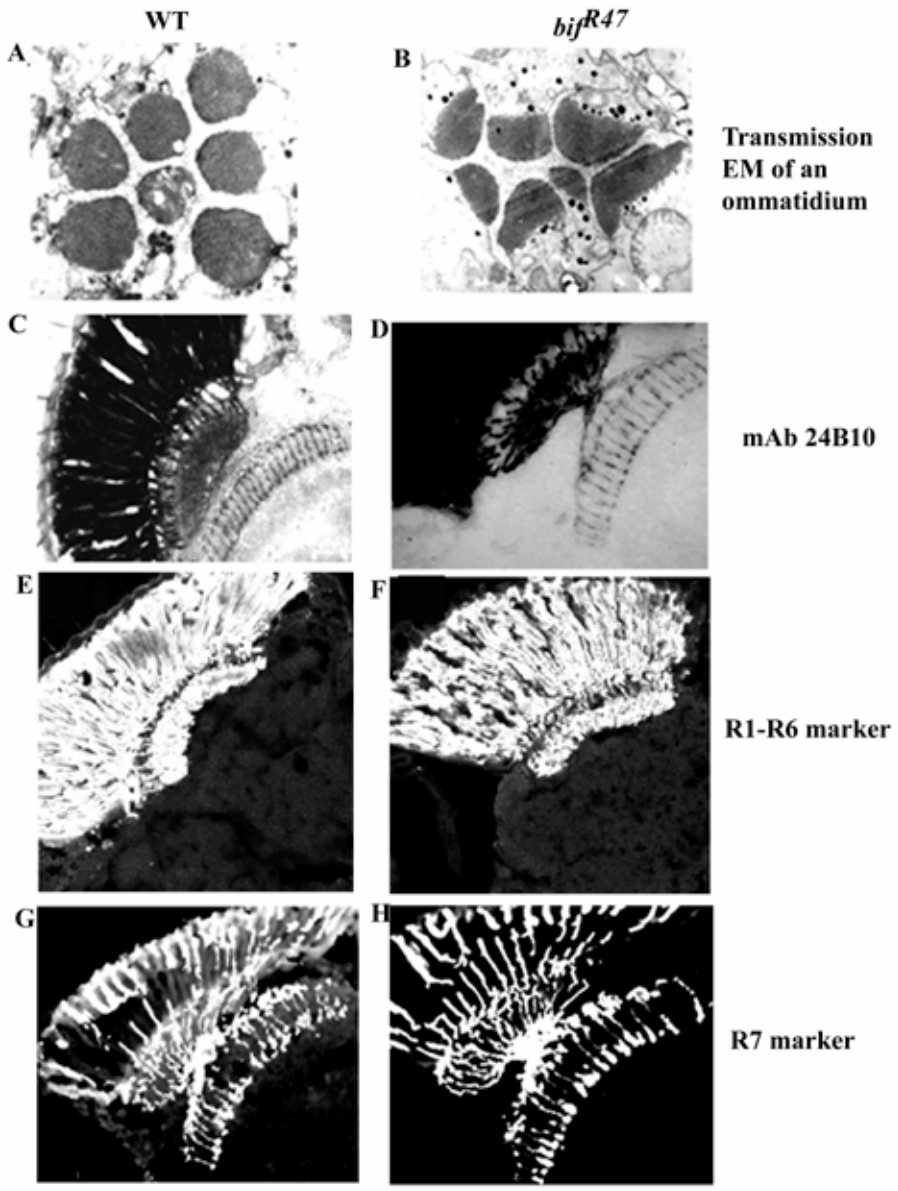

Fig. 4.7: *bif* mutants show normal axon targeting in adult optic lobes
Panels A and B compare the rhabdomere phenotypes seen in *bif* mutants (B), when compared to WT rhabdomeres (A). Note that the mutants show elongated or shorter rhabdomeres that do not form the trapezoid shape that is seen in WT rhabdomeres. Panels C-H show the mutant optic lobes of WT (C, E and G) and *bif* mutants (D, F and H) stained with markers for all or specific subsets of photoreceptor axons. There are no defects seen in the lamina or the medulla of *bif* mutant optic lobes on staining with 24B10 (D); the staining looks similar to WT 24B10 staining (C). No obvious defects are seen in targeting of R1-R6 axons using the *Rh1- lacZ* marker in *bif* mutant (F) when compared to WT (E). Similarly no defects are seen in R7 targeting in *bif* mutants (H) when compared to WT (G) using the *Rh4- lacZ* marker to label R7 axons.

mistargeting phenotype using the Ro^{tau} *lacZ* marker (Fig. 4.8 B, D and F). This indicated that binding of Bif to PP1-87B is essential for its function in axon guidance.

Double labelling with anti-Bif and anti PP1-87B antibodies of wt preparations indicated that both proteins have overlapping expression pattern in most regions of the optic lobe (Fig. 4.9 A-C). Similar to the staining pattern of Bif, anti-PP1 staining in the brain also showed enhanced signal in the brain cortex and the outer layer of the lamina while it was considerably weaker in the axons. In addition, *bif* and *PP1-87B* were found to interact genetically. Transheterozygous flies with one copy of mutant *PP1-87B* and one copy of *bif* showed small breaks and clumping of the axon in the lamina plexus when stained with mAb24B10 (Fig. 4.9 F) whereas the lamina of control flies *pp1*/+ (Fig. 4.9 E) or bif^{R47}/+ (Fig. 4.9 D) were normal. These results indicate that the Bif / PP1-87B complex is probably essential for axon guidance.

4.2.6. PP1 is required for normal axon guidance in the larval stages

Since Bif inhibits the activity of PP1 *in vitro*, it was reasonable to assume that ectopic PP1-87B expression in wt backgrounds should mimic the affect of *bif* mutants on axon guidance. This was indeed the case when *UAS-PP1-87B* was driven with GMR-GAL4 in the eye. Axonal breaks in the lamina similar to those observed in *bif* mutants were observed upon staining of the optic lobes with 24B10 (Fig. 4.10 A, this phenotype was seen in 100% (n=28) of the optic lobes). The R2-R5 axon specific marker also showed mistargeting of a few of the R2-R5 axons into the medulla (Fig. 4.10 B).

The next question was to determine whether *PP1-87B* mutants themselves cause any axonal phenotype in the eye. It was not possible to address this question in homozygous mutants since *PP1-87B* is required for normal cell cycle progression in

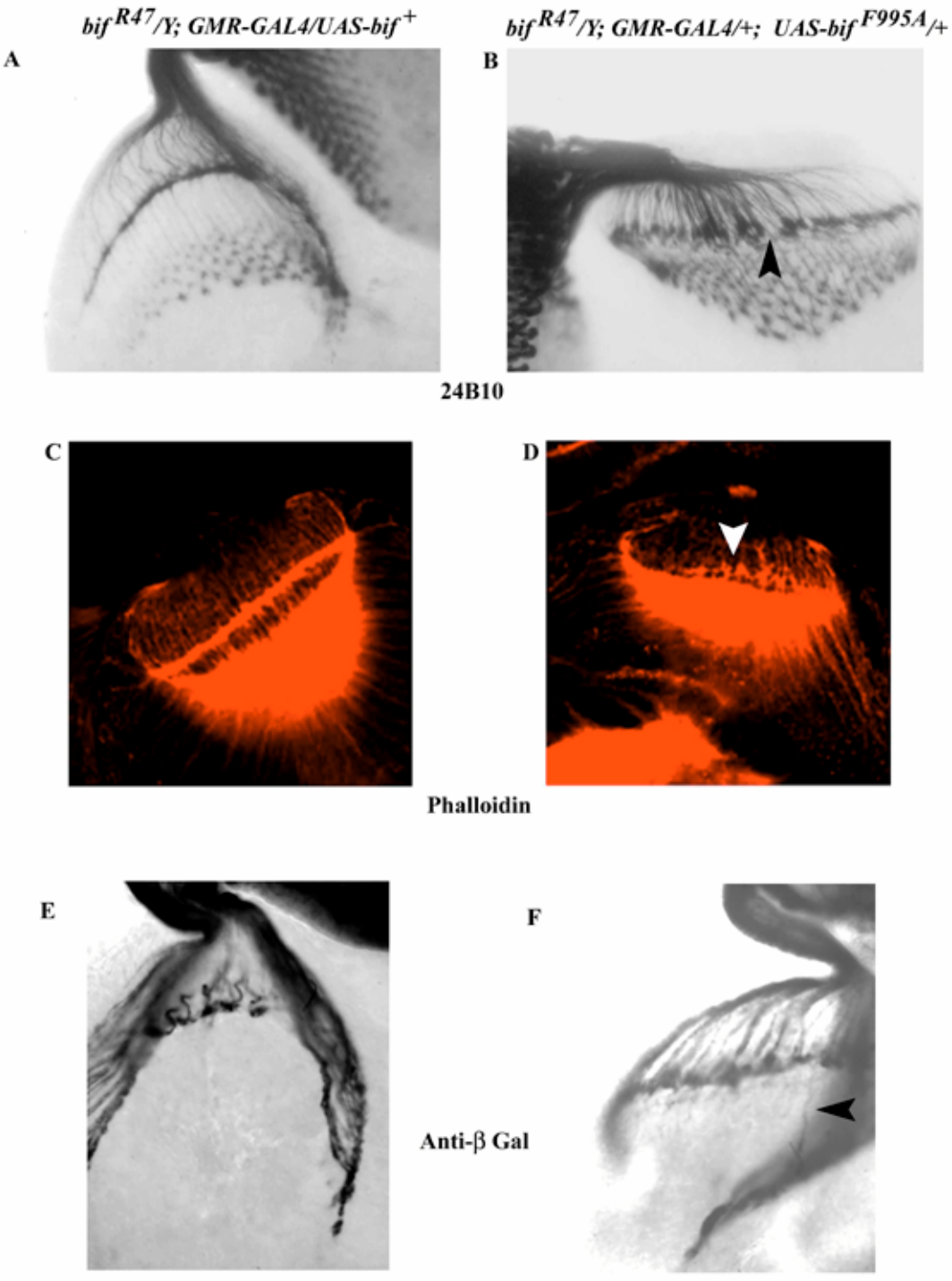

Fig. 4.8: Rescue of the axonal defects using *bif*$^{+}$ and *bif*^{F995A}
Panels A, C and E show the rescue of the bif mutant phenotype using *UAS-Bif*$^{+}$. Note that the axonal phenotype shows rescue using the 24B10 antibody (A), phalloidin (C) and an R2-R5 marker, *Ro*^{tau}*-LacZ* (E). Using *UAS-Bif*^{F995A}, which has a single amino acid change at the 995th position of Bif^{+}, none of the axonal phenotypes, including those seen using 24B10 (B), phalloidin (D) or *Ro*^{tau}*-LacZ* (F) were rescued. Arrowheads in B and D indicate the position of breaks in the lamina. Arrowhead in F shows mistargeted axons that enter the medulla.

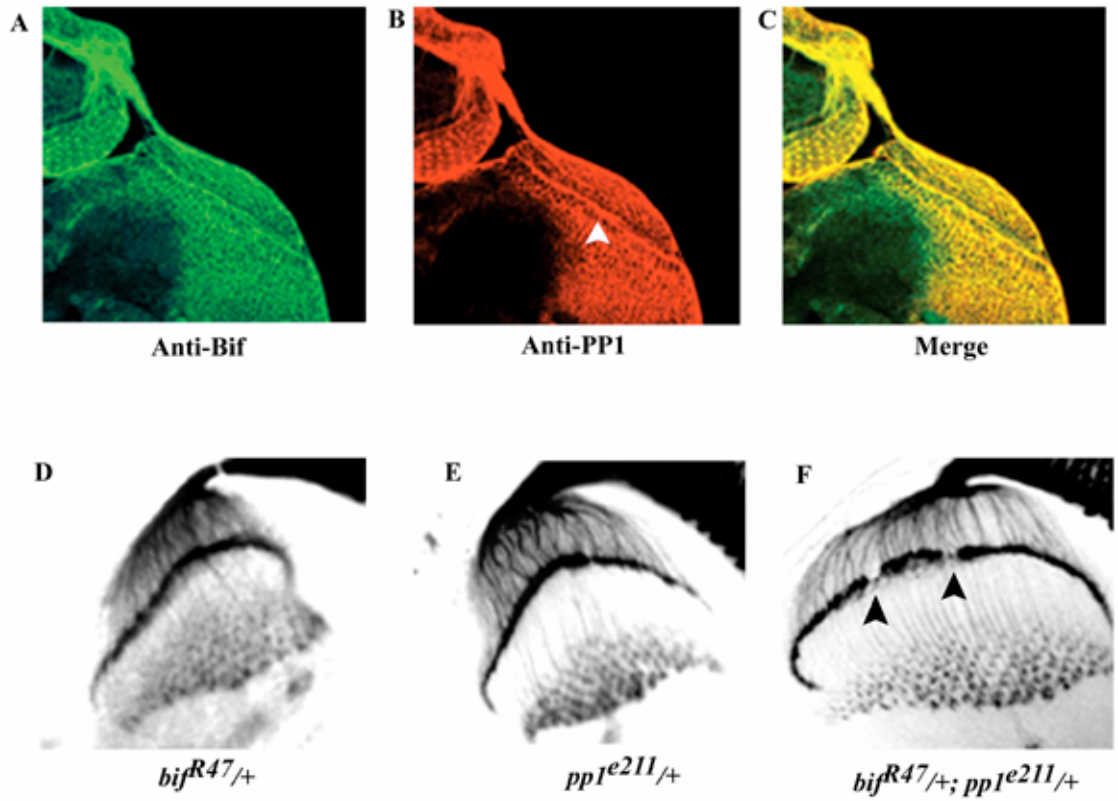

Fig. 4.9: Bif and PP1 co-express in the optic lobe and interact genetically
Panels A-C show expression of Bif (A), PP1 (B) and a merged panel of Bif and PP1 (C). Note that both Bif and PP1 co-express in the WT optic lobe. Panels D-F show 24B10 staining of the photoreceptor axons in controls *bif/+* (D), *pp1/+* (E), both of which show a smooth lamina. However the lamina of *bif/+; pp1/+* larvae shows clumps and breaks (arrowheads in F) indicates that *bif* and *pp1* interact genetically with each other.

the larval brain neuroblasts and hence most *PP1-87B* mutants die in the larval or early pupal stages (Axton et al., 1990). In addition, eye discs in these mutants are severely defective, showing very small discs and defective axonal projections (Fig. 4.10 D). As a first step to determine PP1 function in axon guidance, specific PP1 inhibitors, NIPP1 (Bennett et al., 2003; Beullens et al., 1992; Parker et al., 2002; Van Eynde et al., 1995) and I-2PP1 (Bennett et al., 1999; Bennett et al., 2003; Helps and Cohen, 1999; Huang and Glinsmann, 1976)and reviewed in (Cohen, 2002), were driven post-mitotically in the eye using pGMR-GAL4. In these experiments, the eye disc was formed fairly normally but the photoreceptor axons showed defects (Fig. 4.11 A-D). The lamina formed by the axons expressing either NIPP1 (Fig. 4.11 C) or I-2PP1 (Fig. 4.11 D) was discontinuous with breaks. Using the stronger NIPP1 inhibitor 100% (n=20) showed breaks in the lamina using the 24B10 antibody. Using the weaker I-2PP1 inhibitor 66.7% (n=15) showed breaks in the lamina. The R2-R5-specific marker (*Ro^{tau}-LacZ*) showed axon mistargeting to the medulla mainly with the stronger PP1 inhibitor, NIPP1 in 100% (n=16) of the optic lobed stained (Fig. 4.11 E), the I-2PP1 inhibitor showed a mild mistargeting defect in 61.1% (n=18) with the R2-R5 specific marker (Fig. 4.11 F). These results indicate that PP1 activity is required for photoreceptor axon guidance in visual system.

Since NIPP1 and 1-2PP1 are general PP1 inhibitors and not specific for PP1-87B, we next used different allelic combinations to bypass the early cell cycle defects associated with *PP1-87B* mutations. We used three alleles of *pp1-87B*, *pp1 ^{e211}*, *pp1^{e078}* and *pp1 ^{hs46}* (Axton et al., 1990) to examine the *PP1* phenotype. Using the *pp1 ^{hs46}* allele in trans with the other 2 alleles, allowed larval development to proceed and these animals later died at the pupal stage. In these animals, the larval eye discs formed fairly normally as can be visualised with 22C10 (4.12 A, B). Staining with 24B10

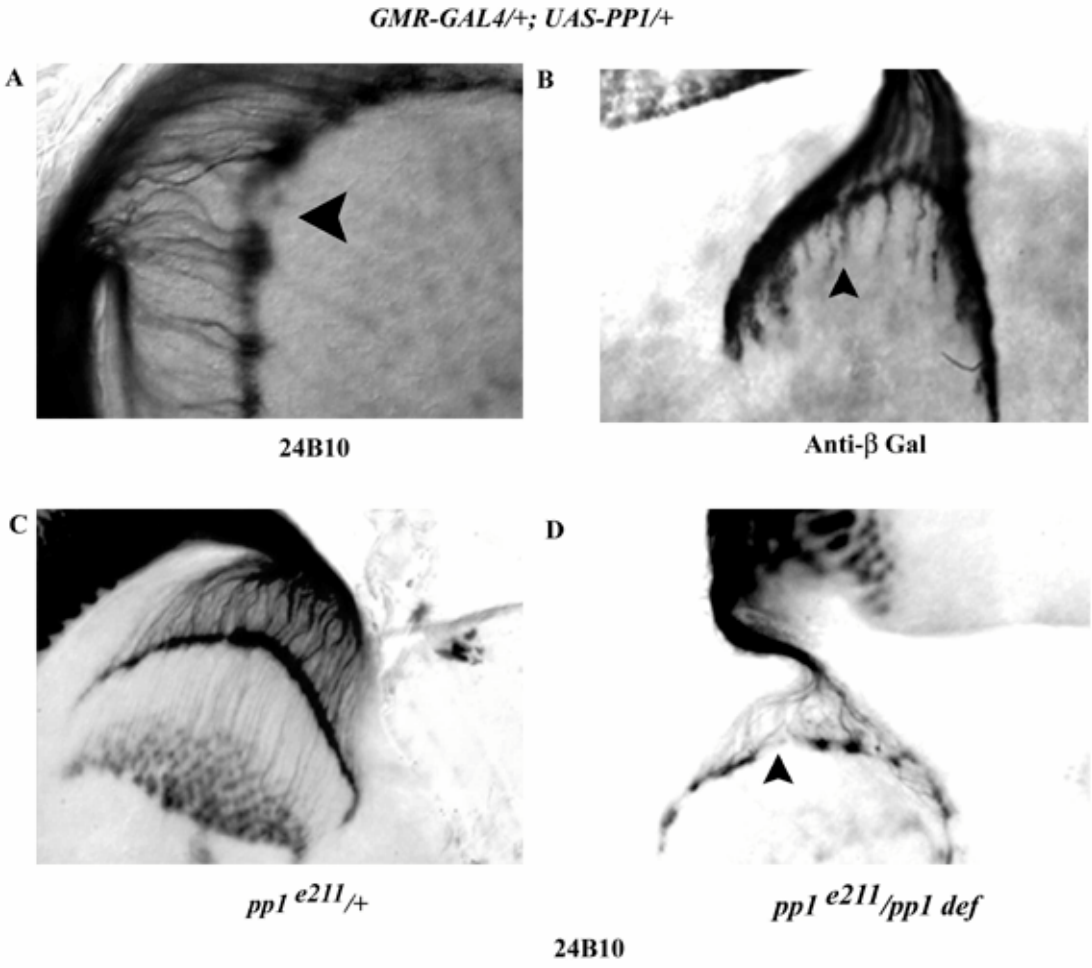

Fig. 4.10: Overexpression of PP1 in the eye and *pp1* mutant phenotype
Panels A and B show phenotypes seen with 24B10 (A) and an R2-R5 axonal marker (B) in the optic lobes of larvae that overexpress PP1 in the eye using *GMR-Gal4*. Note that the lamina shows breaks on staining with 24B10 (arrowhead in A). Panel C shows a *pp1/+* control with no obvious defects on staining with 24B10, while *pp1/def* flies show very severe defects in the larval eye disc and optic lobe as can be detected using mAb 24B10 (D). They show smaller discs and huge breaks in the lamina (arrowhead in D). However, this is probably a secondary consequence of division defects.

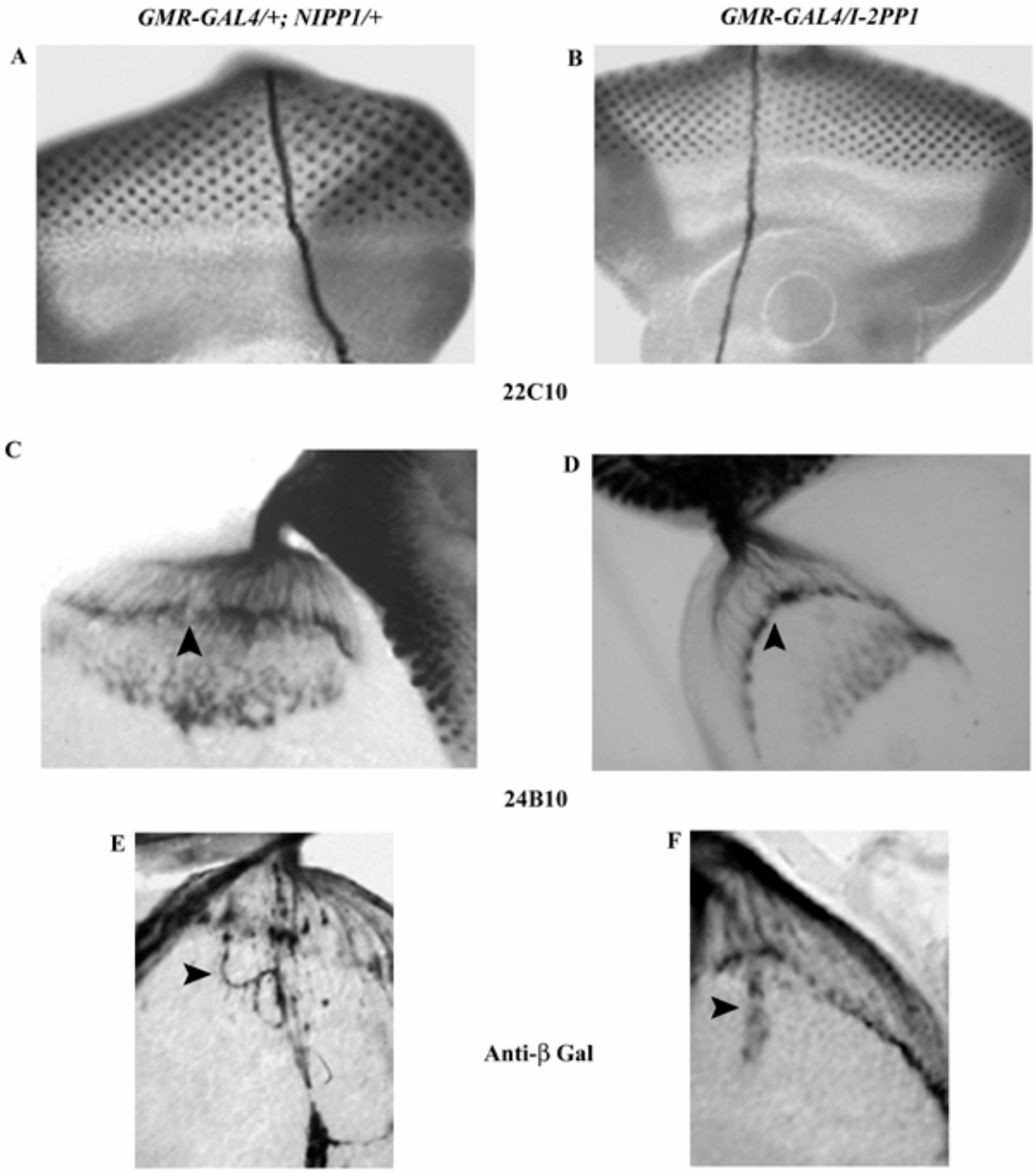

Fig. 4.11: Phenotypes seen on inhibiting PP1 in the larval eye disc
On driving either the *NIPP1* or the *I-2PP1* inhibitors in the larval eye disc, no obvious abnormality was seen in photoreceptor formation using mAb 22C10 (A and B). The lamina in both the cases showed defects on staining with mAb 24B10 with breaks (arrowheads in C and D) and clumping of axons easily observable. The phenotype using the stronger NIPP1 inhibitor of PP1 (C) is more drastic then that seen with the weaker I-2PP1 inhibitor (D). Using the Ro^{tau}-*LacZ* axon marker a very severe defect in R2-R5 targeting was seen on using the stronger PP1 inhibitor (panel E and arrowhead in E), this defect was much milder on droving the weaker PP1 inhibotor in the eye (panel F and arrohead in F).

phenotype was seen in 97.2% of the optic lobes, n=36). Some of the R2-R5 axons in the transheterozygotes were also mistargeted to the medulla (Fig. 4.12 E and F, this phenotype was seen in 100% (n=17) of the cases in *pp1* ^{e078}/*pp1* ^{hs46} transheterozygotes and in 91.6% (n=24) cases in the *pp1* ^{e211}/*pp1* ^{hs46} transheterozygotes. Taken together, these loss of function results further strengthen the view that PP1-87B is required for normal photoreceptor axon guidance.

4.2.7. Bif interacts with other molecules for normal axonal connectivity

Having found that Bif interacts with PP1-87B and is required for proper axonal guidance in the fly eye, I went on to test for genetic interaction between *bif* and other molecules involved in photoreceptor axon guidance. The genetic tests were done using one copy of the *bif* ^{R47} allele, which itself shows no phenotype (Fig. 4.2 A), in combination with one copy of loss of function mutants of other molecules. Axonal defects were observed in double transheterozygous optic lobes, when stained with 24B10, which were transheterozygous for *bif* and the receptor tyrosine phosphatases, *dptp10d* and *rptp69d* (Fig. 4.13 D and E). This phenotype was also seen in female brains, which had one wt X chromosome and the other arm having a deletion of *bif* and *ptp10d* (Fig. 4.13 F). There was no phenotype seen with *bif* ^{R47} in trans with *dock, pak, dlar, ena* and *abl* or with a single copy of just the tyrosine phosphatases (Fig. 4.13 A-C). The various genetic interaction experiments suggest that *bif* is a component of axon guidance pathways involving DPTPs and PP1-87B.

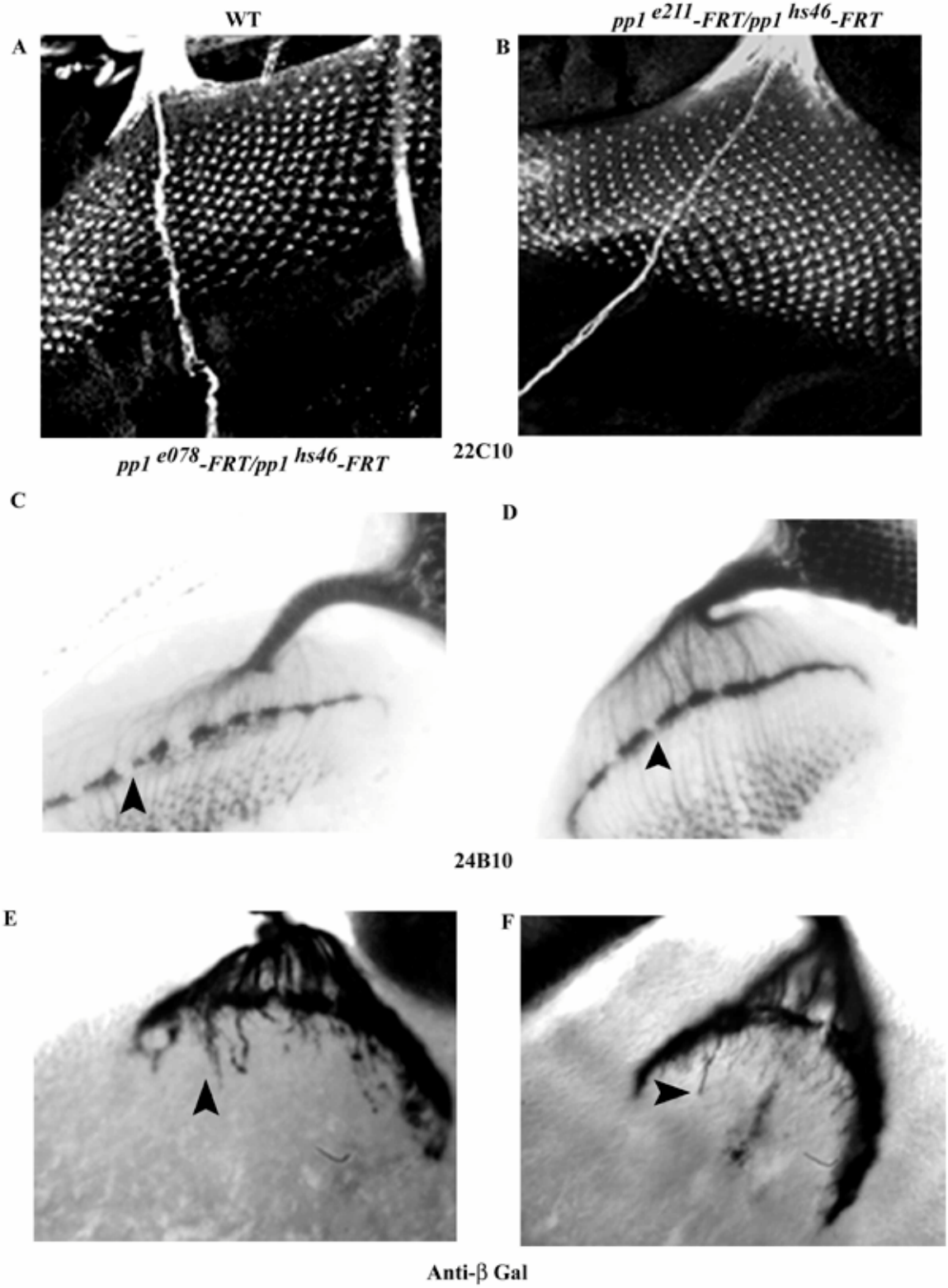

Fig. 4.12: Axonal defects seen in *pp1* mutants
Two alleles of *pp1* ($pp1^{e211}$ and $pp1^{e078}$) were studied in trans with the strong allele of *pp1*, $pp1^{hs46}$. When compared to WT they do not show any obvious defects in 22C10 staining in the larval eye disc (A and B). Both transheterozygous combinations show breaks (arrowheads in C and D) and clumps in the lamina as observed on staining with mAb 24B10 (C and D). Further using the Ro^{tau}-*LacZ* line both transheterozygous combinations show mistargeting of R2-R5 axons into the medulla (arrowheads in E and F).

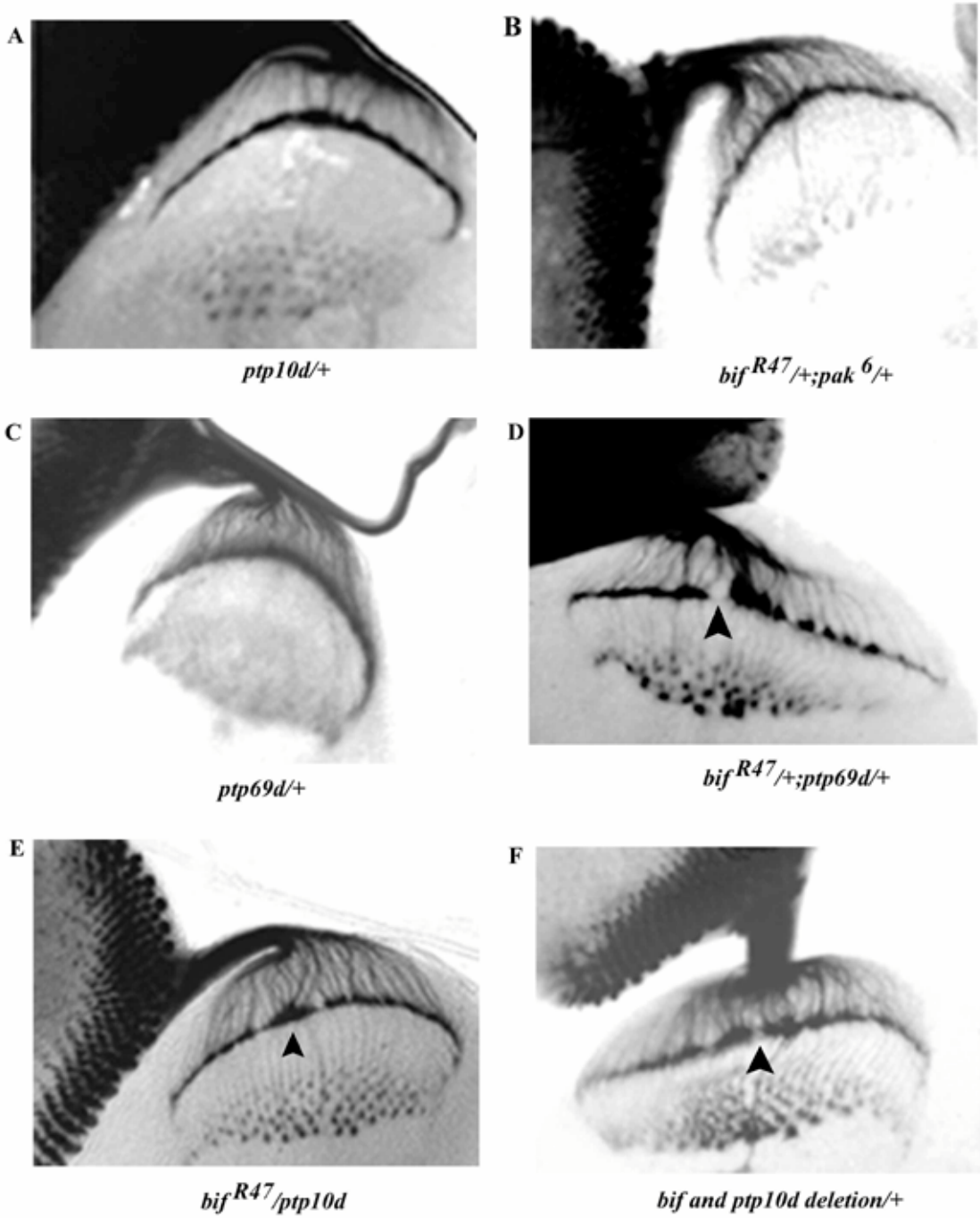

Fig. 4.13: Genetic interaction between *bif* and Receptor Tyrosine Phophatases
The receptor tyrosine phosphatases *rptp69d* and *dptp10d* genetically interacts with *bif*. A and C show control optic lobes from *ptp10d/+* (A) and *ptp69d/+* (B) which do not show any defects when stained with mAb 24B10. B shows *bif/+; pak/+* optic lobe, which again does not show an axonal phenotype. *bif* and *ptp69d* show a genetic interaction; *bif/+; ptp69d/+* optic lobes stained with mAb 24B10 show clumps and breaks (arrowhead in D) in the lamina. A similar phenotype is seen when one copy of *bif* and 1 copy of *ptp10d* are simultaneously removed, which shows breaks and clumps (arrowhead in E) in the lamina. 24B10 Ab stained eye disc from an animal heterozygous for a small deletion that removes both *bif* and *ptp10d* also shows clumps and breaks (arrowhead in F) in the lamina.

4.2.8. Bif directly binds F-actin *in vitro*

bif mutants show defects in the actin cytoskeleton (Bahri et al., 1997) and this work) and it has previously been shown that Bif from embryonic fly extracts can be pulled down using F-actin columns (Sisson et al., 2000), indicating that Bif is part of an actin-associated complex of proteins *in vivo*. So far, the mode of interaction between Bif and F-actin is not clear since Bif does not have any obvious actin binding domain (Bahri et al., 1997)**.** In order to determine whether the interaction of Bif with F-actin is direct, a co-sedimentation assay was performed using F-actin and *in vitro* translated Bif. In this experiment, Bif was pulled down by F-actin, indicating that Bif and F-actin can bind directly to each other (Fig. 4.14 A). Further dissection of the Bif protein mapped the F-actin-binding domain to 2 novel regions in the last 400 amino acids of the protein (Schematic in Fig. 4.14 B). These experiments indicate that the *in vivo* Bif/F-actin complexes may form through direct binding between these two proteins.

4.3. Discussion

This and previous work (Ruan *et al.*, 2002) shows that Bifocal is required for proper targeting of axons of the outer photoreceptors of the *Drosophila* visual system. I also show that this phenotype can be uncoupled from its function in maintaining R cell shape and morphology. In addition, the Bif interacting partner, PP1, is also required for axon guidance in the visual system. Mutations in *pp1* and *bif* show similar phenotypes, indicating that both genes function to promote the termination of R1-6 at the lamina. Furthermore, we have shown that *bif* functions in a genetic pathway that requires not only *PP1* but also the upstream signalling molecules Dptp10D and Rptp69D for proper axon guidance in the fly eye. In addition, we have

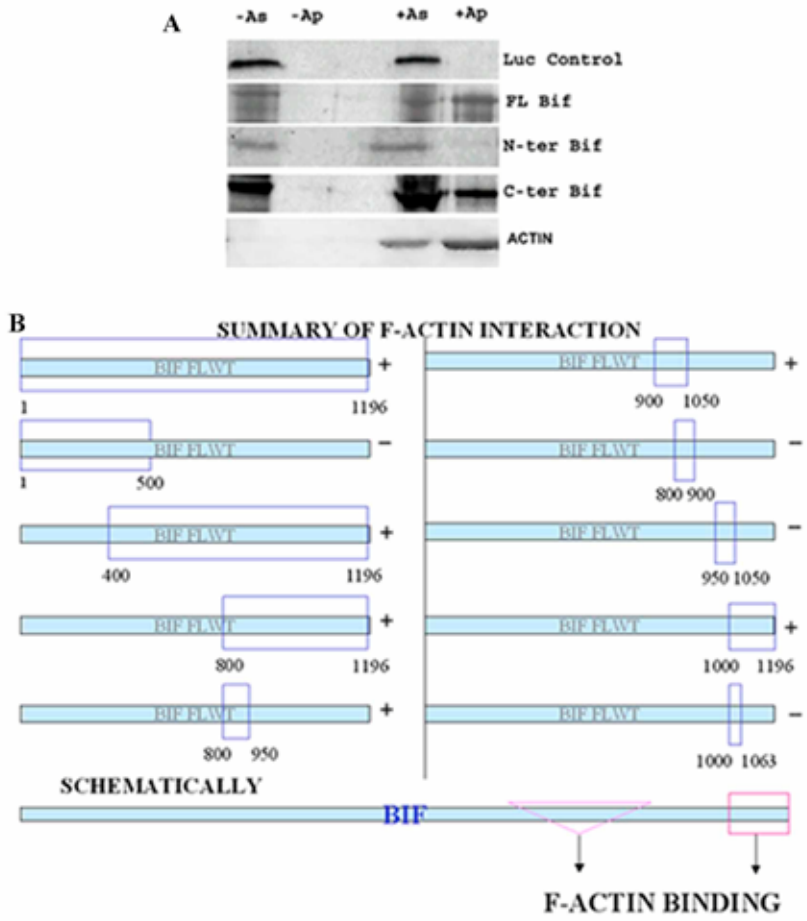

Fig. 4.14: Bif binds F-actin *in vitro*

Panel A shows a series of gels from F-actin co-sedimentation assay. The first rows are *in vitro* translated luciferase controls. Labelled Luciferase does not pellet with F-actin (+Ap). It remains in the supernatant in the presence (+As) or absence (-As) of F-actin. The second row shows *in vitro* translated full length Bifocal (FL Bif) which comes down with the F-actin pellet in the presence of F-actin and remains in the supernatant in the absence of F-actin. The third row shows the N-terminal 500aa of Bifocal (N-ter Bif) that does not come down with the F-actin pellet. The fourth row shows the interaction between the *in vitro* translated C terminal 396 amino acids of Bif (C-ter Bif) and F-actin, where the *in vitro* translated product comes down in a pellet with F-actin (last column, +Ap). The last row is a control gel stained with coomasie blue showing the absence of F-actin in the gel in the lanes –As and –Ap, and the presence of F-actin the lanes denoted by +As and +Ap.

Panel B shows schematic diagrams of the various regions of Bif with + indicating that the region represented in a rectangle box in the figure can bind F-actin *in vitro* and – indicating that the region of Bif represented in a rectangle box in the figure cannot bind F-actin *in vitro*. The last diagram in panel B schematically shows the 2 regions of Bif that can bind F-actin *in vitro*.

shown that Bif can directly bind F-actin and thus might provide a link connecting this axon guidance pathway to the underlying actin cytoskeleton.

The rescue experiments utilising the two different isoforms of *bif* demonstrate that the function of Bif in photoreceptor axon guidance can be uncoupled from its function in the maintenance of cell shape and morphology in photoreceptor cells (Bahri et al., 1997), indicating that Bif has a dual role in the fly visual system, normal axon connectivity in the larval stages and the formation of normal rhabdomeres in the adult eye. It is somewhat surprising to find that the two isoforms of Bif behave differently with respect to axon guidance since both isoforms contain the PP1 and actin binding sites. One possible explanation is that the additional sequences present in the bif^{+} isoform accounts for Bif function in axon guidance. The precise role of these sequences is not clear at present. It is possible for these sequences to affect protein folding or mediate binding to other partners. In this regard, one possibility is for these sequences to effect the subcellular localisation of one Bif isoform to the axons while the other isoform that lacks it remains in the cell body. It is not possible to distinguish between these possibilities, at the present time, since specific antibodies that recognise different isoforms of Bif are not available. It is also possible that expression of the longer isoform of Bif may also lead to some of the shorter isoform produces and hence one can only say at this point that although I have shown that the shorter bif^{10DA} isoform is not sufficient to rescue the eye defects it may be necessary for Bif axonal function in the eye. This possibility can only be anwered if one were to do rescue experiments to look at rescue of the eye defects and the axon guidance defects with three constructs; one that can make both the isoforms (using the natural promoter of *bif*, the second that is deficient for the longer isoform (this could be done by using a

frame shift in the extra coding region) and the this that is deficient for the shorter bif^{10DA} isoform (this could be made using a splice site mutation).

Mutations in the conserved phosphatase-binding motif in Bif, which abolish binding of Bif to PP1-87B, render the protein ineffective or less effective to function in axon guidance. Similar affects on Bif activity in the eye have been reported for these mutations (Helps et al., 2001). Another interesting aspect is that Bif can associate with cytoskeletal actin both in vivo (Sisson et al., 2000) and in vitro (this work). Changes in the actin cytoskeleton are essential for remodeling of the axon growth cone. These data suggest that, in addition to its regulatory effect on the phosphatase activity, Bif might serve as a direct link between PP187B and the actin cytoskeleton. Similar observations were reported for PP1 inhibitors in mammals. It has been shown that neurabins, the inhibitors for the PP1 homologue in mammals, PP1c, bind actin and serve as linkers between the actin cytoskeleton and the plasma membrane at the cadherin-based cell-cell adhesion sites. Neurabin I is seen to be highly concentrated at the synapse of developed neurons and in the lamellapodia of growth cones during the development of neurons suggesting that it could be required for synapse formation or function (MacMillan et al., 1999; McAvoy et al., 1999; Oliver et al., 2002; Terry-Lorenzo et al., 2002). Although it does not share any sequence homology with mammalian neurabins, Bif could be a functional homologue of the neurabins in the *Drosophila* larval visual system by associating with PP187B and the actin cytoskeleton. Such functions of Bif might consequently affect the phosphorylation status of various actin-binding proteins like myosin II (reviewed in (Tan et al., 1992) and cofilin (reviewed in (Lawler, 1999), which are known to undergo phosphorylation and dephosphorylation.

A role for PP1 itself in axonal connectivity in the larval optic lobe is supported by two observations. Firstly, driving PP1 inhibitors in the fly eye results in axon

defects. These inhibitors are not specific to PP187B, nevertheless they do support the notion that the phosphatase activity of PP1 is required for proper axon guidance. Secondly, transallelic combinations of *PP187B* mutants, which are able to bypass the earlier defects of cell cycle arrest that are usually seen in homozygotes of strong *pp187B* mutants, reveal axon targeting defects in the larval lamina. In these genetic combinations, formation of the R cells of the larval eye disc are not adversely affected, suggesting that the axon guidance phenotype of *pp187B* mutants is not simply due to the lack of R cells in the disc. Protein phosphatase 1 (PP1) is one of the most abundant eukaryotic protein phosphatases that dephosphorylates serine and threonine residues of its target proteins. The activities of various PP1 catalytic (PP1c) subunits are extensively regulated in various organisms and tissue types within a single organism. PP1c binds various regulatory molecules, which could bring the phosphatase to its site of action (reviewed in (Cohen, 2002) or act as adaptors for the phosphatase at its site of function. There are 5 related PP1c subunits in *Drosophila* (Carvalho et al., 2001; Dombradi et al., 1990b; Dombradi et al., 1993). *Drosophila* PP1s are very similar proteins encoded by different loci in the fly genome and they are variably regulated at different points in development (Alphey et al., 1997; Asztalos et al., 1993; Axton et al., 1990; Baksa et al., 1993; Bennett et al., 1999; Carvalho et al., 2001; Dombradi et al., 1990a; Dombradi et al., 1990b; Dombradi and Cohen, 1992; Dombradi et al., 1993; Helps et al., 2001; Helps et al., 1998; Raghavan et al., 2000) and reviewed in (Cohen, 2002). It is conceivable that Bif acts as one of the catalytic units of PP1 in the fly eye and is required either as a complex with PP1 and the actin cytoskeleton or required for recruiting PP1 to subcellular sites where the PP1 activity is required to modulate the actin cytoskeleton. The former hypothesis seems more plausible as *bif* mutant larval and pupal eye discs do not show any obvious changes in PP1 staining (Fig. 4.15 A-D).

PP1 staining in the pupal eye disc is very similar to Bif and F-actin and the staining in *bif* mutant is similar to F-actin in *bif* mutants (Fig. 4.15 D), indicating no obvious change in localisation from WT (Fig. 4.15 C) in the pupal eye disc. However, there could be minor defects not easily observable with the confocal, and the PP1 antibody cross reacting with any of the other 4 isoforms of PP1 present in *Drosophila* cannot be excluded.

Based on the genetic interaction between *bif* and the receptor tyrosine phosphatase genes, *dptp10d* and *dptp69d,* and its functional interactions with *PP1* and F-actin, a possible model for Bif function in axon guidance could be as follows: activation of receptor molecules leads to signalling events that activate Bif in the growth cone which in turn lead to inhibition of PP1 activity and changes in the actin cytoskeleton to support axon outgrowth and guidance. In this scenario, PP1 must have a threshold level of activity as absence of PP1-87B also causes axon guidance defects. Bif might participate in lowering PP1 activity to the threshold level but must not abolish all PP1 activity in order to allow normal photoreceptor axon guidance.

Finally, *bif* mutants affect axon targeting in the larval optic lobe but these defects seem to be corrected in the adult. How this axon defect is rectified in the adult stages remains unclear and probably occurs during the extensive regeneration that occurs during the pupal stages of fly development.

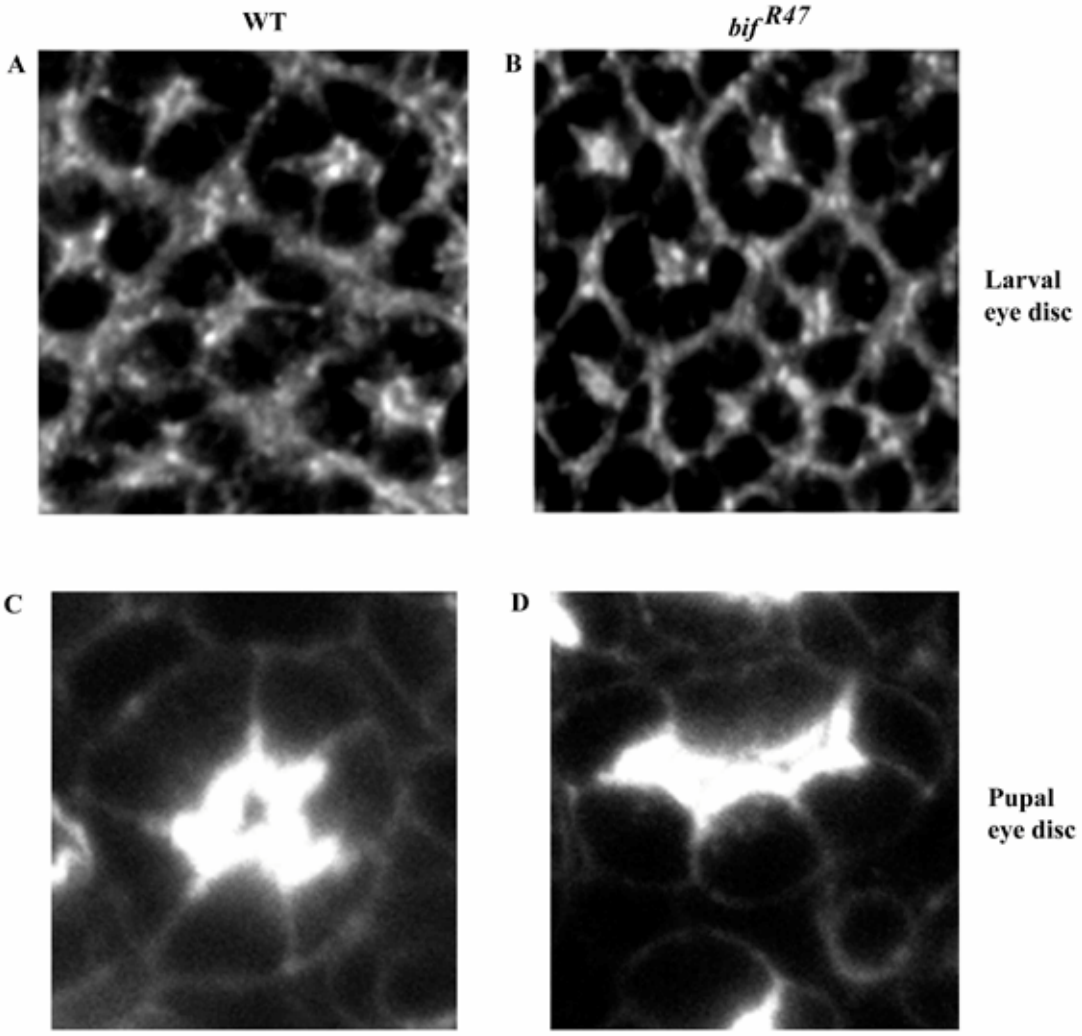

Fig. 4.15: WT and *bif* mutant eye discs showing expression of PP1 protein
Panels A and B show larval eye discs stained with anti-PP1 antibody. In both WT (A) and *bif* (B) eye discs, PP1 is expressed in the photoreceptor cells. Panels C and D show anti PP1 staining in 55 hour pupal eye discs, where PP1 is expressed in a pattern similar to F-actin in WT (C) and *bif* mutant (D) eye discs. PP1 expression is seen enriched in a star like pattern in WT eye discs (C) and in a more compressed pattern in *bif*^{R47} mutant eye discs (D).

4.4. Future directions

Future work pertaining to this chapter includes:

1. It has been shown previously that overexpression of Bif in cells causes excess F-actin being formed. It will be interesting to see how the F-actin cytoskeleton is affected when PP1 is over-expressed alone, as well as when both Bif and PP1 are over-expressed.
2. To do genetic experiments to find the hierarchy between Bif, PP1 and Msn. This part of the work would involve overexpression of Bif, PP1 and Msn individually in various mutant backgrounds and looking at the affects of transheterozygous and double mutant combinations on larval photoreceptor axon targeting.

Chapter 5

Role of Bifocal and Homer in Oogenesis

5.1. Introduction:

Drosophila Homer (Hom), the *Drosophila* homologue of the vertebrate Homer (Brakeman *et al.*, 1997) is an F-actin binding protein (Shiraishi *et al.*, 1999). Mutants in *hom* show defects in locomotor activity and mating behaviour (Diagana *et al.*, 2002). As mentioned in the previous chapters of this thesis Bifocal (Bif) is a novel protein, which has been shown to co-localise with F-actin and is required for normal photoreceptor rhabdomere formation and axon guidance (Helps et al., 2001; Ruan et al., 2002). Bif has been shown to form a complex with both F-actin and microtubules (Sisson et al., 2000). Total loss of function of *bif* or *hom* are viable and fertile with no obvious embryonic defects (Bahri et al., 1997; Diagana et al., 2002). Here I show that simultaneous loss of both Homer (Diagana *et al.*, 2002) and Bifocal (Bahri et al., 1997), gives rise to essentially sterile females which show defects in oogenesis.

The large cells of the *Drosophila* egg chamber make it an excellent system for identifying genes involved in the generation of cell polarity. Early on during oogenesis, a microtubule organising centre (MTOC) forms within the oocyte, which directs the transport of newly synthesised material along microtubules from the nurse cells into the developing oocyte. Then, at stages 7–8, the oocyte microtubule cytoskeleton undergoes a dramatic re-organisation in response to a signal from the overlying posterior follicle cells (Theurkauf *et al.*, 1992). This re-organisation of the microtubules is also required for posteriorly localised

molecules, like Staufen and *osk* RNA, to move from the anterior of the oocyte to the posterior cortex where they are localised as a tight crescent throughout the rest of oogenesis (illustrated in Fig. 5.1A) (St Johnston, 1993).

The MTOC is disassembled and microtubules become nucleated at the anterior cortex of the oocyte, generating a gradient of microtubules with their `plus' ends tightly focused at the posterior pole (Gonzalez-Reyes *et al.*, 1995). As microtubule inhibitors and mutations which disrupt microtubule organisation (Benton *et al.*, 2002) or microtubule motor function (Clark *et al.*, 1994) block the proper localisation of polar markers such as *oskar* mRNA, microtubules are thought to play a critical role in the establishment of oocyte polarity. Although the evidence that microtubules contribute to the establishment of oocyte polarity is compelling, the role of the actin cytoskeleton in this process is less clear. Rather surprisingly, however, several genes identified by their mRNA mislocalisation phenotype were found, upon cloning, to code for conserved actin-binding proteins. Several of these mutations, such as those affecting profilin (Manseau *et al.*, 1996), disrupt oocyte polarity, probably in part as an indirect consequence of changes in microtubule organisation. The new functional analysis of Dmoesin (Jankovics *et al.*, 2002; Polesello *et al.*, 2002), however, shows that the actin-rich cortex plays a second role in the localisation of posterior determinants within the *Drosophila* oocyte.

The data**,** to date, suggest that, during oogenesis, *oskar* mRNA is first transported to the ends of microtubules by the plus-end directed motor kinesin I (Brendza *et al.*, 2000). Then, upon arrival at the posterior pole of the oocyte, *oskar* mRNA becomes tethered at the cortex and once tethered gets translated to give Osk proteins (so far two isoforms of Osk are known). The proteins then undergo modifications (most probably phosphorylation) and these proteins enable more *osk*

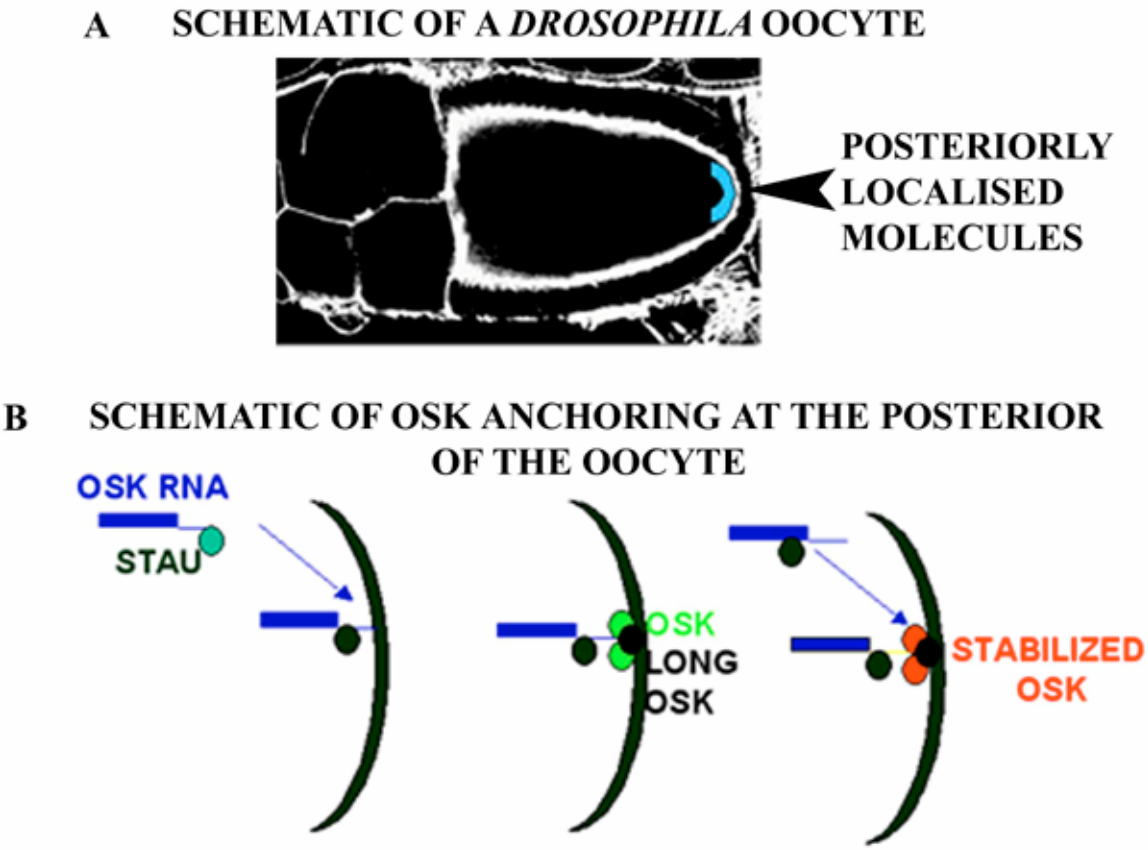

Fig. 5.1: Schematic of an oocyte and Osk localisation at the posterior cortex of the Oocyte adapted from (Riechmann *et al.*, 2002)
A shows a schematic of the posterior localisation of molecules in a stage 10 oocyte and B shows a cartoon of Osk localisation and anchoring to the posterior of the oocyte.

RNA to come to the posterior and give rise to an effective feed back loop mechanism (a schematic of this process is shown in Fig. 5.1B). It has also been shown that the longer isoform of Osk plays an important role in anchoring Osk protein and RNA to the posterior cortex of the oocyte (Markussen *et al.*, 1995; Riechmann *et al.*, 2002; Rongo *et al.*, 1995; Vanzo and Ephrussi, 2002).

The existence of a cortical anchor for posterior determinants is likely to serve several related functions. First, an anchor is absolutely required to maintain the polar localisation of posterior determinants during 'cytoplasmic streaming', when the ooplasm swirls in a washing-machine-like vortex (Theurkauf *et al.*, 1992). In fact, *oskar* mRNA must remain tethered at the cortex until early embryogenesis (Tetzlaff *et al.*, 1996). Second, an anchor may also be required at late stages 8-9 to capture residual posterior determinants as they enter the oocyte from nurse cells (Erdelyi *et al.*, 1995). Finally, the anchor may be an important element of the feed-forward loop described above, helping to break oocyte symmetry by generating a molecular memory of prior mRNA and protein localisation (reviewed in (Baum, 2002). The actin cytoskeleton may play a role as an anchor for the posterior group molecules as is apparently the case of asymmetric localisation of determinants in the neuroblasts (Broadus and Doe, 1997; Jan and Jan, 1998).

Analysis of the *bif; hom* double mutants indicates simultaneous loss of both of these molecules in flies, while not affecting *osk* mRNA transport and translation, delocalises *osk* RNA and proteins from the posterior cortex (Babu *et al.*, 2004). Further, the analysis of these double mutants helps shed some more light into the fairly elusive mechanism of anchoring of Osk to the posterior cortex. So far apart from moesin (Jankovics *et al.*, 2002; Polesello *et al.*, 2002), the only other

molecules known to be involved in Osk anchoring in the oocyte are Osk itself (Vanzo and Ephrussi, 2002) and Stau (Micklem *et al.*, 2000).

Latrunculin A disruption of actin microfilaments, which causes delocalisation of Bifocal but not Homer from the posterior cortex of wild type oocytes, causes only minor defects in the anchoring of *osk* gene products; however Latrunculin A disruption in the absence of Homer, but not in the absence of Bifocal, causes severe defects in posterior anchoring of *osk* RNA and proteins. Our data suggest that two processes, one that requires Bifocal and an intact F-actin cytoskeleton and a second process requiring Homer but independent of an intact F-actin cytoskeleton, may act redundantly to mediate posterior anchoring of the *osk* gene products.

5.2. Results:

5.2.1. Bif and Homer (Hom) are 2 F-actin binding proteins localised apically in Neuroblasts

Both Bif and Hom show asymmetric localisation at the apical cortex of mitotic embryonic neuroblasts (Fig. 5.2 A-C), indicating that these two F-actin binding proteins may be involved in neuroblast asymmetric divisions. However, animals lacking both the maternal and zygotic components of either gene are fertile, viable and show no obvious defects in embryonic CNS development. This prompted me to make double mutants of *bif* and *hom.* However, although double homozygous mutant females are viable, they show defects in oogenesis, with the great majority of the eggs produced remaining unfertilised as judged by the lack of staining in eggs using an antibody directed against the sperm tail (Graner et al., 1994; Karr, 1991) (Fig. 5.3 A, B). Further, on staining the oocytes with Anti-Bif and Anti-Hom antibodies, I found

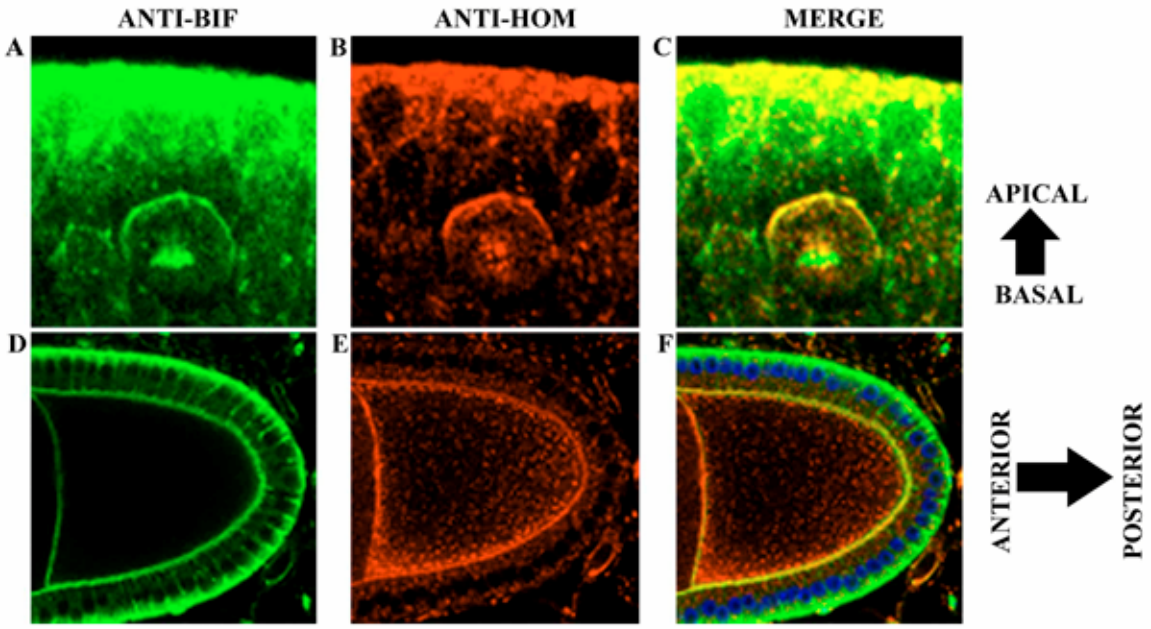

Fig. 5.2: Bif and Hom localisation in Neuroblasts and oocytes
A and B show Bif (green) and Hom (red) localisation in embryonic Neuroblasts (NB) and C is a merge of the figures A and B. Note that Bif and Hom show apical enrichment in the NB. The DNA stain in this figure is also in green and indicates that the NB is in metaphase. D and E show Bif (green) and Hom (red) staining in the oocyte and F is a merge of figures D and E. Note that Bif shows a cortical localisation in the oocyte while Hom shows a predominantly cytoplasmic as well as a cortical staining in the oocyte. DNA is stained in blue and indicated the location of the follicle cell nuclei.

that both molecules co-localise in the cortex of the oocyte and Homer also shows cytoplasmic staining in the oocyte (Fig. 5.2 D-F).

In the few fertilised embryos that do undergo development, the numbers of Vasa positive germ cells are drastically reduced (from ~33 in wt, n=15; to 7 in double mutants, n=12; Fig. 5.3 C, D), suggesting possible defects in the function or localisation of posterior determinants during oogenesis.

5.2.2. *bif;hom* double mutants show defects in the anchoring of *osk* RNA and proteins

Analyses of wt, *bif* and *hom* single mutants as well as double mutant oocytes indicate that the two genes act in a redundant manner for the correct anchoring of posteriorly but not anteriorly localised molecules, in stage 10 oocytes. Posterior group molecules, include *oskar* (*osk*) RNA and the 2 isoforms of Osk proteins (Rongo *et al.*, 1995) and Staufen (Stau) (St Johnston *et al.*, 1991). A fusion protein in which β-Galactosidase has been fused to the N-terminal extension of the long form of the Osk protein (referred to as Osk-βGal) is used as a marker for the long form of the Osk protein, which has been shown to have a role in the posterior cortical maintenance of Osk (Gunkel *et al.*, 1998; Vanzo and Ephrussi, 2002). All of these components are localised as a tight posterior cortical crescent in wild type (wt) oocytes (Schematic in Fig. 5.1 A and Fig. 5.4 A-D). In most double mutant oocytes, these molecules, when detectable, are present largely at the posterior region, however in contrast to wt oocytes, they show a diffuse distribution that extends into regions of the posterior cytoplasm distinctly interior to the posterior cortex (Fig. 5.4 E-H). In about 30% of the cases, Osk or Stau protein cannot be detected (Fig. 5.4 I and K and see Table 5.1 for quantification). The defects seen in the oocytes of double mutants are essentially

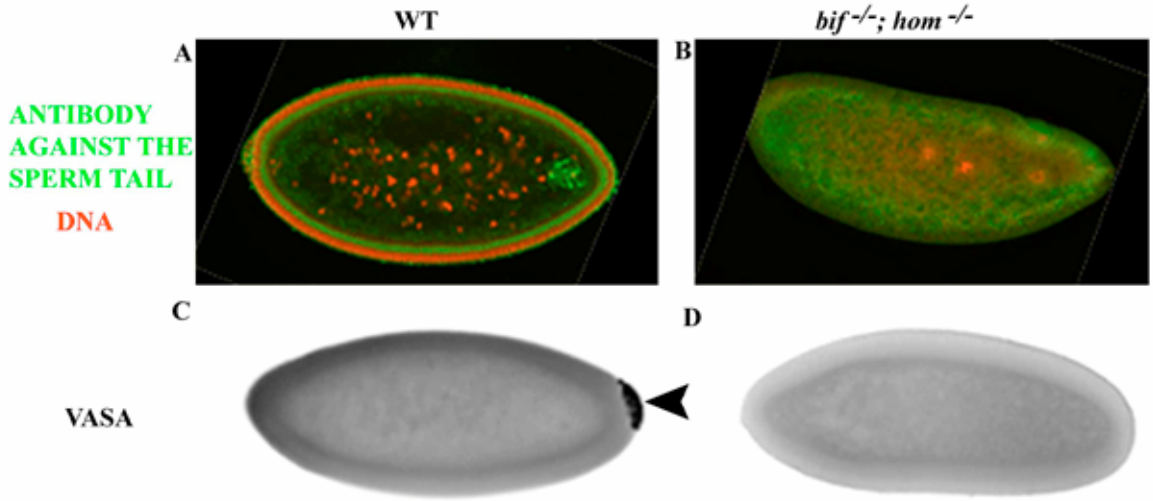

Fig. 5.3: Sperm tail and pole cell staining in WT and double mutant embryos
A and B show staining of wild type (A) and *bif* $^{-/-}$*; hom* $^{-/-}$ (B) embryos stained with an antibody that recognises the sperm tail (DROP 1.1 in green). Note that WT embryos show a coiled staining of the sperm tail while this staining is absent in the double mutant embryos. DNA is shown stained in red in the figures. C and D show Vasa staining in WT (C) and *bif* $^{-/-}$*; hom* $^{-/-}$ double mutants (D), on the few embryos that are fertilised. Note that the cells staining Vasa positive at the posterior pole of WT embryos (arrowhead in C) are absent in the double mutant embryos.

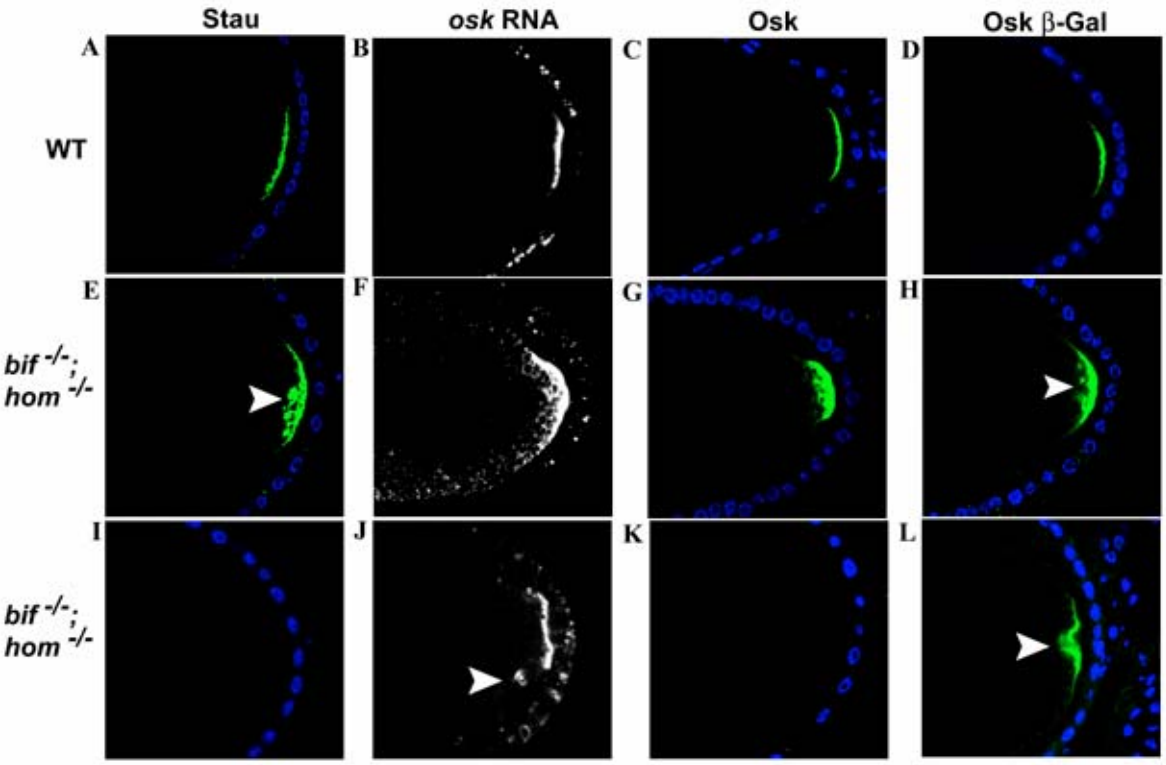

Fig. 5.4: Loss of both *bifocal* and *homer* causes defective anchoring of the posterior determinants in oocytes

Stage 10 WT and *bif;hom* double mutant oocytes showing the localisation of Stau (green), *osk* RNA (white), Osk (green) and Osk-βGal (green). Two sets of double mutant oocytes are shown (E-L) to illustrate the different severity of the phenotypes observed; for example Stau and Osk can either be loosely cytoplasmic (E, G, H) or undetectable (I, L). Arrowheads point to sites of cytoplasmic localisation. DNA staining (blue) marks the position of follicle cell nuclei.

Table 5.1: Phenotypes seen in *bif;hom* double mutant oocytes

genotype	STAUFEN			*oskar* RNA			OSKAR			Osk-β Gal		
	Faint or Loss of stain	Diffuse stain	Cytopl-asmic stain	Faint or Loss of stain	Diffuse stain	Cytopl-asmic stain	Faint or Loss of stain	Diffuse stain	Cytopl-asmic stain	Faint or Loss of stain	Diffuse stain	Cytopl-asmic stain
WT stg 9	1/30 (3.3%)	1/30 (3.3%)	0/30 (0%)	0/8 (0%)	0/8 (0%)	0/8 (0%)	0/24 (0%)	1/24 (4.2%)	0/24 (0%)	0/17 (0%)	0/17 (0%)	0/17 (0%)
WT stg 10A	0/14 (0%)	0/14 (0%)	0/14 (0%)	0/7 (0%)	0/7 (0%)	0/7 (0%)	0/11 (0%)	0/11 (0%)	0/11 (0%)	0/23 (0%)	1/23 (4.3%)	0/23 (0%)
WT stg 10B	1/27 (3.7%)	0/27 (0%)	0/27 (0%)	1/14 (7.1%)	0/14 (0%)	0/14 (0%)	1/14 (7.1%)	0/14 (0%)	0/14 (0%)	1/29 (3.4%)	0/29 (0%)	0/29 (0%)
bif$^{-/-}$; *hom*$^{-/-}$ stg 9	0/26 (0%)	2/26 (7.6%)	0/26 (0%)	1/20 (5%)	0/20 (0%)	0/20 (0%)	1/36 (2.8%)	2/36 (5.6%)	0/36 (0%)	0/11 (0%)	2/11 (18.1%)	0/11 (0%)
bif$^{-/-}$; *hom*$^{-/-}$ stg 10A	0/12 (0%)	7/12 (58.3%)	1/12 (8.3%)	1/16 (6.25%)	8/16 (50%)	2/16 (12.5%)	0/22 (0%)	8/22 (36.4%)	3/22 (13.6%)	4/15 (26.7%)	6/15 (40%)	0/15 (0%)
bif$^{-/-}$; *hom*$^{-/-}$ stg 10B	12/27 (44.4%)	8/27 (29.6%)	4/27 (14.8%)	2/18 (11.1%)	12/18 (66.7%)	3/18 (16.7%)	8/25 (32%)	15/25 (60%)	0/25 (0%)	5/20 (25%)	14/20 (70%)	0/20 (0%)

In *bif; hom* double mutant oocytes the localisation of the posterior group molecules show a range of phenotypes. I have artificially divided these into three classes (some examples are shown in Fig. 5.4). Note that diffuse staining indicates staining at the posterior of the oocyte where the posterior group molecules are not present as a tight cortical crescent but show a predominantly posterior cortical and cytoplasmic staining (as seen in Fig. 5.4G). Whereas cytoplasmic staining indicates staining that shows a distinct cytoplasmic localisation of the Protein or RNA along with a posterior staining (an example is shown in Fig. 5.4F).

absent in the single mutant oocytes. These findings indicate that whereas *bif* and *hom* are individually dispensable, together they are required for the localisation of the posterior components of the oocytes. These defects in localisation are specific for the posterior group molecules since the anterior/dorsal localisation of Gurken (Neuman-Silberberg and Schupbach, 1996) and anterior localisation of *bicoid* RNA(Berleth *et al.*, 1988) are unaffected (Fig. 5.6 A-D). It is well known that the F-actin cytoskeleton is necessary for the proper anchoring of molecules to the cell cortex (Broadus and Doe, 1997; Jan and Jan, 1998). Therefore, it seemed likely that Bif and Hom could be acting via the F-actin cytoskeleton and would then be localised in the cortex in a manner similar to F-actin, which is visualised using phalloidin staining. To address this question, two sets of staining, one with Phalloidin and Bif and the other with Phalloidin and Hom were done on wt oocytes. Staining with anti-Bif (Helps et al., 2001) antibody indicates that Bif localises to the oocyte cortex in a manner very similar to that seen for F-actin (Fig. 5.8 A, B). The staining seen with the anti-Homer antibody is highly punctated and, although localisation is cortically enriched, Hom is also present in the cytoplasm (Fig. 5.8 E. F). This cortical staining seen in wt oocytes (and nurse cells) is absent in mutant oocytes stained with the corresponding antibodies, confirming the specificity of both antibodies and that the mutants are protein nulls (Fig. 5.8 I, J).

Several observations indicate that the defect in posterior localisation of the *osk* gene products is due to defective anchoring and not transport or translation of *osk* RNA. *Osk* RNA as well as Stau are localised normally in stage 9 double mutant oocytes (Fig. 5.5 A-D). Consistent with this, both the F-actin and microtubule cytoskeletons in the double mutants are indistinguishable from those in the wt oocytes (Fig. 5.6 E-H). Not only does the polarity of the microtubules appear normal as

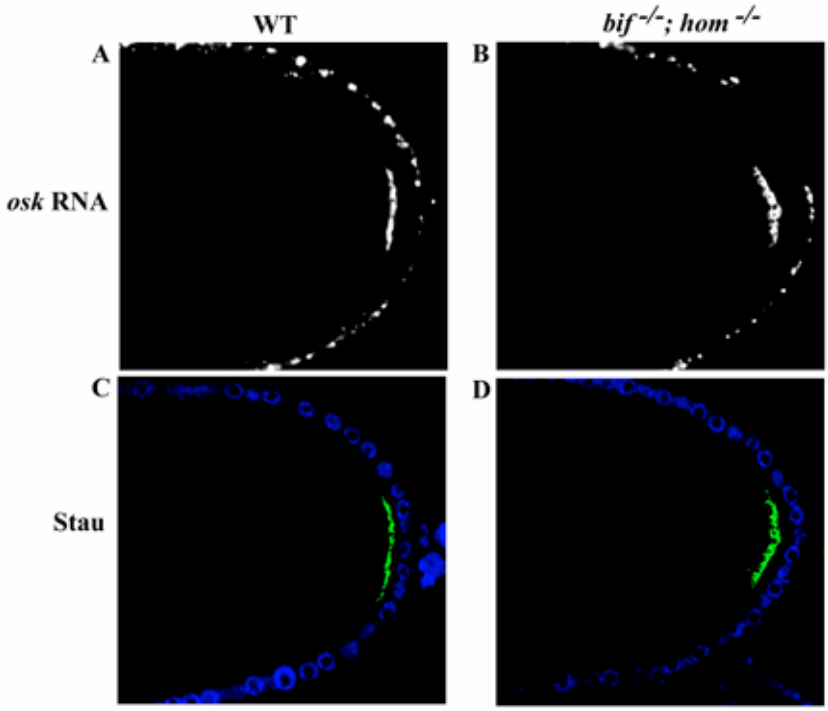

Fig. 5.5: Normal localisation of *osk* RNA and Stau protein in stage 9 double mutant oocytes
osk RNA (white) and Stau (green) localisation in WT (A and C) and double mutant (B and D) stage 9 oocytes; the normal localisation seen at stage 9 indicate that the defects seen in stage 10 double mutant oocytes are due to defects in anchoring.

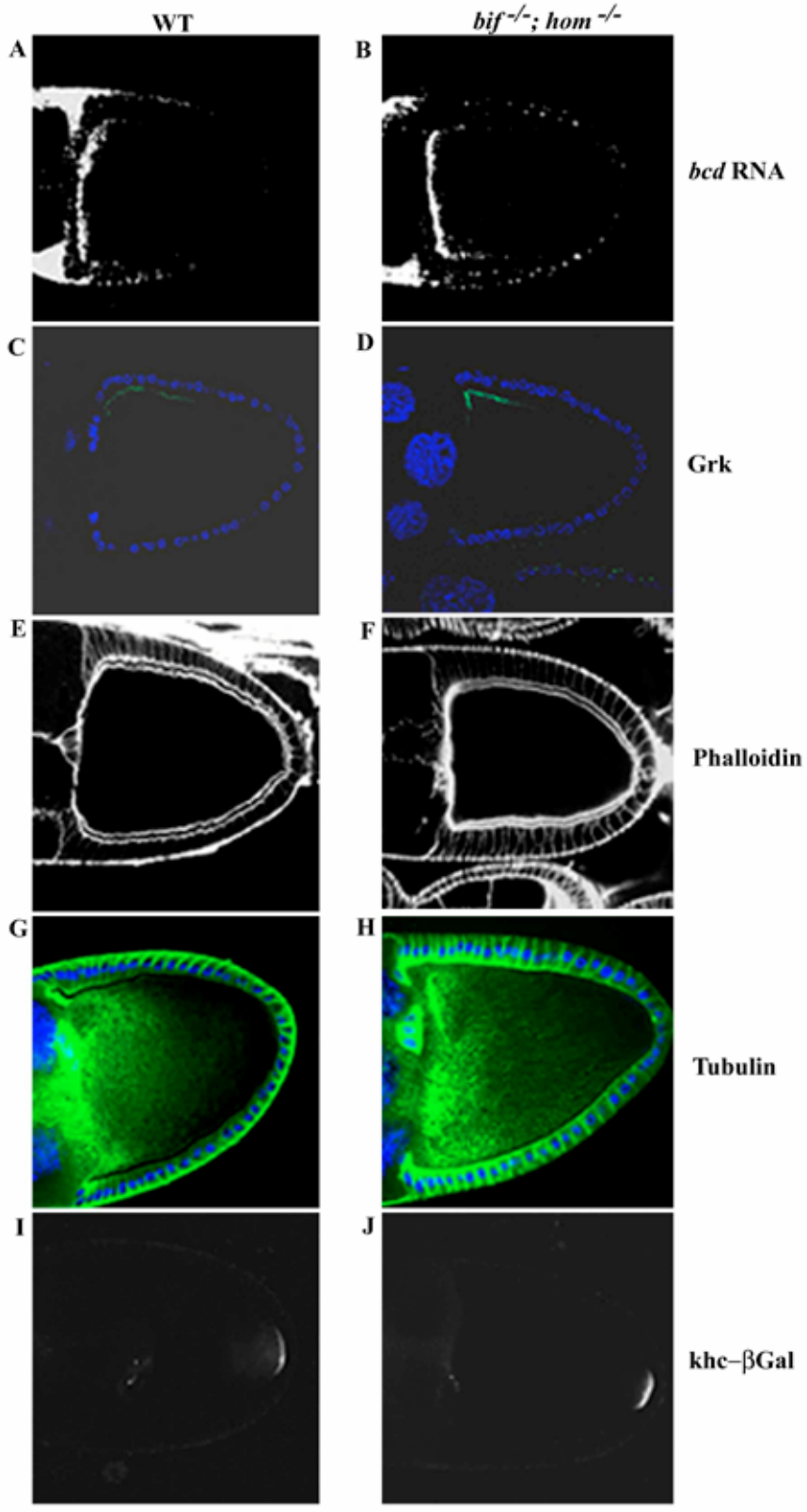

Fig. 5.6: Normal localisation of Anterior and cytoskeletal components in the double mutant oocytes

Stage 10 WT (A, C, E, G and I) and double mutant (B, D, F, H and J) oocytes assessed with *bcd* RNA in situ (A and B), anti Gurken antibody (C and D), phalloidin (E and F), tubulin (G and H) and khc-βGal (I and J) all of which appear to be normal.

assayed using a *kinesin heavy chain* (*khc*) β-Gal marker (Brendza *et al.*, 2000; Clark *et al.*, 1994) (Fig. 5.6 I and J), the cytoskeleton dependent cytoplasmic streaming occurs normally in stage 10 double mutant oocytes as is seen with wt oocytes (Fig. 5.7, *cappuccino* mutant oocytes which show enhanced streaming were analysed as a control). Taken together these observations indicate that the double mutant oocytes retain, at a gross level, normal cytoskeletal structure. They can transport *osk* mRNA to the posterior cortex, and translate it appropriately, but do not maintain the posterior anchoring of the *osk* gene products.

5.2.3. Role of F-actin in the localisation of Osk, Bif and Hom

An intact F-actin cytoskeleton is thought to be required for asymmetric protein localisation in several contexts (reviewed in (Jan and Jan, 1998). In the oocyte, loss or reduction of the actin binding proteins moesin and tropomyosin have been shown to affect the posterior anchoring of Osk in the oocyte and the embryo, respectively (Erdelyi *et al.*, 1995; Jankovics *et al.*, 2002; Polesello *et al.*, 2002; Tetzlaff *et al.*, 1996). To assess the requirement for an intact microfilament cytoskeleton for the anchoring of *osk* RNA and proteins in the oocyte, the localisation of these molecules were examined in wt oocytes treated with an actin de-polymerising drug Latrunculin A (Spector *et al.*, 1983) (Lat A). Following treatment with 20μM Lat A, cortical F-actin in the oocytes was largely undetectable with phalloidin; yet, unexpectedly, both Osk proteins (short and Osk-βGal) and *osk* RNA remain localised to the posterior cortex of the great majority of wt oocytes from stage 9-10B (Fig. 5.9 A-C and see Table 5.2 for quantification); in around 17% of the Lat A treated wt oocytes, mild defects in anchoring are observed; *osk* RNA and proteins show a diffuse localisation at the posterior cortex however in no cases were they seen concentrated in the cytoplasm or

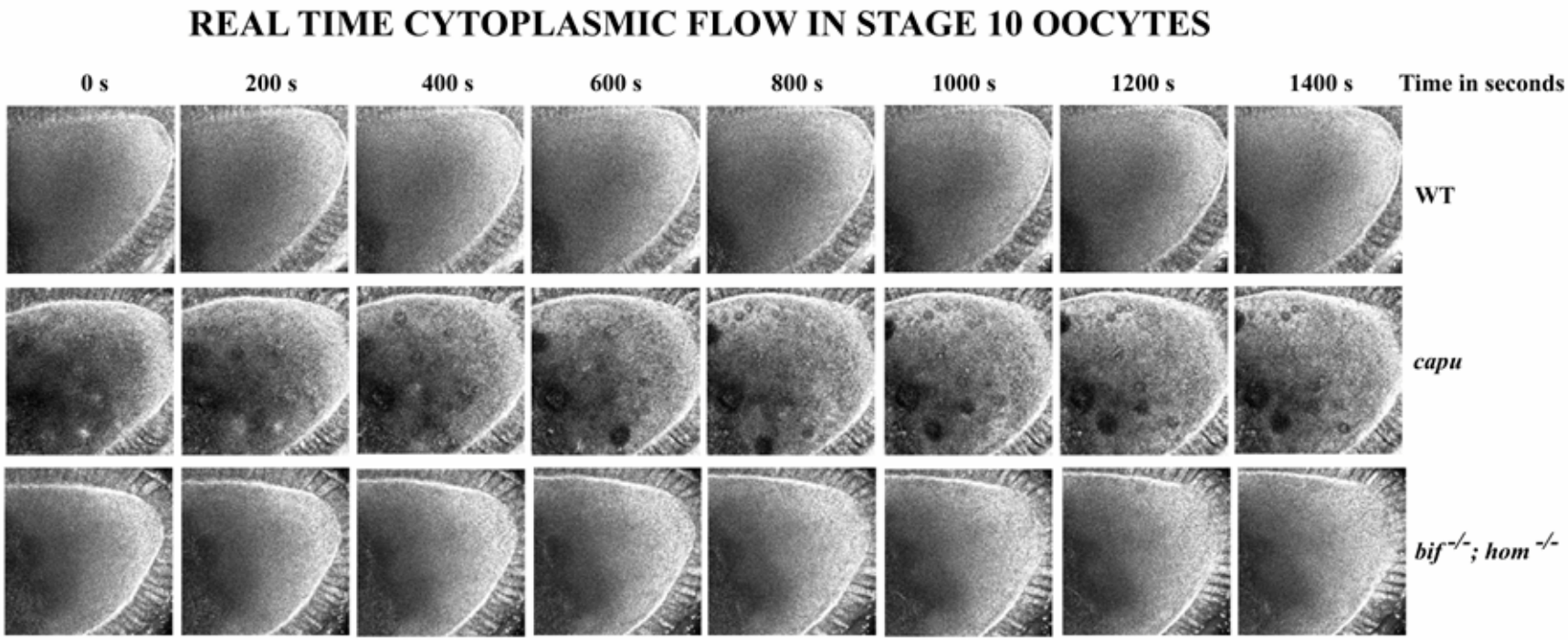

Fig. 5.7: Time lapse of cytoplasmic streaming in oocytes
Different time points taken of cytoplasmic streaming motion in a live oocyte.
The first panel analyses wt oocytes for up to 23 minutes and 20 seconds. The second and third panels show *capu* mutant oocytes and the double mutant oocytes respectively, analysed at the same time points. Note that the changes in the cytoplasm at the various time points in the *capu* oocyte are very easily observable and occur to a much lesser extent in WT and *bif* $^{-/-}$*; hom* $^{-/-}$ oocytes.

become delocalised or undetectable (as seen in the *hom*/*bif* double mutant oocytes) as would be expected if an intact F-actin cytoskeleton were to be an absolute requirement for the normal anchoring of Osk. These mild affects on protein localisation in the oocyte are in distinct contrast to those seen in embryonic neuroblasts where severe and high penetrance defects in asymmetric protein localisation are observed following disruption of microfilaments (Broadus and Doe, 1997). These observations suggest that the role of microfilaments in the anchoring of proteins to the cortex may differ in the different cellular contexts.

Additional experiments were performed to ascertain that the mild affect on Osk posterior anchoring following disruption of microfilaments is not peculiar to Lat A treatment. In fact the posterior cortical localisation of Osk remain in the great majority of oocytes even after treatment with cytochalasin D (CD), Lat A followed by CD, CD followed by Lat A and up to 100μM Lat A. (Fig. 5.10 A-C and, see Table 5.3 for quantification). These results are consistent with previous reports of CD disruption of F-actin, e.g. (Cha *et al.*, 2002); however, they indicate that an intact F-actin cytoskeleton although required for the normal posterior anchoring of Osk in a small proportion of oocytes is probably not the only factor involved in normal anchoring of Osk to the posterior cortex. There are at least two possible explanations for these observations. First, there remains a small amount of residual F-actin even after sequential treatment with Lat A and CD, which is sufficient to anchor Osk normally in a small fraction of the drug, treated oocytes. Alternatively, there may be other factors besides an intact F-actin cytoskeleton, which can, in parallel, contribute towards the posterior anchoring of *osk* RNA and protein.

Since disrupting the F-actin cytoskeleton did not seem to have a drastic affect on the localisation of Osk in the oocyte, I went on to assess the requirement for intact

microfilaments on Homer and Bif localisation. Both Bif and Hom localise to the cortex (and in the case of Hom also the cytoplasm) of wt oocytes (Fig. 5.8 A, E). Following depolymerisation of F-actin with Lat A, such that cortical F-actin becomes undetectable in the oocyte, Hom localisation appears unchanged from the wt pattern in all oocytes (Fig. 5.8 G, H, n=49) but Bif becomes highly diffuse with essentially no detectable enrichment at the cortex (Fig. 5.8 C, D, n=55). This appears to be an affect on Bif localisation and not stability since the levels of the protein are not reduced as judged by Western analysis.

These findings raise the possibility that *bif* function might be dependent on intact F-actin; however Hom localisation is Lat A insensitive, suggesting that its function in the oocyte may not require intact microfilaments. However, the possibility that Lat A treatment allows for the retention of a small amount of the F-actin cytoskeleton and this is stabilised in some way by Homer, hence there is a severe anchoring defect only in the absence of Hom in the Lat A treated oocytes, cannot be excluded.

5.2.4. Hom is required for Osk anchoring in the absence of an intact F-actin cytoskeleton

These data raise the possibility that there are two processes, one that is microfilament dependent and requires Bif and another, which is not dependent on intact microfilaments and requires Hom. Either process is sufficient to anchor the *osk* gene products to the posterior cortex of the great majority of the oocytes. One prediction of this hypothesis is that *hom* should be necessary to anchor posterior components in the absence of intact F-actin. Indeed when *hom* single mutant oocytes were treated with Lat A, I found a large amount of cytoplasmic Osk at stages 9 and 10

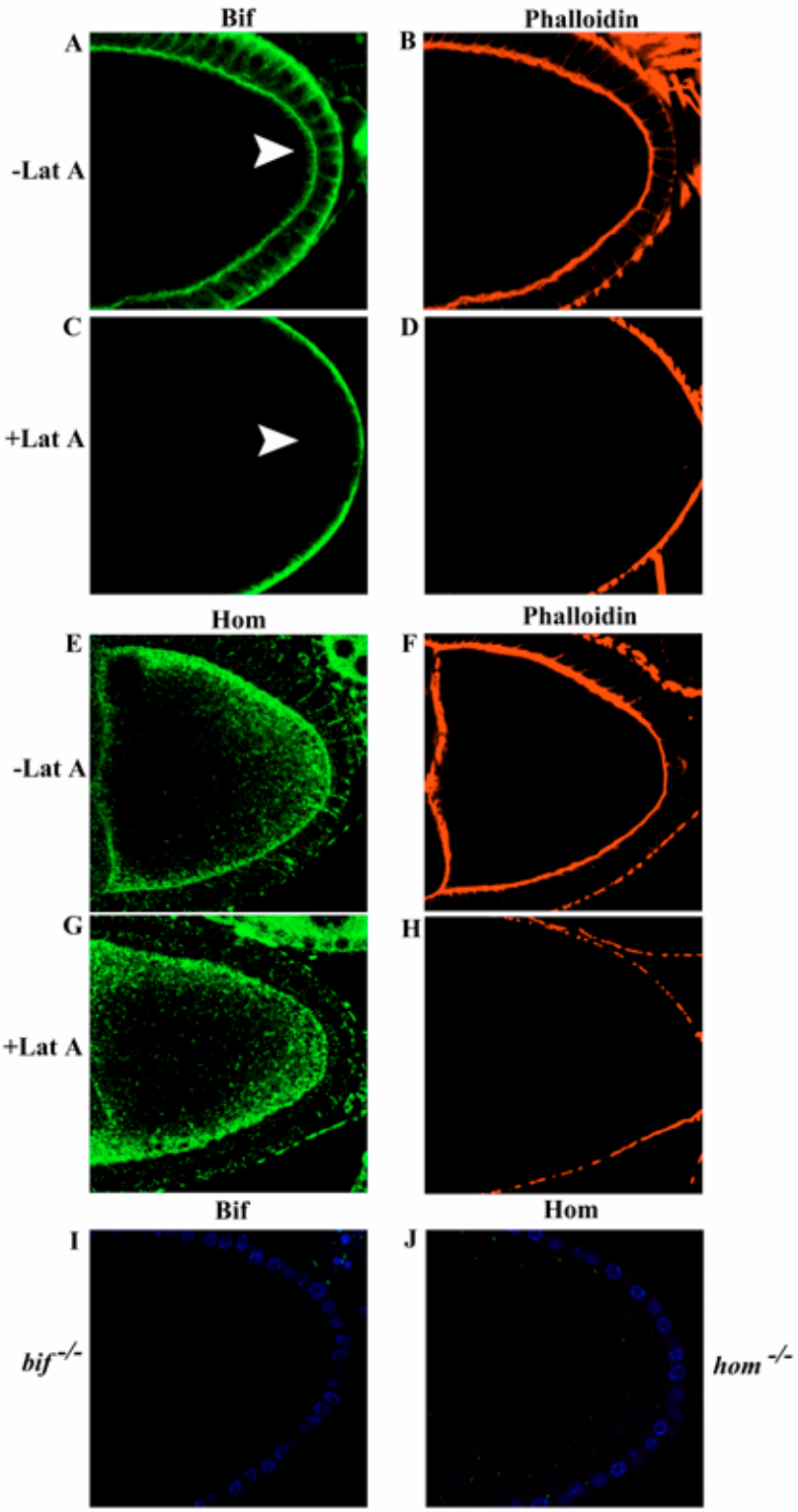

Fig. 5.8: Bifocal and Homer localisation in the presence and absence of intact microfilaments

Anti-Bif (green) and phalloidin (red) staining of Lat A treated and untreated WT oocytes (A-D). Note that cortical Bif staining (arrowheads) in the oocyte disappears in the absence of an intact F-actin cytoskeleton. Anti-Hom (green) and phalloidin (red) staining in the presence and absence of Lat A treatment (E-H). Note that Hom staining at the cortex of the oocyte remains even in the absence of an intact F-actin cytoskeleton. I and J are Anti- Bif (I) and anti-Hom (J) staining of their respective mutant oocytes. In these oocytes the follicle cell nuclei are in blue. Note that in Lat A treated ovaries, residual phalloidin staining remains on the exterior border of the follicle cells although it is totally absent from the oocyte cortex, perhaps due to a lower actin turnover in the follicle cells.

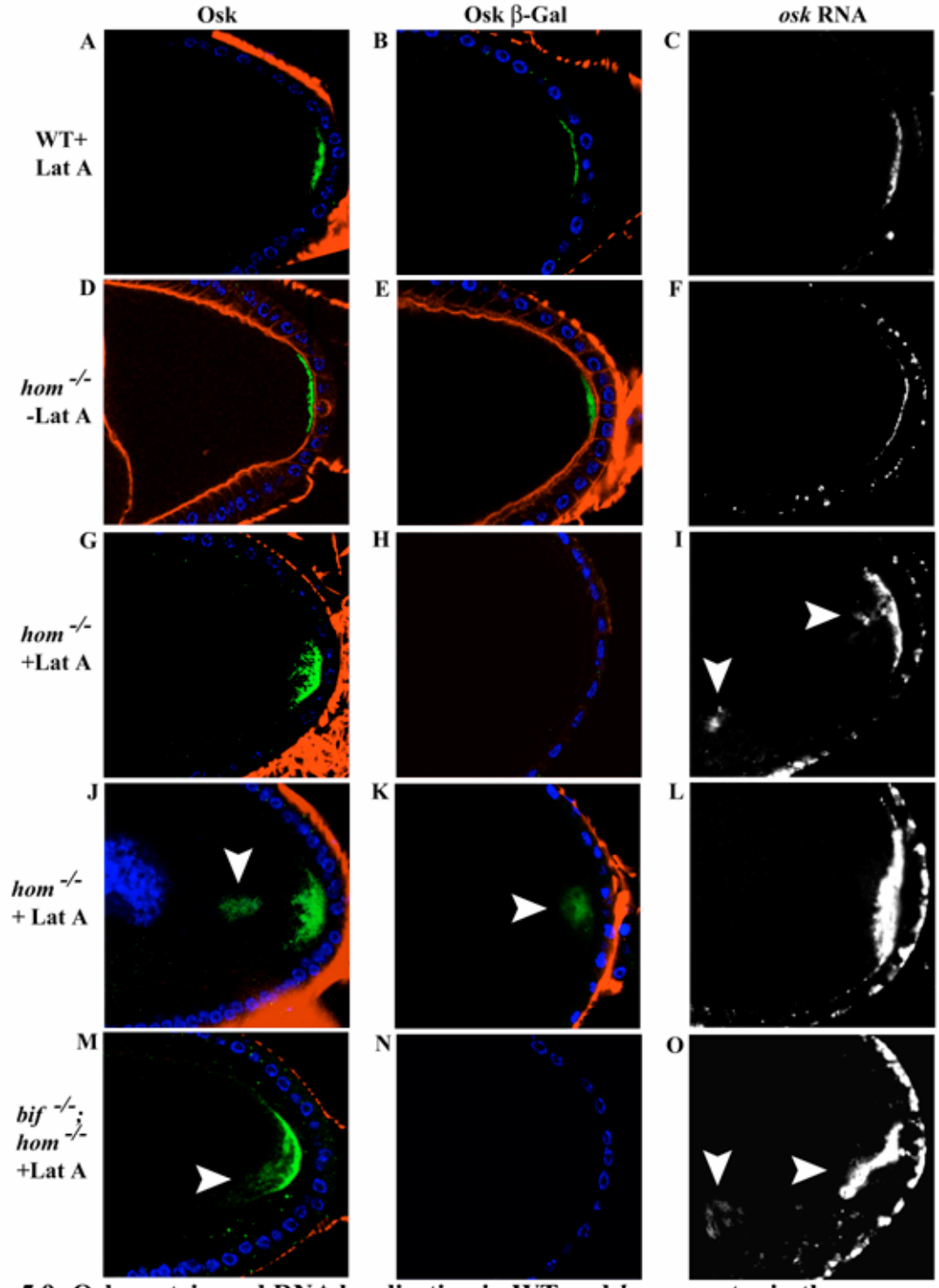

Fig. 5.9: Osk protein and RNA localisation in WT and *hom* oocytes in the presence or absence of intact microfilaments

In the great majority of WT stage 10 oocytes (A-C), in which the cortical F-actin (phalloidin, red) has been rendered undetectable by Lat A treatment, Osk (green, A), Osk-βGal (green, B) and *osk* RNA (white, C) are localised as a tight posterior crescent similar to that of untreated WT oocytes (see Table 5.2 for quantification). DNA staining showing the position of the follicle cell nuclei (blue). In hom oocytes not treated with Lat A (D-F), cortical F-actin (red) can be seen and Osk protein (D), Osk-βGal (E) and *osk* RNA (F) localisation are WT. In Lat A treated *hom* oocytes (G-L), the cortical F-actin is undetectable. *osk* RNA and proteins show diffuse (G, I, J, L) and in some cases prominent cytoplasmic localisation (arrowheads, I-K). In several cases the Osk-βGal line does not show any staining in *hom* mutants treated with Lat A (example in H). Similar results are seen with Lat A treatment of *bif; hom* double mutants (M-O; cytoplasmic localisation of Osk and *osk* RNA are indicated by arrowheads in M and O).

Table 5.2: Lat A treatment of oocytes

Lat A TREATMENT	*oskar* RNA			OSKAR			Osk-β Gal		
	Faint or Loss of stain	Diffuse stain	Cytopl-asmic stain	Faint or Loss of stain	Diffuse stain	Cytopl-asmic stain	Faint or Loss of stain	Diffuse stain	Cytopl-asmic stain
WT+LatA	2/19 (10.5%)	2/19 (10.5%)	0/19 (0%)	2/75 (2.7%)	11/75 (14.7%)	0/75 (0%)	3/32 (9.4%)	0/32 (0%)	0/32 (0%)
hom $^{-/-}$+ LatA	13/34 (38.2%)	11/34 (32.3%)	5/34 (14.7%)	6/91 (6.6%)	56/91 (61.5%)	17/91 (18.7%)	23/45 (51.1%)	8/45 (17.8%)	5/45 (11.1%)
bif $^{-/-}$+ LatA	-	-	-	0/16 (0%)	3/16 (18.7%)	0/16 (0%)	-	-	-
bif $^{-/-}$*; hom* $^{-/-}$+ Lat A	3/15 (20%)	7/15 (46.7%)	3/15 (20%)	3/25 (12%)	14/25 (56%)	4/25 (16%)	10/18 (55.6%)	5/18 (27.8%)	1/18 (5.6%)

In *hom* mutant oocytes treated with Latrunculin A (LatA) the localisation *Osk* RNA and proteins show varying phenotypes. These results have been artificially divided into three classes (some examples are shown in Fig. 5.8). Note that diffuse staining indicates staining at the posterior of the oocyte where the posterior group molecules are not present as a tight cortical crescent but show a predominantly posterior cortical and cytoplasmic staining an example of this is shown in Fig. 5.8 G. Whereas cytoplasmic staining indicates staining that shows a distinct cytoplasmic localisation of the Protein or RNA along with a posterior staining as is seen in Fig. 5.8 J.

near the posterior pole and there was a large reduction in the Osk-βGal signal (Fig. 5.9 G-L, Table 5.2). This could indicate that the loss of the longer Osk isoform may be the primary defect seen in Lat A treated *hom* mutants since this longer Osk isoform is known to be essential for *osk* RNA and protein anchoring (Vanzo and Ephrussi, 2002). The defects induced by depolymerising F-actin in *homer* oocytes are similar to but more severe than those seen in *bif; homer* double mutant oocytes. This is probably due to the fact that F-actin disruption also leads to premature streaming in stage 9 and enhanced streaming in stage 10 oocytes, (Manseau *et al.*, 1996) hence accentuating the affects of the loss of Osk anchoring at the posterior cortex. The above results demonstrate that disruption of F-actin in the absence of *homer* function disrupts anchoring of the o*sk* gene products. Similar results were obtained when *hom* mutants were treated with just CD or treated successively with Lat A and CD or vice versa (Fig. 5.10 D-F and Table 5.3). Cytochalasin D does not cause loss of F-actin as seen with phalloidin staining, and causes changes in the cortical F-actin as well as causing some of the F-actin to be seen in the cytoplasm, this affect is not seen with Lat A. This could be attributed to the difference in the mechanism of action between CD and Lat A (Spector *et al.*, 1989). However, despite this difference between CD and Lat A, the affects of these drugs singly or in combination on Osk posterior anchoring are similar, causing mild defects in Osk posterior anchoring in only 1/5 of the treated wt oocytes and severe defects in the great majority of treated *hom* oocytes. A second prediction is that disruption of microfilaments in the absence of *bif* should not affect anchoring of Osk. Indeed most wt and *bif* single mutant oocytes treated with Lat A showed largely wt anchoring of the Osk gene products (Fig. 5.11 A and Table 5.2 for quantification), similar to Lat A treatment of wt oocytes. These results are consistent with the notion

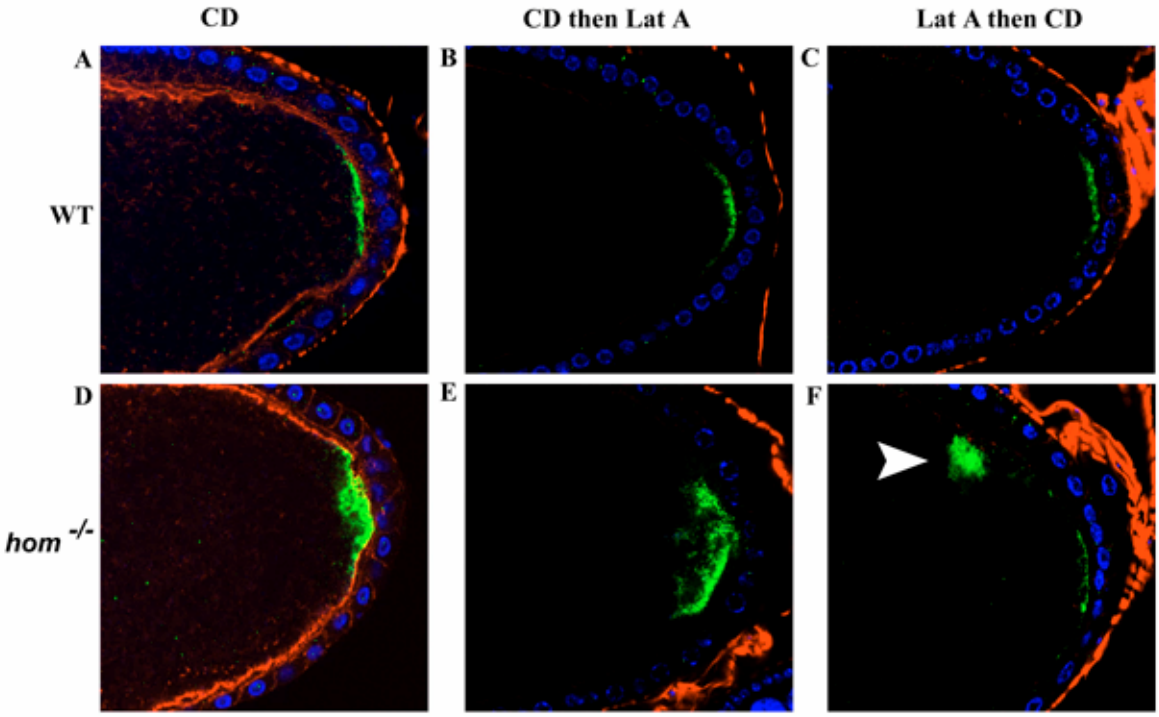

Fig. 5.10: Osk localisation in drug treated WT and *hom* mutants
Wild type stage 9 and 10 oocytes were treated with CD alone (A), CD followed by Lat A (B) and Lat A followed by CD (C). Phalloidin staining in these oocytes is in red. Osk protein (green) in these oocytes was detected using anti- Osk antibody. The protein localisation in most cases is still predominantly at the posterior cortex as in the wt oocytes. Similar experiments with *hom* mutant oocytes treated with CD alone (D), CD followed by Lat A (E) and Lat A followed by CD (F) all show enhanced diffuse or cytoplasmic staining (arrowhead in F) of Osk after drug treatment. Table 5.3 quantities the phenotypes represented in this figure. DNA staining (blue) shows the position of the follicle cell nuclei.

Table 5.3: Lat A and CD treatment of oocytes

DRUG TREATMENT	OSKAR		
	Faint or Loss of stain	Diffuse stain	Cytopl-asmic stain
WT+CD	0/23 (0%)	6/23 (26%)	0/19 (0%)
hom $^{-/-}$+ CD	0/11 (0%)	3/11 (27.2%)	5/11 (45.5%)
WT+CD+ Lat A	0/18 (0%)	4/18 (22%)	0/18 (0%)
hom $^{-/-}$+ CD+lat A	3/18 (16.7%)	4/18 (22.2%)	8/18 (44.4%)
WT+LatA + CD	0/15 (0%)	3/15 (20%)	0/15 (0%)
hom $^{-/-}$+ LatA+CD	1/10 (10%)	5/10 (50%)	3/10 (30%)

In *hom* mutant oocytes treated with Cytochalasin D (CD) alone or in combination with Latrunculin A (LatA) the localisation of Oskar protein shows a range of phenotypes. The results have been artificially divided into three classes along with the control oocytes treated under the same conditions (some examples are shown in Fig. 5.10).

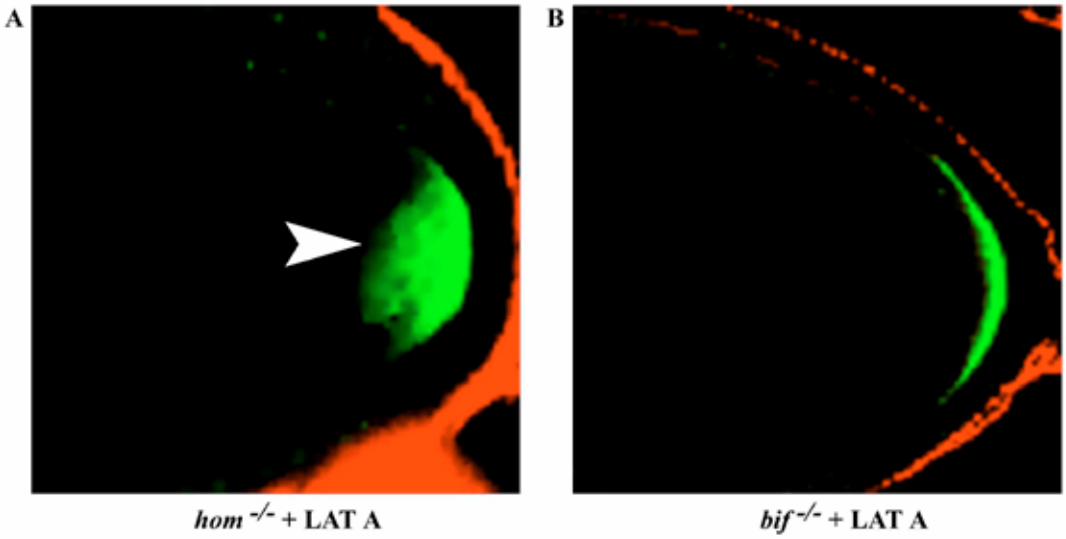

Fig. 5.11: Osk localisation in *bif* and *hom* mutants treated with Lat A
Osk localisation in *hom* mutants treated with Lat A (A) and a similar staining in *bif* mutants (B) treated with Lat A under the same conditions. Note that the posterior, cortical localisation of Osk is unaffected in *bif* mutants after Lat A treatment, whereas *hom* mutants show a diffuse staining of Osk (Arrowhead in A).

that Bif functions in an F-actin dependent manner in maintaining Osk to the posterior of the oocyte.

If there are two independent mechanisms which act redundantly for normal Osk anchoring at the posterior cortex then it would follow that the *bif; hom* double mutants in the absence of an intact F-actin cytoskeleton would show a similar phenotype to *hom* single mutants treated with Lat A and not a more severe phenotype. This is indeed the case seen on testing *osk* RNA and Osk proteins in Lat A treated double mutant oocytes (Fig. 5.9 M-O; quantification in Table 5.2).

5.2.5. Homer forms a complex with Osk

Since Hom posterior cortical localisation remains unchanged following F-actin disruption, its ability to localise Osk to the posterior may be because it forms a complex with Osk or because it binds *osk* RNA. As the molecule has a coiled-coiled domain and an EVH domain, it seems unlikely to bind RNA, which was indeed the case where control regions S1 and S3 of Stau act as negative and positive controls in the assay as has been shown earlier (Li *et al.*, 1997; Ramos *et al.*, 2000) (Fig. 5.12 B).

Co-immunoprecipitation experiments, using *Drosophila* ovarian extracts indicate that Hom and Osk form a complex *in vivo.* Further, the stability of this complex is not dependent on an intact F-actin cytoskeleton (Fig. 5.12 A).

5.2.6. Bif and Hom Localisation in *moe* mutants

Recent studies have shown that Drosophila Moesin is essential to link the cortical F-actin to the oocyte cell membrane (Jakovics *et al.*, 2002; Polesello *et al.*, 2002). When *moesin* function is compromised cortical F-actin can detach from the cell membrane and “fall” into the oocyte cytoplasm and this results in the mislocalisation

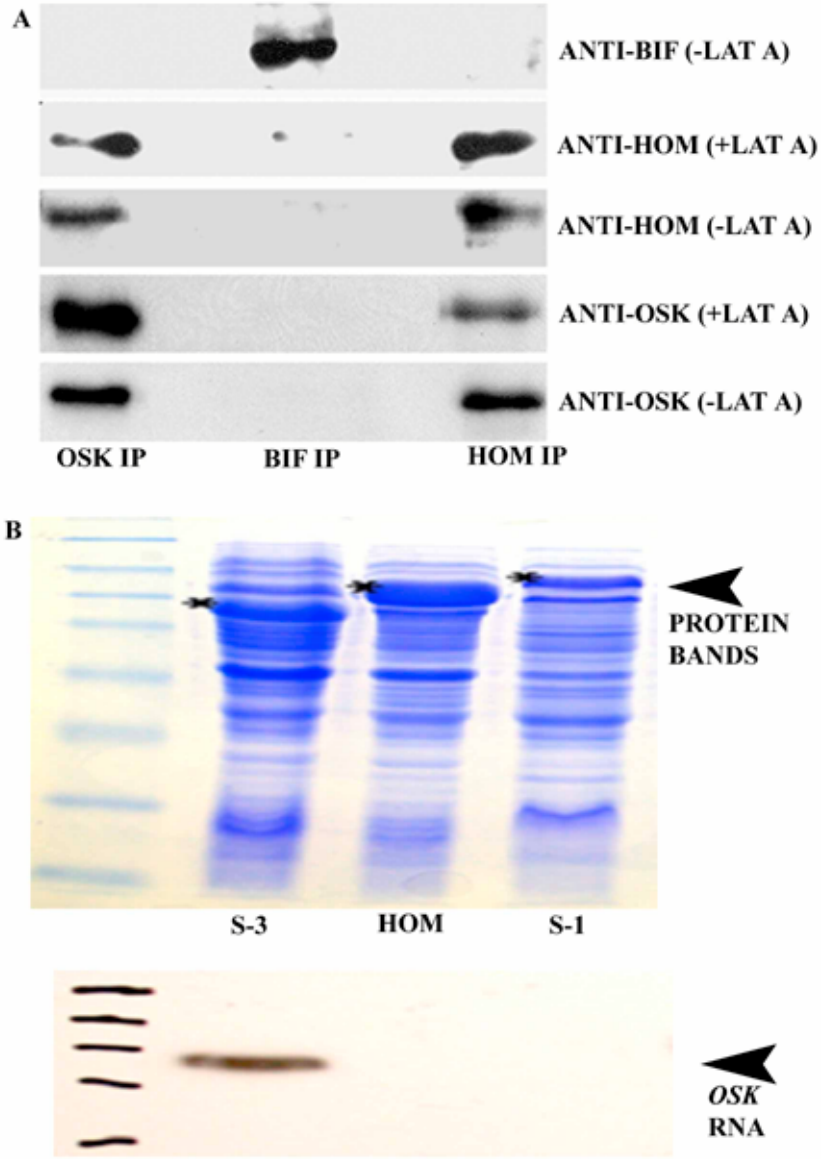

Fig. 5.12: Immuno-precipitations and RNA binding assays
A: Western blot analysis of co-IP's from extracts of ovaries treated or not treated with Lat A. Anti-Osk, anti-Bif and anti-Hom co-IP's are probed with the antibodies indicated. Osk appears to complex with Hom in extracts derived from Lat A treated and untreated ovaries. Bif does not co-IP with Osk or Hom and serves as a control. Note that the amount of Osk brought down in the Hom IP with Lat A is similar to the amount of Osk brought down in the absence of Lat A.
B: A coomasie stained gel of GST fused Stau regions (S-3 and S-1, lanes 2 and 4) and GST-Hom (lane 3) to show that there was equal protein in all lanes for the RNA binding assay. The lower panel shows that only the S-3 fragment of Staufen pulls down radiolabelled *osk* RNA (seen as the single band on autorad). The S-1 region of Stau and Hom do not bind *osk* RNA.

of Osk. We have examined the affects of loss of *moesin* function on the localisation of both Bif and Hom. Bif localisation corresponds to that of F-actin in the cytoplasm and the cortex and most of the regions in the cortex lacking phalloidin staining show reduced or loss of Bif staining (Fig. 5.13 A-D). Hom staining in *dmoe* oocytes is present in the cortex in a pattern similar to cortical F-actin and in the regions where the cortical actin appears to fall into the cytoplasm, Hom staining is similar to F-actin staining (Fig. 5.13 E-H). One reasonable interpretation of these observations is that when the cortical actin cytoskeleton becomes detached from the cell membrane in *dmoe* mutant oocytes components of the Osk anchoring machinery (including both Bif and Hom) along with Osk also become detached with the F-actin from the cell membrane giving rise to the observed Osk mislocalisation phenotype. This situation is different from LatA treatment, which leads to depolymerisation of the F-actin cytoskeleton but does not cause change to the localisation of some of the components (e.g. Hom) of the anchoring machinery from the cortex to the cytoplasm.

5.3. Discussion and model

In this chapter I have described the identification of two molecules, Bifocal and Homer that act together for the normal anchoring of posterior group molecules to the posterior cortex. These molecules seem to be localised in a actin dependent (Bif) and actin independent way (Hom) and are together required for the normal anchoring of posterior group molecules. One of the surprising findings in this chapter is the fact that an intact F-actin cytoskeleton does not seem to be absolutely required for normal anchoring of posterior group molecules (Osk) to the posterior cortex.

The novel results I have presented in this chapter, bring to light the possibility that the maintenance of Osk at the posterior of the oocyte may be mediated by two distinct

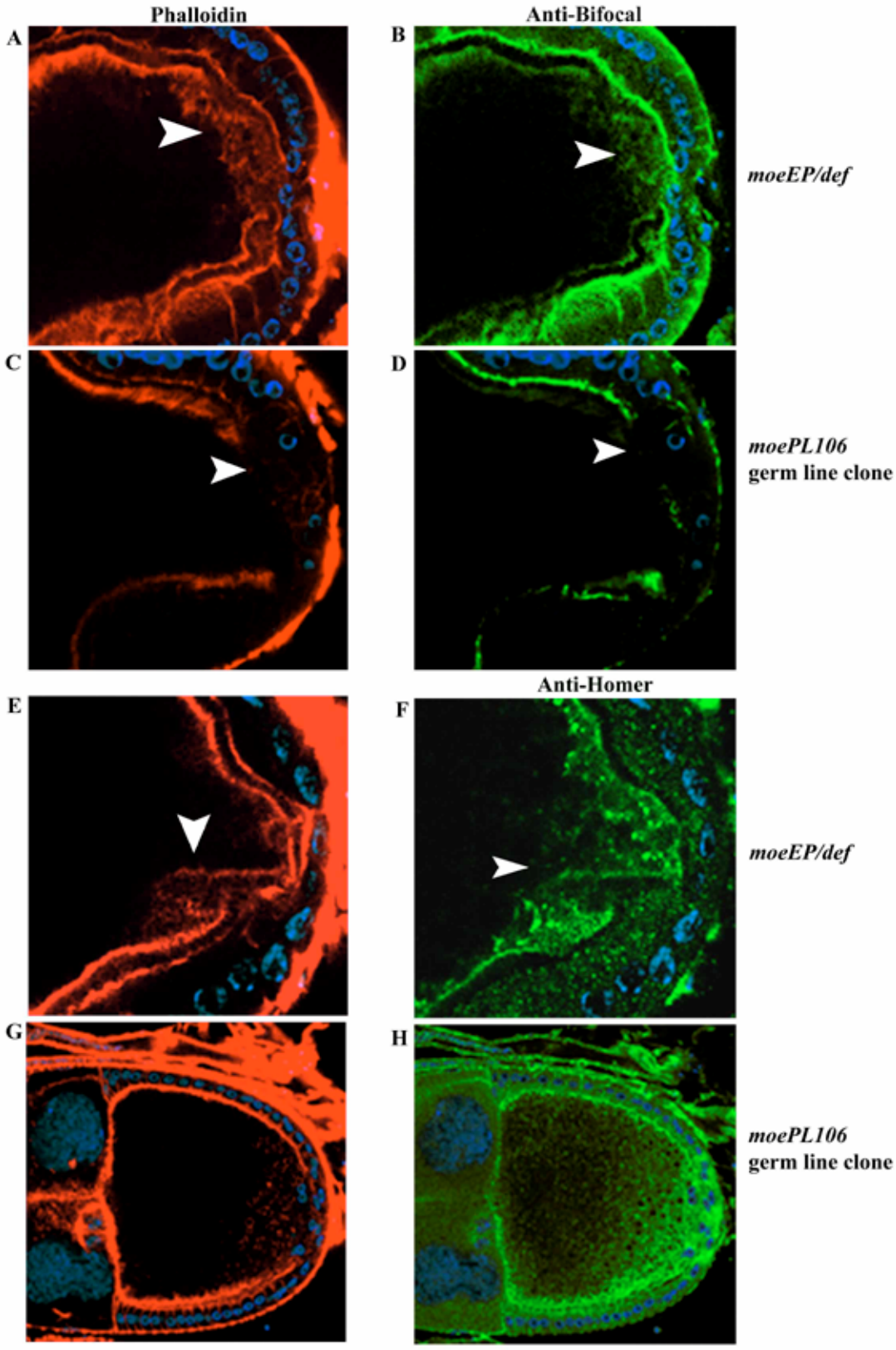

Fig. 5.13: Bif and Hom localisation in *moe* mutants

A-D shows *moe* mutants with phalloidin (A, C) and anti-Bif (B, D) staining. Note that when F-actin is seen in the oocyte cytoplasm (Arrowhead in A), Bif is also seen in the cytoplasm (arrowhead in B) and regions showing lack of F-actin (arrowhead in C) show loss of Bif staining (arrowhead in D).

E-H show shows *moe* mutants with phalloidin (E, G) and anti-Hom (F, H) staining. Note that when F-actin is seen in the oocyte cytoplasm (Arrowhead in E), Hom is also seen in the cytoplasm (arrowhead in F). DNA staining is in blue in all figures and the moe mutant used is indicated on the right.

mechanisms either of which is sufficient, at least for the great majority of the oocytes. One mechanism does not require an intact F-actin cytoskeleton and Hom seems to be an important player in this process. Homer can complex with Osk and the stability of this complex is not dependent on an intact F-actin cytoskeleton. The second mechanism requires an intact F-actin cytoskeleton. Bif seems to be required for this mechanism. Previous work has shown that over-expression of Bif can promote actin polymerisation in cultured cells (Ruan *et al.*, 2002). Since it is also known that F-actin forms a complex with Bif in *Drosophila* embryonic lysates (Sisson et al., 2000) and that Bif binds directly to F-actin filaments *in vitro* (previous chapter), it is possible that Bif acts to stabilise actin filaments. In this scenario its absence may cause subtle changes in the F-actin cytoskeleton that may affect its capacity to anchor molecules at the cortex when *hom* is absent. In contrast *hom* can function and is required to anchor Osk in the absence of an intact F-actin cytoskeleton or in the absence of *bif* function. Only when both mechanisms are disrupted in the oocyte, either through the simultaneous disruption of both *homer* and *bif*, or when F-actin is disrupted in the absence of *homer*, do the *osk* gene products fail to remain anchored to the posterior cortex (schematically represented in Fig. 5.14).

Recent data has shown that Moesin, an actin binding molecules with ERM domains is required for anchoring Osk to the posterior cortex of the oocyte and in *moe* mutants F-actin falls off from the cortex into the ooplasm. On testing Bif and Hom localisation in *moe* mutants, both Bif and Homer are seen to ‘fall off’ the cortex like F-actin and they both show weak or no staining where the F-actin is not visible. This indicates that both Bif and Hom are affected in *moe*, again consistent with the notion that both Bif and Hom have to be affected in order to show defects in Osk anchoring. It is conceivable that both Bif and Hom act downstream of Moe in the oocyte.

One of the major shortcomings of this study is that it fails to address the mechanism of anchoring of Osk to the oocyte cortex, especially in the absence of an intact F-actin cytoskeleton. It is conceivable that there could be molecules at the cortex that are required along with Hom to keep Osk anchored normally to the cortex. Some of the possible candidates that may be part of one or both of the proposed pathways would be cortical molecules like spectrins, integrins and tropomyosins.

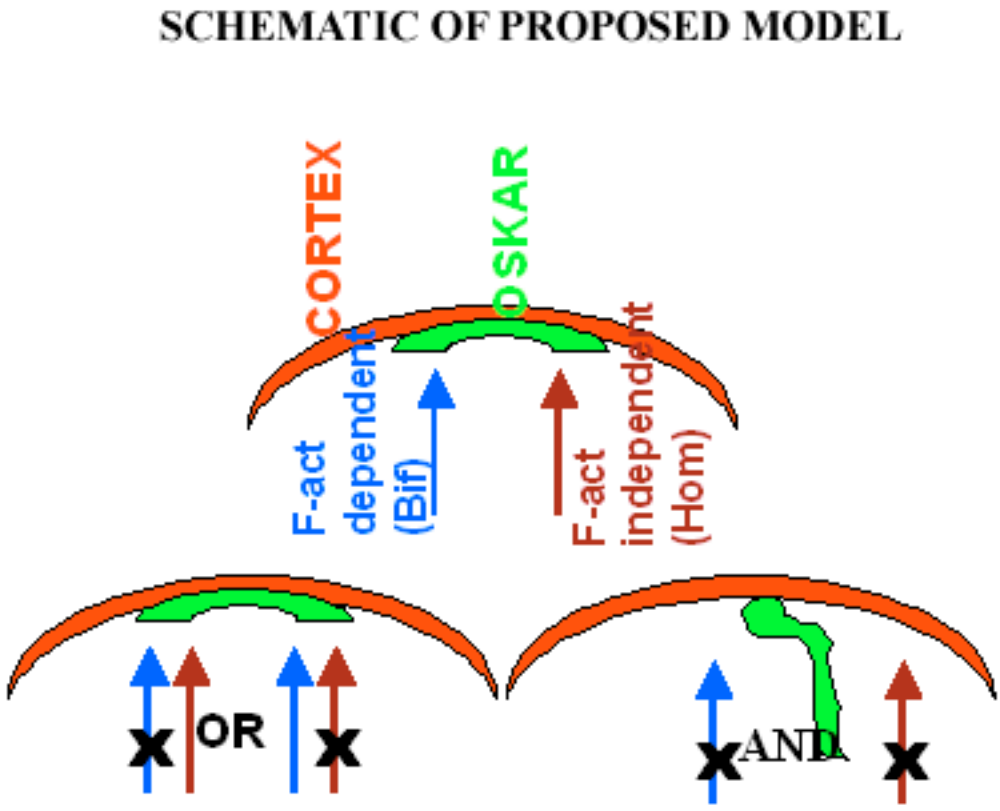

Fig. 5.14: Model
A schematic model proposing that the posterior cortical anchoring of the *osk* gene products in oocyte is mediated by an F-actin dependent pathway requiring *bif* and a second parallel pathway requiring *hom* which does not require intact F-actin; either pathway can promote anchoring of the the *osk* gene products at the posterior cortex of the great majority of oocytes. Posterior is towards the top of the Figure.

One of the problems involved in looking at molecules required for anchoring Osk is that these molecules may have an essential function early in oogenesis, hence germ line clone screens may not necessarily identify many of the molecules involved in the anchoring process as they may have earlier functions and one may not get late stage 9/10 oocytes.

This work has shed light on the possibility that there may be two redundant pathways acting to anchor Osk to the posterior cortex of the oocyte, this would also mean that mutations affecting any one of the pathways alone would not give rise to an obvious anchoring phenotype. Two possible screens that could throw light on the other molecules involved in the F-actin independent process of anchoring Osk would be-

1. To look for mutants that fail to anchor Osk in the absence of Bif but in the presence of Hom, this would effectively target molecules in the F-actin independent machinery.
2. To look for mutations that cause disruption of Hom localisation in the oocyte in the absence of an intact F-actin cytoskeleton (treatment of Lat A). This would effectively help one identify molecules upstream of Hom that are required for the localisation of Hom in the oocyte.

5.4. Future directions:

It will be interesting to identify additional molecules involved in pathways and elucidate the mechanisms that are required to localise Homer to the posterior cortex of the oocyte in the absence of an intact actin cytoskeleton.

Chapter 6

GENERAL DISCUSSION

This work has been focused on the function of *Drosophila* Bifocal in eye development, photoreceptor axon guidance and oogenesis. Work in this thesis has also explored genetic interactions between Bif and PP1, F-actin and Hom using both the eye imaginal disc and the oocyte as models

Chapter 3 outlines the interaction between Bif and PP1 and illustrates the importance of this interaction for normal eye development in *Drosophila*. This work reveals that the short, 4 amino acid long, PP1 binding site present in Bif is essential for the normal function of Bif in the eye. Mutating a single amino acid in the PP1 binding motif prevents Bif from rescuing the eye phenotypes seen in *bif* mutants.

This work shows for the first time that a regulatory subunit of PP1 (Bif) is of functional significance *in vivo* in conjunction with PP1 (Helps et al., 2001). It has been known for some time now that PP1 has a function in fly development. PP1-87B has been shown to be required for normal mitosis in the larval brain (Axton et al., 1990). Mutations in *pp1-87B* have also been shown to have behavioural defects related to habituation and associative learning (Asztalos et al., 1993). PP1β-9C has been shown to be required for the normal attachment of muscles to muscle attachment sites in *Drosophila* larvae (Raghavan et al., 2000). However none of the PP1 interacting proteins, until recently, have been shown to have an *in vivo* role in *Drosophila* dependent on their interaction with PP1. Recent work has shown that there are other

molecules that regulate PP1 *in vivo* as is seen in the case of the genes *Trithorax* and *Smad Anchor for Receptor Activation* (Bennett *et al.*, 2003; Rudenko *et al.*, 2003).

It will be interesting to find out the mechanisms that regulate the function of Bif in the *Drosophila* eye. It would be possible find molecules that interact genetically with *bif* in the eye, by forward genetic screening methods to find enhancers and suppressers of the rhabdomere phenotype seen in *bif* mutants.

Chapter 4 elaborates on the role of Bif in larval photoreceptor axon guidance and how this process is uncoupled from the role of Bif in normal rhabdomere development. Further, it shows the role of PP1 and Bif interaction for normal axon targeting in the *Drosophila* larval brain. This chapter also shows the role of PP1 itself in photoreceptor axon targeting as well as the genetic interactions between Bif and the Protein tyrosine phosphatases PTP10D and DPTP69D. The last part of this chapter deals with the direct interaction between Bif and F-actin.

Although it has been shown previously that Bif is required for normal photoreceptor axon targeting (Ruan *et al.*, 2002), this work shows for the first time that PP1 could also be involved in axon guidance in *Drosophila*. Both *Ptp10d* and *Dptp69d* have been shown to have a function in axon guidance in *Drosophila* (Desai and Purdy, 2003; Garrity et al., 1999; Newsome et al., 2000b; Sun et al., 2000). My work shows that Bif genetically interacts with these two tyrosine phosphatases in the larval brain.

It would be interesting to find other molecules that interact with Bif in the process of photoreceptor axon guidance. The axon guidance defects in *bif* mutants can be visualised using the $Ro^{tau}LacZ$ marker, which labels the R2-R5 axons that send their projections to the second neuropile of the optic lobe, the lamina. In *bif* mutants most of these axons enter the medulla which is the third neuropile of the optic lobe. A screen

that looks for suppressors of this phenotype in the bif mutant background would enable one to find molecules that genetically interact with *bif* in the process of photoreceptor axon guidance.

Another aspect this work brings to light is the fact that the *bif* mutant phenotype that is observable in the larval stages cannot be detected in adult brains. It would be interesting to find the mechanisms that allow for this repair of mistargeted axons. This repair probably occurs during the extensive regeneration that takes place during the pupal stages. One method of finding molecules responsible for this repair of the axon guidance phenotype would be to do a genetic screen in the *bif* mutant background and look for molecules that themselves show no phenotype in larval or adult photoreceptor axon targeting, but show a phenotype in both larval and adult axon targeting in the presence of homozygous *bif* mutation.

Lastly, this work would also serve as some of the initial data to find the genetic relationship between Bif, F-actin, PP1 and a protein kinase Misshapen (Msn), that has been previously shown to interact with Bif *in vivo* (Ruan *et al.*, 2002). I am currently studying the genetic relationship between these 3 molecules using both *Drosophila* genetics and the cell culture assay systems as tools to study the hierarchy between these molecules.

Chapter 5 deals with the genetic interaction between *hom* and *bif* and how this interaction is required for the normal anchoring of Osk to the posterior cortex of the *Drosophila* oocyte. This chapter also introduces data that lead to the hypothesis that there may be an F-actin dependent and an F-actin independent process which act redundantly to allow for normal anchoring of Osk to the posterior cortex of the oocyte. Either of these mechanisms is sufficient for this process and there are defects in Osk

anchoring only when both the Osk anchoring mechanisms are disrupted in the oocyte. Further Hom complexes with Osk and this could help with its anchoring of Osk to the posterior cortex.

It will be very interesting to find other components of both the F-actin dependent and the F-actin independent pathways and see how they relate to Bif and Hom. One method of finding F-actin independent molecules would be by doing a germline screen in the *bif* mutant background and looking at Osk localisation in the mutants. Or by doing a germline screen and then looking at Osk localisation in the absence of an intact F-actin cytoskeleton in the mutants obtained in this screen.

Finding molecules in the F-actin dependent pathway would involve doing a germline screen in the *hom* mutant background and looking at Osk localisation in these double mutants.

I am currently in the process of finding known molecules that could be in the F-actin independent pathway by making double mutants of *bif* and other known cytoskeletal molecules like tropomyosin and spectrin and looking at Osk localisation in these double mutants.

The **appendix** (pages 145-149) describes a deficiency screen done with homozygous or heterozygous *bif* mutants and one copy of the deficiency. The fact that it gave rise to dominant interactors of *bif* that seem to be involved in axon guidance in the embryo is very interesting, as it suggests that Bif may be involved in embryonic axon guidance in addition to its role in photoreceptor axon guidance. The next step in this direction would involve finding the molecules within the deficiencies that interact with *bif*. Using smaller deficiencies to narrow down the genes within the deficiencies and using the RNAi injection method would allow for finding the genes that interact

genetically with *bif*. Finding the molecules that genetically interact with *bif* would also throw some light on the role of Bif in the process of embryonic axon guidance.

Although this thesis looks at the function of *bif* in three different tissues in *Drosophila*, it brings out the relationship between Bif and F-actin in all three cases. Bif co-localises with F-actin in the eye discs (larval and pupal), optic lobe and the ovary and in all three tissues Bif seems to function in regulating a cytoskeletal process. In the pupal eye discs loss of *bif* function gives rise to defects in the F-actin rich rhabdomeres and these defects can be further seen in the adult eye (Bahri et al., 1997). In the larval optic lobes loss of *bif* function gives rise to defects in photoreceptor axon targeting and clumping of the axons at the lamina of the optic lobes. This phenotype in turn gives rise to abnormal F-actin localisation in the lamina. These results indicate that Bif is required for a normal actin cytoskeleton both in the eye and the optic lobe.

At the molecular level, the organisation of the actin cytoskeleton seems to be dependent on the Bif-PP1 interaction, suggesting that PP1 may influence actin movement or operate in a pathway that regulates actin distribution within the cell. Bif has several potential Ser/Thr phosphorylation sites around the PP1-binding motif, the carboxy-terminal sequence of Bif, RRSSTIM, could serve as a potential phosphorylation site for PKA (as well as for a number of other kinases). It is possible that phosphorylation of Bif could affect PP1 binding and/or activity, allowing the Bif-PP1 complex to modulate signalling processes. Another possibility is that the Bif-PP1c complex might be required to dephosphorylate proteins associated with actin (Helps et al., 2001).

Actin-binding proteins can bind actin monomers, cross-link actin filaments into bundles of F-actin, sever actin filaments, or cap their growing ends. Some actin

binding proteins such as myosin II and cofilin are known to undergo phosphorylation (Lawler, 1999; Tan et al., 1992). Dephosphorylation of such proteins, possibly by PP1 complexes, may affect a redistribution of the actin cytoskeleton. It has been previously shown that myosin interacts with PP1, hence enabling PP1 to regulate myofibrillar contractility at the neuronal synapses (Hubbard and Cohen, 1993; Tanaka et al., 1998). Further it has been shown that neurabins I and II localise PP1c to the actin cytoskeleton at the plasma membrane (MacMillan et al., 1999; McAvoy et al., 1999; Satoh et al., 1998), this raises the possibility that PP1 along with Bif and/or other cytokeletal molecules could dephosphorylate actin binding proteins, hence affecting a redistribution of the actin cytoskeleton. Further Bif itself binds F-actin *in vitro* hence strengthening the argument that Bif, Bif-PP1 complex or/and the complex between Bif and other as yet unidentified molecules could have a major role to play in organisation and stability of the actin cytoskeleton.

Chapter 5 of this thesis also shows the importance of the cytoskeletal functions of Bif in the oocyte. Double mutants of *bif* and *hom* show defects in anchoring of Osk to the posterior cortex of the oocyte, indicating defects in the cytoskeletal organisation of the posterior cortex in these double mutants. Homer has been shown to be required for normal retinotopic axon targeting in *Xenopus* (Foa *et al.*, 2001). This indicates that Hom has a function in normal cytoskeletal development. Further both these molecules bind F-actin *in vitro* (Cai, 2002; Shiraishi *et al.*, 1999) suggesting a role for F-actin in this anchoring process. This also suggests that, as in the case of PP1, the molecules that interact with Bif either physically or genetically are, like Bif, themselves involved in formation, maintenance or stability of the cytoskeleton.

Although we demonstrate the possibility of F-actin dependent and F-actin independent mechanisms to anchor Osk to the posterior cortex, it is clear that both

mechanisms are required for the normal anchoring of the posterior group molecules in the oocyte. Further the fact that Bif seems to be part of the F-actin dependent mechanism indicates that there is a close interrelation between Bif and F-actin during different stages and in different tissues of the fruit fly. Bif seems to affect actin differently in different tissues of *Drosophila.* It is probable that there are other cytoskeletal molecules that mediate the F-actin independent anchoring mechanism, again linking both Bif and Hom to the F-actin cytoskeleton.

Further work would be needed to find the other cytoskeletal molecules involved in this process as well as to find other functions of Bif in embryonic axonal development.

Appendix 1.1

Deficiency screen to find deficiencies that dominantly interact with Bifocal

The previous chapters of this thesis have described the direct interaction between Bif and PP1, and the genetic interaction between Bif and the phosphatases Ptp69d and Ptp10d as well as the genetic interaction between Bif and Hom.

To find other molecules that could potentially interact with Bif genetically, I undertook a genetic screen that would identify regions in the second and third chromosomes that showed dominant interaction with the bif^{R47} mutant allele.

A schematic of how the screen was performed is shown in Fig. 6.1, and the results obtained from the screen are shown in Table 6.1. The lines that gave a dominant lethal phenotype with bif^{R47} were analysed with mAb BP102 and mAb1D4 (anti-Fasciclin II). BP102 stains the anterior and posterior commissures and the longitudinal connectives from stage 12 of *Drosophila* embryonic development (Seeger *et al.*, 1993). It can be seen from Fig. 6.2 that the dominant interactors of *bif* mutant show an axonal morphology phenotype in combination with bif^{R47} mutant. Axonal phenotypes were also seen on staining with anti-Fas II (Fig. 6.3). Fas II is a homologue of the vertebrate neural cell adhesion molecule (NCAM) (Grenningloh *et al.*, 1990; Grenningloh *et al.*, 1991). Anti- Fas II staining includes the three fascicles in the longitudinal connectives of the *Drosophila* embryo.

The results of the deficiency screen described here suggest a role for Bif in axon guidance in the embryo, although this phenotype is not present in *bif* mutants

alone. This work could be carried on further to find the molecule within each deficiency that genetically interacts with *bif* and gives rise to an axon guidance phenotype. It would also be interesting to further characterise the phenotype seen in the mutants.

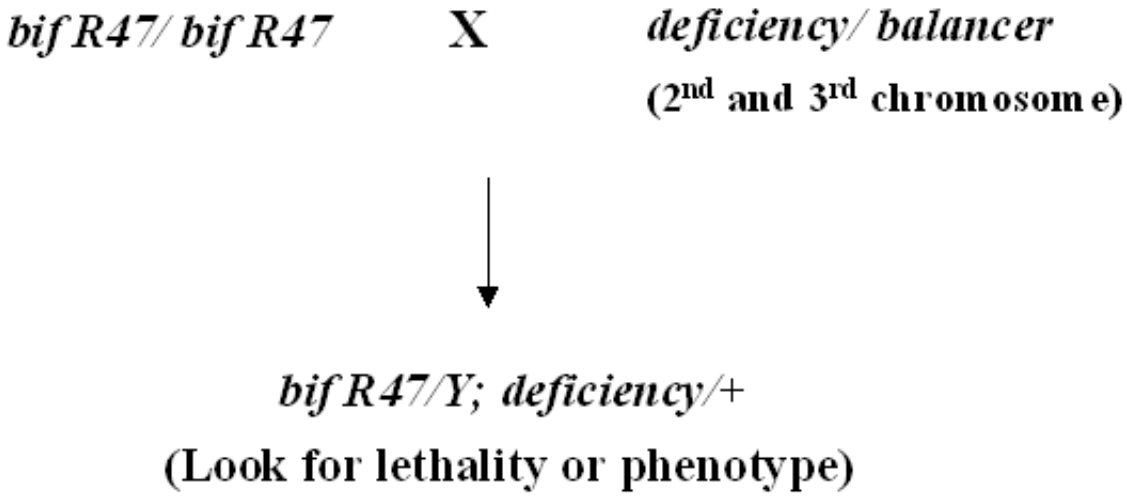

Fig. 6.1: Scheme of to find molecules that genetically interact with *bif* (dominant interactors)
bif ^{R47} females were crossed to the deficiency kit on the 2nd and 3rd chromosomes and the resulting male progeny which are *bif* mutant and have one copy of the deficiency were scored for lethality or any other observable phenotype. The deficiencies that dominantly interact with *bif* and their phenotypes are listed in Table 6.1.

Table 6.1: Deficiencies that genetically interact with *bif*

Deficiency	**Region uncovered by The deficiencies**	**Phenotype seen in genotype *bif*^{R47}/Y; *deficiency*/+ or *bif*^{R47}/+; *deficiency*/+**
Df(2R)eve, cn^{1} and *Df(2R)X1, Mef2*^{X1}	Mapped to 46C3-46C11	Males lethal and show a phenotype with 1D4 and BP102 (Fig. 6.1 C, D)
Df(2L)TW161, cn^{1} *bw*^{1}	Mapped to 38A6-40B1	Males show upheld wings
Df(2L)ast2 and *Df(2L)ast6*	Mapped to 21E1-21E3	Males show a rough eye phenotype (Observable under light microscope)
Df(3L)Ly, Df(3L)BK10, ru^{1} *sens*$^{Ly-1}$ *red*^{1} *cv-c*^{1} *Sb*$^{sbd-1}$ *sr*^{1} *e*^{1}	Mapped to 70A2- 71F	Males lethal and show a phenotype with 1D4 and BP102 (Fig. 6.1 E, F) Females show a rough eye phenotype (Observable under light microscope)
Df(3R)9A99, th^{1} *st*^{1} *cp*^{1} *in*^{1} *kni*$^{ri-1}$ *kni*^{6} *cu*^{1} *e*^{s} *ca*^{1}	Mapped to 83F2- 84B2	Males lethal and show a phenotype with 1D4 and BP102 (Fig. 6.1 G, H).

Deficiencies in the 2nd and 3rd chromosomes that dominantly interact with *bif* mutants

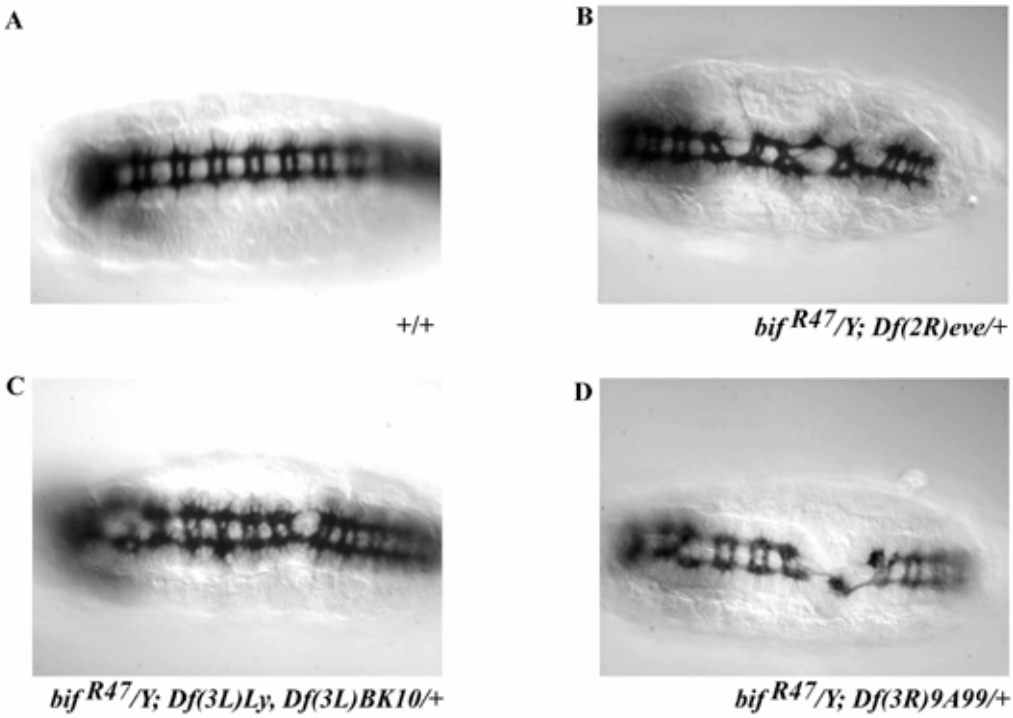

Fig. 6.2: BP102 staining of stage 16 embryos
WT (A) and *bif* ^{R47}*/Y; Df/+* stage 16 embryos were stained with the monoclonal Ab BP102, axon morphology defects were seen with all 3 deficiencies pulled out in the screen (B-D). Breaks are seen in the commissures and the connectives in all 3 cases. The phenotype seen with a dominant interaction of *Df(3L)Ly, Df(3L)BK10* is the weakest (C) with the other 2 dominant interaction showing a variety of defects in the VNC.

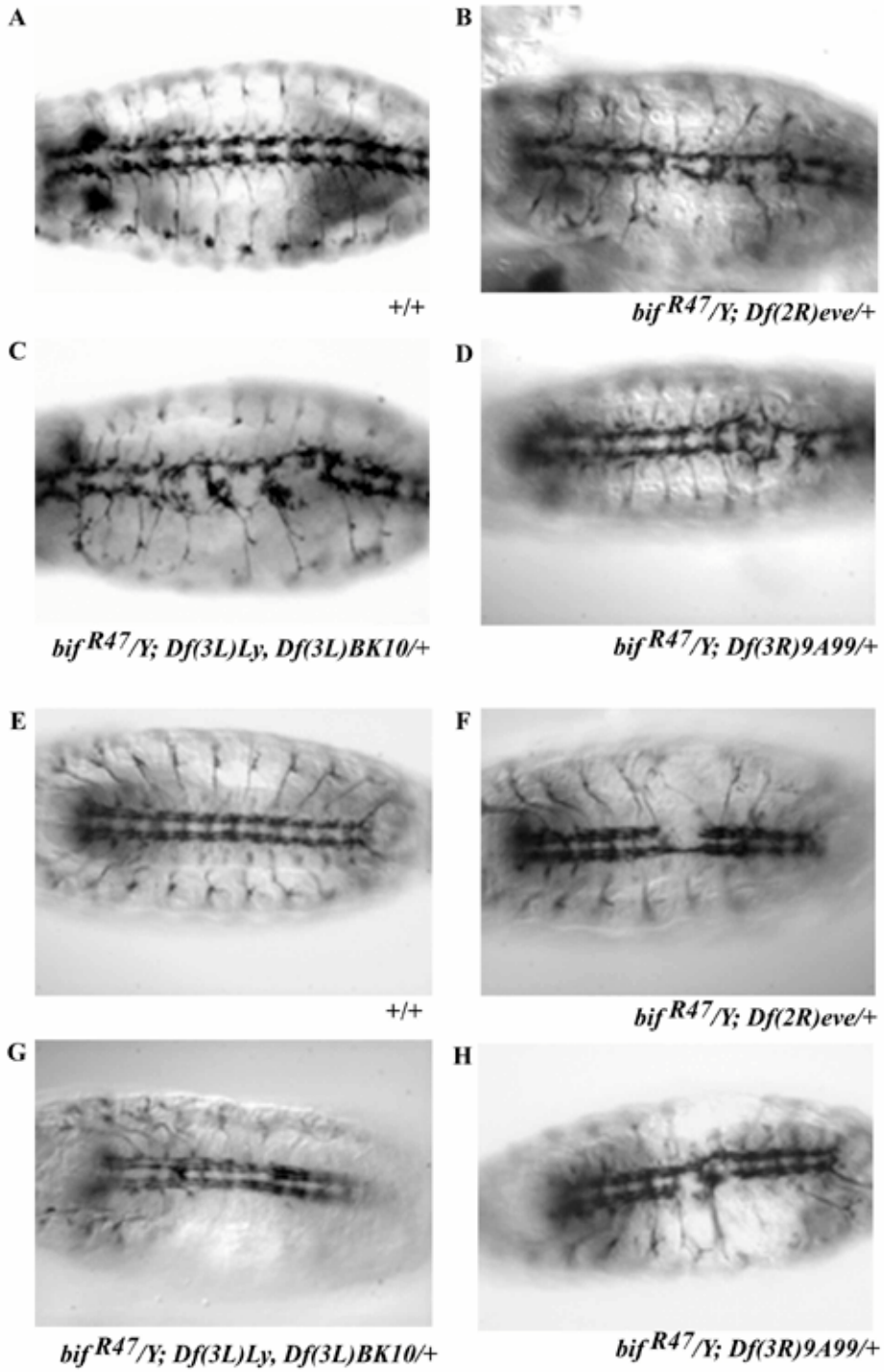

Fig. 6.3: 1D4 staining of stage 15 and 16 embryos
WT (A and E) and *bif*^{R47}*/Y; Df/+* stage 15 (B-D) and stage 16 (F-H) embryos were stained with monoclonal Ab 1D4 which stains the 3 commisures of the embryonic midline. All 3 of the dominant interactions show breaks in the commissural axons.

REFERENCES

Adams, M. D., Celniker, S. E., Holt, R. A., Evans, C. A., Gocayne, J. D., Amanatides, P. G., Scherer, S. E., Li, P. W., Hoskins, R. A., Galle, R. F.*, et al.* (2000). The genome sequence of Drosophila melanogaster. Science *287*, 2185-2195.

Allen, P. B., Kwon, Y. G., Nairn, A. C., and Greengard, P. (1998). Isolation and characterization of PNUTS, a putative protein phosphatase 1 nuclear targeting subunit. In J Biol Chem, pp. 4089-4095.

Alphey, L., Parker, L., Hawcroft, G., Guo, Y., Kaiser, K., and Morgan, G. (1997). KLP38B: a mitotic kinesin-related protein that binds PP1. In J Cell Biol, pp. 395-409.

Arikawa, K., Hicks, J. L., and Williams, D. S. (1990) Identification of actin filaments in the rhabdomeral microvilli of Drosophila photoreceptors.

Asztalos, Z., von Wegerer, J., Wustmann, G., Dombradi, V., Gausz, J., Spatz, H. C., and Friedrich, P. (1993). Protein phosphatase 1-deficient mutant Drosophila is affected in habituation and associative learning. J Neurosci *13*, 924-930.

Awasaki, T., Saito, M., Sone, M., Suzuki, E., Sakai, R., Ito, K., and Hama, C. (2000). The Drosophila trio plays an essential role in patterning of axons by regulating their directional extension. In Neuron, pp. 119-131.

Axton, J. M., Dombradi, V., Cohen, P. T., and Glover, D. M. (1990). One of the protein phosphatase 1 isoenzymes in Drosophila is essential for mitosis. Cell *63*, 33-46.

Babu, K., Cai, Y., Bahri, S., Yang, X., and Chia, W. (2004). Roles of Bifocal, Homer, and F-actin in anchoring Oskar to the posterior cortex of Drosophila oocytes. Genes Dev *18*, 138-143.

Bahri, S. M., Yang, X., and Chia, W. (1997). The Drosophila bifocal gene encodes a novel protein which colocalizes with actin and is necessary for photoreceptor morphogenesis. Mol Cell Biol *17*, 5521-5529.

Baksa, K., Morawietz, H., Dombradi, V., Axton, M., Taubert, H., Szabo, G., Torok, I., Udvardy, A., Gyurkovics, H., Szoor, B., and et al. (1993). Mutations in the protein phosphatase 1 gene at 87B can differentially affect suppression of position-effect variegation and mitosis in Drosophila melanogaster. In Genetics, pp. 117-125.

Bateman, J., Shu, H., and Van Vactor, D. (2000). The guanine nucleotide exchange factor trio mediates axonal development in the Drosophila embryo. In Neuron, pp. 93-106.

Baum, B. (2002). Drosophila oogenesis: generating an axis of polarity. Curr Biol *12*, R835-837.

Bennett, D., Szoor, B., and Alphey, L. (1999). The chaperone-like properties of mammalian inhibitor-2 are conserved in a Drosophila homologue. In Biochemistry, pp. 16276-16282.

Bennett, D., Szoor, B., Gross, S., Vereshchagina, N., and Alphey, L. (2003). Ectopic expression of inhibitors of protein phosphatase type 1 (PP1) can be used to analyze roles of PP1 in Drosophila development. Genetics *164*, 235-245.

Benton, R., Palacios, I. M., and St Johnston, D. (2002). Drosophila 14-3-3/PAR-5 is an essential mediator of PAR-1 function in axis formation. Dev Cell *3*, 659-671.

Berleth, T., Burri, M., Thoma, G., Bopp, D., Richstein, S., Frigerio, G., Noll, M., and Nusslein-Volhard, C. (1988). The role of localization of bicoid RNA in organizing the anterior pattern of the Drosophila embryo. Embo J *7*, 1749-1756.

Beullens, M., Van Eynde, A., Stalmans, W., and Bollen, M. (1992). The isolation of novel inhibitory polypeptides of protein phosphatase 1 from bovine thymus nuclei. In J Biol Chem, pp. 16538-16544.

Bollen, M., and Stalmans, W. (1992). The structure, role, and regulation of type 1 protein phosphatases. In Crit Rev Biochem Mol Biol, pp. 227-281.

Bossing, T., and Brand, A. H. (2002). Dephrin, a transmembrane ephrin with a unique structure, prevents interneuronal axons from exiting the Drosophila embryonic CNS. In Development, pp. 4205-4218.

Brakeman, P. R., Lanahan, A. A., O'Brien, R., Roche, K., Barnes, C. A., Huganir, R. L., and Worley, P. F. (1997). Homer: a protein that selectively binds metabotropic glutamate receptors. Nature *386*, 284-288.

Brand, A. H., and Perrimon, N. (1993). Targeted gene expression as a means of altering cell fates and generating dominant phenotypes. Development *118*, 401-415.

Brendza, R. P., Serbus, L. R., Duffy, J. B., and Saxton, W. M. (2000). A function for kinesin I in the posterior transport of oskar mRNA and Staufen protein. Science *289*, 2120-2122.

Brittis, P. A., Lemmon, V., Rutishauser, U., and Silver, J. (1995). Unique changes of ganglion cell growth cone behavior following cell adhesion molecule perturbations: a time-lapse study of the living retina. Mol Cell Neurosci *6*, 433-449.

Broadus, J., and Doe, C. Q. (1997). Extrinsic cues, intrinsic cues and microfilaments regulate asymmetric protein localization in Drosophila neuroblasts. Curr Biol *7*, 827-835.

Brose, K., Bland, K. S., Wang, K. H., Arnott, D., Henzel, W., Goodman, C. S., Tessier-Lavigne, M., and Kidd, T. (1999). Slit proteins bind Robo receptors and have an evolutionarily conserved role in repulsive axon guidance. Cell *96*, 795-806.

Burden-Gulley, S. M., Pendergast, M., and Lemmon, V. (1997). The role of cell adhesion molecule L1 in axonal extension, growth cone motility, and signal transduction. Cell Tissue Res *290*, 415-422.

Cai, Y. (2002) The Mechanism of Drosophila Neuroblast Asymmetric Division, National University of Singapore, Singapore.

Carvalho, A. B., Dobo, B. A., Vibranovski, M. D., and Clark, A. G. (2001). Identification of five new genes on the Y chromosome of Drosophila melanogaster. Proc Natl Acad Sci U S A *98*, 13225-13230.

Cha, B. J., Serbus, L. R., Koppetsch, B. S., and Theurkauf, W. E. (2002). Kinesin I-dependent cortical exclusion restricts pole plasm to the oocyte posterior. Nat Cell Biol *4*, 592-598.

Chou, T. B., and Perrimon, N. (1996). The autosomal FLP-DFS technique for generating germline mosaics in Drosophila melanogaster. Genetics *144*, 1673-1679.

Clandinin, T. R., Lee, C. H., Herman, T., Lee, R. C., Yang, A. Y., Ovasapyan, S., and Zipursky, S. L. (2001). Drosophila LAR regulates R1-R6 and R7 target specificity in the visual system. Neuron *32*, 237-248.

Clandinin, T. R., Lee, C. H., Herman, T., Lee, R. C., Yang, A. Y., Ovasapyan, S., and Zipursky, S. L. (2001). Drosophila LAR regulates R1-R6 and R7 target specificity in the visual system. In Neuron, pp. 237-248.

Clark, I., Giniger, E., Ruohola-Baker, H., Jan, L. Y., and Jan, Y. N. (1994). Transient posterior localization of a kinesin fusion protein reflects anteroposterior polarity of the Drosophila oocyte. Curr Biol *4*, 289-300.

Cohen, P. (1989). The structure and regulation of protein phosphatases. In Annu Rev Biochem, pp. 453-508.

Cohen, P. (1992). Signal integration at the level of protein kinases, protein phosphatases and their substrates. Trends Biochem Sci *17*, 408-413.

Cohen, P. T. (2002). Protein phosphatase 1--targeted in many directions. J Cell Sci *115*, 241-256.

Cook, T., and Desplan, C. (2001). Photoreceptor subtype specification: from flies to humans. Semin Cell Dev Biol *12*, 509-518.

Cox, D. N., Lu, B., Sun, T. Q., Williams, L. T., and Jan, Y. N. (2001a). Drosophila par-1 is required for oocyte differentiation and microtubule organization. Curr Biol *11*, 75-87.

Cox, D. N., Seyfried, S. A., Jan, L. Y., and Jan, Y. N. (2001b). Bazooka and atypical protein kinase C are required to regulate oocyte differentiation in the Drosophila ovary. Proc Natl Acad Sci U S A *98*, 14475-14480.

de Cuevas, M., and Spradling, A. C. (1998). Morphogenesis of the Drosophila fusome and its implications for oocyte specification. Development *125*, 2781-2789.

Dearborn, R., Jr., He, Q., Kunes, S., and Dai, Y. (2002). Eph receptor tyrosine kinase-mediated formation of a topographic map in the Drosophila visual system. In J Neurosci, pp. 1338-1349.

Desai, C., and Purdy, J. (2003). The neural receptor protein tyrosine phosphatase DPTP69D is required during periods of axon outgrowth in Drosophila. Genetics *164*, 575-588.

Desai, C. J., Garrity, P. A., Keshishian, H., Zipursky, S. L., and Zinn, K. (1999). The Drosophila SH2-SH3 adapter protein Dock is expressed in embryonic axons and facilitates synapse formation by the RP3 motoneuron. Development *126*, 1527-1535.

Diagana, T. T., Thomas, U., Prokopenko, S. N., Xiao, B., Worley, P. F., and Thomas, J. B. (2002). Mutation of Drosophila homer disrupts control of locomotor activity and behavioral plasticity. J Neurosci *22*, 428-436.

Dietrich, W. (1909). Die Facetenaugen der Dipteren. Z Wiss Zool *92*, 465-539.

Dombradi, V., Axton, J. M., Barker, H. M., and Cohen, P. T. (1990). Protein phosphatase 1 activity in Drosophila mutants with abnormalities in mitosis and chromosome condensation. FEBS Lett *275*, 39-43.

Dombradi, V., Axton, J. M., Brewis, N. D., da Cruz e Silva, E. F., Alphey, L., and Cohen, P. T. (1990). Drosophila contains three genes that encode distinct isoforms of protein phosphatase 1. Eur J Biochem *194*, 739-745.

Dombradi, V., and Cohen, P. T. (1992). Protein phosphorylation is involved in the regulation of chromatin condensation during interphase. In FEBS Lett, pp. 21-26.

Dombradi, V., Mann, D. J., Saunders, R. D., and Cohen, P. T. (1993). Cloning of the fourth functional gene for protein phosphatase 1 in Drosophila melanogaster from its chromosomal location. Eur J Biochem *212*, 177-183.

Egloff, M. P., Johnson, D. F., Moorhead, G., Cohen, P. T., Cohen, P., and Barford, D. (1997). Structural basis for the recognition of regulatory subunits by the catalytic subunit of protein phosphatase 1. Embo J *16*, 1876-1887.

Erdelyi, M., Michon, A. M., Guichet, A., Glotzer, J. B., and Ephrussi, A. (1995). Requirement for Drosophila cytoplasmic tropomyosin in oskar mRNA localization. Nature *377*, 524-527.

Fernald, R. D. (2000). Evolution of eyes. Curr Opin Neurobiol *10*, 444-450.

Foa, L., Rajan, I., Haas, K., Wu, G. Y., Brakeman, P., Worley, P., and Cline, H. (2001). The scaffold protein, Homer1b/c, regulates axon pathfinding in the central nervous system in vivo. Nat Neurosci *4*, 499-506.

Fujita, S. C., Zipursky, S. L., Benzer, S., Ferrus, A., and Shotwell, S. L. (1982). Monoclonal antibodies against the Drosophila nervous system. Proc Natl Acad Sci U S A *79*, 7929-7933.

Garrity, P. A., Lee, C. H., Salecker, I., Robertson, H. C., Desai, C. J., Zinn, K., and Zipursky, S. L. (1999). Retinal axon target selection in Drosophila is regulated by a receptor protein tyrosine phosphatase. Neuron *22*, 707-717.

Garrity, P. A., Rao, Y., Salecker, I., McGlade, J., Pawson, T., and Zipursky, S. L. (1996). Drosophila photoreceptor axon guidance and targeting requires the dreadlocks SH2/SH3 adapter protein. Cell *85*, 639-650.

Gehring, W. J. (2002). The genetic control of eye development and its implications for the evolution of the various eye-types. Int J Dev Biol *46*, 65-73.

Gehring, W. J., and Ikeo, K. (1999). Pax 6: mastering eye morphogenesis and eye evolution. Trends Genet *15*, 371-377.

Gonzalez-Reyes, A., Elliott, H., and St Johnston, D. (1995). Polarization of both major body axes in Drosophila by gurken-torpedo signalling. Nature *375*, 654-658.

Graner, M., Stupka, K., and Karr, T. L. (1994). Biochemical and cytological characterization of DROP-1: a widely distributed proteoglycan in Drosophila. Insect Biochem Mol Biol *24*, 557-567.

Grenningloh, G., Bieber, A. J., Rehm, E. J., Snow, P. M., Traquina, Z. R., Hortsch, M., Patel, N. H., and Goodman, C. S. (1990). Molecular genetics of neuronal recognition in Drosophila: evolution and function of immunoglobulin superfamily cell adhesion molecules. Cold Spring Harb Symp Quant Biol *55*, 327-340.

Grenningloh, G., Rehm, E. J., and Goodman, C. S. (1991). Genetic analysis of growth cone guidance in Drosophila: fasciclin II functions as a neuronal recognition molecule. Cell *67*, 45-57.

Gunkel, N., Yano, T., Markussen, F. H., Olsen, L. C., and Ephrussi, A. (1998). Localization-dependent translation requires a functional interaction between the 5' and 3' ends of oskar mRNA. Genes Dev *12*, 1652-1664.

Halder, G., Callaerts, P., and Gehring, W. J. (1995). Induction of ectopic eyes by targeted expression of the eyeless gene in Drosophila. Science *267*, 1788-1792.

Halter, D. A., Urban, J., Rickert, C., Ner, S. S., Ito, K., Travers, A. A., and Technau, G. M. (1995). The homeobox gene repo is required for the differentiation and maintenance of glia function in the embryonic nervous system of Drosophila melanogaster. Development *121*, 317-332.

Hanson, M. a. (1993). The Development of the Optic Lobe. In The Development of Drosophila melanogaster, M. a. Martinez-Arias, ed. (Cold spring Harbour Laboratory Press).

Harris, R., Sabatelli, L. M., and Seeger, M. A. (1996). Guidance cues at the Drosophila CNS midline: identification and characterization of two Drosophila Netrin/UNC-6 homologs. Neuron *17*, 217-228.

Hay, B. A., Maile, R., and Rubin, G. M. (1997). P element insertion-dependent gene activation in the Drosophila eye. Proc Natl Acad Sci U S A *94*, 5195-5200.

Hay, B. A., Wolff, T., and Rubin, G. M. (1994). Expression of baculovirus P35 prevents cell death in Drosophila. In Development, pp. 2121-2129.

Hedgecock, E. M., Culotti, J. G., and Hall, D. H. (1990). The unc-5, unc-6, and unc-40 genes guide circumferential migrations of pioneer axons and mesodermal cells on the epidermis in C. elegans. Neuron *4*, 61-85.

Helps, N. R., Barker, H. M., Elledge, S. J., and Cohen, P. T. (1995). Protein phosphatase 1 interacts with p53BP2, a protein which binds to the tumour suppressor p53. In FEBS Lett, pp. 295-300.

Helps, N. R., and Cohen, P. T. (1999). Drosophila melanogaster protein phosphatase inhibitor-2: identification of a site important for PP1 inhibition. In FEBS Lett, pp. 72-76.

Helps, N. R., Cohen, P. T., Bahri, S. M., Chia, W., and Babu, K. (2001). Interaction with protein phosphatase 1 Is essential for bifocal function during the morphogenesis of the Drosophila compound eye. Mol Cell Biol *21*, 2154-2164.

Helps, N. R., Vergidou, C., Gaskell, T., and Cohen, P. T. (1998). Characterisation of a novel Drosophila melanogaster testis specific PP1 inhibitor related to mammalian inhibitor-2: identification of the site of interaction with PP1. In FEBS Lett, pp. 131-136.

Hing, H., Xiao, J., Harden, N., Lim, L., and Zipursky, S. L. (1999). Pak functions downstream of Dock to regulate photoreceptor axon guidance in Drosophila. Cell *97*, 853-863.

Hiramoto, M., Hiromi, Y., Giniger, E., and Hotta, Y. (2000). The Drosophila Netrin receptor Frazzled guides axons by controlling Netrin distribution. Nature *406*, 886-889.

Huang, F. L., and Glinsmann, W. (1976). A second heat-stable protein inhibitor of phosphorylase phosphatase from rabbit muscle. In FEBS Lett, pp. 326-329.

Huang, Z., and Kunes, S. (1998). Signals transmitted along retinal axons in Drosophila: Hedgehog signal reception and the cell circuitry of lamina cartridge assembly. In Development, pp. 3753-3764.

Hubbard, M. J., and Cohen, P. (1993). On target with a new mechanism for the regulation of protein phosphorylation. Trends Biochem Sci *18*, 172-177.

Huynh, J. R., Petronczki, M., Knoblich, J. A., and St Johnston, D. (2001a). Bazooka and PAR-6 are required with PAR-1 for the maintenance of oocyte fate in Drosophila. Curr Biol *11*, 901-906.

Huynh, J. R., Shulman, J. M., Benton, R., and St Johnston, D. (2001b). PAR-1 is required for the maintenance of oocyte fate in Drosophila. Development *128*, 1201-1209.

Iwai, Y., Hirota, Y., Ozaki, K., Okano, H., Takeichi, M., and Uemura, T. (2002). DN-cadherin is required for spatial arrangement of nerve terminals and ultrastructural organization of synapses. In Mol Cell Neurosci, pp. 375-388.

Iwai, Y., Usui, T., Hirano, S., Steward, R., Takeichi, M., and Uemura, T. (1997). Axon patterning requires DN-cadherin, a novel neuronal adhesion receptor, in the Drosophila embryonic CNS. Neuron *19*, 77-89.

Jan, Y. N., and Jan, L. Y. (1998). Asymmetric cell division. Nature *392*, 775-778.

Jankovics, F., Sinka, R., Lukacsovich, T., and Erdelyi, M. (2002). MOESIN Crosslinks Actin and Cell Membrane in Drosophila Oocytes and Is Required for OSKAR Anchoring. Curr Biol *12*, 2060-2065.

Jarman, A. P. (2000). Developmental genetics: vertebrates and insects see eye to eye. Curr Biol *10*, R857-859.

Johnson, D. F., Moorhead, G., Caudwell, F. B., Cohen, P., Chen, Y. H., Chen, M. X., and Cohen, P. T. (1996). Identification of protein-phosphatase-1-binding domains on the glycogen and myofibrillar targetting subunits. In Eur J Biochem, pp. 317-325.

Kaprielian, Z., Runko, E., and Imondi, R. (2001). Axon guidance at the midline choice point. Dev Dyn *221*, 154-181.

Karr, T. L. (1991). Intracellular sperm/egg interactions in Drosophila: a three-dimensional structural analysis of a paternal product in the developing egg. Mech Dev *34*, 101-111.

Kennedy, T. E. (2000). Cellular mechanisms of netrin function: long-range and short-range actions. Biochem Cell Biol *78*, 569-575.

Kidd, T., Bland, K. S., and Goodman, C. S. (1999). Slit is the midline repellent for the robo receptor in Drosophila. Cell *96*, 785-794.

Kidd, T., Brose, K., Mitchell, K. J., Fetter, R. D., Tessier-Lavigne, M., Goodman, C. S., and Tear, G. (1998a). Roundabout controls axon crossing of the CNS midline and defines a novel subfamily of evolutionarily conserved guidance receptors. Cell *92*, 205-215.

Kidd, T., Russell, C., Goodman, C. S., and Tear, G. (1998b). Dosage-sensitive and complementary functions of roundabout and commissureless control axon crossing of the CNS midline. Neuron *20*, 25-33.

Kim-Ha, J., Kerr, K., and Macdonald, P. M. (1995). Translational regulation of oskar mRNA by bruno, an ovarian RNA-binding protein, is essential. Cell *81*, 403-412.

Kimmel, B. E., Heberlein, U., and Rubin, G. M. (1990). The homeo domain protein rough is expressed in a subset of cells in the developing Drosophila eye where it can specify photoreceptor cell subtype. Genes Dev *4*, 712-727.

Knoblich, J. A. (2001). The Drosophila nervous system as a model for asymmetric cell division. Symp Soc Exp Biol, 75-89.

Kolodkin, A. L., and Ginty, D. D. (1997). Steering clear of semaphorins: neuropilins sound the retreat. Neuron *19*, 1159-1162.

Kolodkin, A. L., Matthes, D. J., and Goodman, C. S. (1993). The semaphorin genes encode a family of transmembrane and secreted growth cone guidance molecules. Cell *75*, 1389-1399.

Kolodkin, A. L., Matthes, D. J., O'Connor, T. P., Patel, N. H., Admon, A., Bentley, D., and Goodman, C. S. (1992). Fasciclin IV: sequence, expression, and function during growth cone guidance in the grasshopper embryo. Neuron *9*, 831-845.

Kolodziej, P. A., Timpe, L. C., Mitchell, K. J., Fried, S. R., Goodman, C. S., Jan, L. Y., and Jan, Y. N. (1996). frazzled encodes a Drosophila member of the DCC immunoglobulin subfamily and is required for CNS and motor axon guidance. Cell *87*, 197-204.

Kraut, R., Chia, W., Jan, L. Y., Jan, Y. N., and Knoblich, J. A. (1996). Role of inscuteable in orienting asymmetric cell divisions in Drosophila. Nature *383*, 50-55.

Krueger, N. X., Van Vactor, D., Wan, H. I., Gelbart, W. M., Goodman, C. S., and Saito, H. (1996). The transmembrane tyrosine phosphatase DLAR controls motor axon guidance in Drosophila. In Cell, pp. 611-622.

Kunes, S. (1999). Stop or go in the target zone. In Neuron, pp. 639-640.

Kunes, S. (2000). Axonal signals in the assembly of neural circuitry. Curr Opin Neurobiol *10*, 58-62.

Kunes, S., and Steller, H. (1993). Topography in the Drosophila visual system. Curr Opin Neurobiol *3*, 53-59.

Kunes, S., Wilson, C., and Steller, H. (1993). Independent guidance of retinal axons in the developing visual system of Drosophila. J Neurosci *13*, 752-767.

Land, M. F., and Fernald, R. D. (1992). The evolution of eyes. Annu Rev Neurosci *15*, 1-29.

Lantz, V., Chang, J. S., Horabin, J. I., Bopp, D., and Schedl, P. (1994). The Drosophila orb RNA-binding protein is required for the formation of the egg chamber and establishment of polarity. Genes Dev *8*, 598-613.

Lasko, P. F., and Ashburner, M. (1990). Posterior localization of vasa protein correlates with, but is not sufficient for, pole cell development. Genes Dev *4*, 905-921.

Lawler, S. (1999). Regulation of actin dynamics: The LIM kinase connection. Curr Biol *9*, R800-802.

Lee, C. H., Herman, T., Clandinin, T. R., Lee, R., and Zipursky, S. L. (2001). N-cadherin regulates target specificity in the Drosophila visual system. Neuron *30*, 437-450.

Li, P., Yang, X., Wasser, M., Cai, Y., and Chia, W. (1997). Inscuteable and Staufen mediate asymmetric localization and segregation of prospero RNA during Drosophila neuroblast cell divisions. Cell *90*, 437-447.

Lin, H., and Spradling, A. C. (1995). Fusome asymmetry and oocyte determination in Drosophila. Dev Genet *16*, 6-12.

Longley, R. L., Jr., and Ready, D. F. (1995). Integrins and the development of three-dimensional structure in the Drosophila compound eye. In Dev Biol, pp. 415-433.

Luo, L. (2000). Trio quartet in D. (melanogaster). In Neuron, pp. 1-2.

MacMillan, L. B., Bass, M. A., Cheng, N., Howard, E. F., Tamura, M., Strack, S., Wadzinski, B. E., and Colbran, R. J. (1999). Brain actin-associated protein

phosphatase 1 holoenzymes containing spinophilin, neurabin, and selected catalytic subunit isoforms. J Biol Chem *274*, 35845-35854.

Manseau, L., Calley, J., and Phan, H. (1996). Profilin is required for posterior patterning of the Drosophila oocyte. Development *122*, 2109-2116.

Mardon, G., Solomon, N. M., and Rubin, G. M. (1994). dachshund encodes a nuclear protein required for normal eye and leg development in Drosophila. Development *120*, 3473-3486.

Markussen, F. H., Michon, A. M., Breitwieser, W., and Ephrussi, A. (1995). Translational control of oskar generates short OSK, the isoform that induces pole plasma assembly. Development *121*, 3723-3732.

Martin, K. A., Poeck, B., Roth, H., Ebens, A. J., Ballard, L. C., and Zipursky, S. L. (1995). Mutations disrupting neuronal connectivity in the Drosophila visual system. Neuron *14*, 229-240.

Maurel-Zaffran, C., Suzuki, T., Gahmon, G., Treisman, J. E., and Dickson, B. J. (2001). Cell-autonomous and -nonautonomous functions of LAR in R7 photoreceptor axon targeting. Neuron *32*, 225-235.

McAvoy, T., Allen, P. B., Obaishi, H., Nakanishi, H., Takai, Y., Greengard, P., Nairn, A. C., and Hemmings, H. C., Jr. (1999). Regulation of neurabin I interaction with protein phosphatase 1 by phosphorylation. Biochemistry *38*, 12943-12949.

Micklem, D. R., Adams, J., Grunert, S., and St Johnston, D. (2000). Distinct roles of two conserved Staufen domains in oskar mRNA localization and translation. Embo J *19*, 1366-1377.

Mitchell, K. J., Doyle, J. L., Serafini, T., Kennedy, T. E., Tessier-Lavigne, M., Goodman, C. S., and Dickson, B. J. (1996). Genetic analysis of Netrin genes in Drosophila: Netrins guide CNS commissural axons and peripheral motor axons. Neuron *17*, 203-215.

Morrison, D. K., Murakami, M. S., and Cleghon, V. (2000). Protein kinases and phosphatases in the Drosophila genome. J Cell Biol *150*, F57-62.

Nakanishi, H., Obaishi, H., Satoh, A., Wada, M., Mandai, K., Satoh, K., Nishioka, H., Matsuura, Y., Mizoguchi, A., and Takai, Y. (1997). Neurabin: a novel neural tissue-specific actin filament-binding protein involved in neurite formation. In J Cell Biol, pp. 951-961.

Navarro, C., Lehmann, R., and Morris, J. (2001). Oogenesis: Setting one sister above the rest. Curr Biol *11*, R162-165.

Neuman-Silberberg, F. S., and Schupbach, T. (1996). The Drosophila TGF-alpha-like protein Gurken: expression and cellular localization during Drosophila oogenesis. Mech Dev *59*, 105-113.

Newsome, T. P., Asling, B., and Dickson, B. J. (2000a). Analysis of Drosophila photoreceptor axon guidance in eye-specific mosaics. Development *127*, 851-860.

Newsome, T. P., Schmidt, S., Dietzl, G., Keleman, K., Asling, B., Debant, A., and Dickson, B. J. (2000b). Trio combines with dock to regulate Pak activity during photoreceptor axon pathfinding in Drosophila. Cell *101*, 283-294.

Oliver, C. J., Terry-Lorenzo, R. T., Elliott, E., Bloomer, W. A., Li, S., Brautigan, D. L., Colbran, R. J., and Shenolikar, S. (2002). Targeting protein phosphatase 1 (PP1) to the actin cytoskeleton: the neurabin I/PP1 complex regulates cell morphology. In Mol Cell Biol, pp. 4690-4701.

Osorio, D., and Bacon, J. P. (1994). A good eye for arthropod evolution. Bioessays *16*, 419-424.

Oster, S. F., and Sretavan, D. W. (2003). Connecting the eye to the brain: the molecular basis of ganglion cell axon guidance. Br J Ophthalmol *87*, 639-645.

Ott, H., Bastmeyer, M., and Stuermer, C. A. (1998). Neurolin, the goldfish homolog of DM-GRASP, is involved in retinal axon pathfinding to the optic disk. J Neurosci *18*, 3363-3372.

Palmer, A., and Klein, R. (2003). Multiple roles of ephrins in morphogenesis, neuronal networking, and brain function. Genes Dev *17*, 1429-1450.

Parker, L., Gross, S., Beullens, M., Bollen, M., Bennett, D., and Alphey, L. (2002). Functional interaction between NIPP1 and PP1 in Drosophila: consequences of over-expression of NIPP1 in flies and suppression by co-expression of PP1. In Biochem J.

Pellettieri, J., and Seydoux, G. (2002). Anterior-posterior polarity in C. elegans and Drosophila--PARallels and differences. Science *298*, 1946-1950.

Perez, S. E., and Steller, H. (1996). Migration of glial cells into retinal axon target field in Drosophila melanogaster. J Neurobiol *30*, 359-373.

Pichaud, F., and Desplan, C. (2002). Cell biology: a new view of photoreceptors. Nature *416*, 139-140.

Pichaud, F., Treisman, J., and Desplan, C. (2001). Reinventing a common strategy for patterning the eye. Cell *105*, 9-12.

Polesello, C., Delon, I., Valenti, P., Ferrer, P., and Payre, F. (2002). Dmoesin controls actin-based cell shape and polarity during Drosophila melanogaster oogenesis. Nat Cell Biol *4*, 782-789.

Queenan, A. M., Barcelo, G., Van Buskirk, C., and Schupbach, T. (1999). The transmembrane region of Gurken is not required for biological activity, but is necessary for transport to the oocyte membrane in Drosophila. Mech Dev *89*, 35-42.

Raghavan, S., Williams, I., Aslam, H., Thomas, D., Szoor, B., Morgan, G., Gross, S., Turner, J., Fernandes, J., VijayRaghavan, K., and Alphey, L. (2000). Protein phosphatase 1beta is required for the maintenance of muscle attachments. Curr Biol *10*, 269-272.

Ramos, A., Grunert, S., Adams, J., Micklem, D. R., Proctor, M. R., Freund, S., Bycroft, M., St Johnston, D., and Varani, G. (2000). RNA recognition by a Staufen double-stranded RNA-binding domain. Embo J *19*, 997-1009.

Rao, Y., Pang, P., Ruan, W., Gunning, D., and Zipursky, S. L. (2000). brakeless is required for photoreceptor growth-cone targeting in Drosophila. Proc Natl Acad Sci U S A *97*, 5966-5971.

Rao, Y., and Zipursky, S. L. (1998). Domain requirements for the Dock adapter protein in growth- cone signaling. In Proc Natl Acad Sci U S A, pp. 2077-2082.

Ready, D. F., Hanson, T. E., and Benzer, S. (1976). Development of the Drosophila retina, a neurocrystalline lattice. Dev Biol *53*, 217-240.

Riechmann, V., and Ephrussi, A. (2001). Axis formation during Drosophila oogenesis. Curr Opin Genet Dev *11*, 374-383.

Riechmann, V., Gutierrez, G. J., Filardo, P., Nebreda, A. R., and Ephrussi, A. (2002). Par-1 regulates stability of the posterior determinant Oskar by phosphorylation. Nat Cell Biol *4*, 337-342.

Rongo, C., Gavis, E. R., and Lehmann, R. (1995). Localization of oskar RNA regulates oskar translation and requires Oskar protein. Development *121*, 2737-2746.

Ruan, W., Long, H., Vuong, D. H., and Rao, Y. (2002). Bifocal is a downstream target of the Ste20-like serine/threonine kinase misshapen in regulating photoreceptor growth cone targeting in Drosophila. Neuron *36*, 831-842.

Rudenko, A., Bennett, D., and Alphey, L. (2003). Trithorax interacts with type 1 serine/threonine protein phosphatase in Drosophila. EMBO Rep *4*, 59-63.

Sastry, S. K., and Burridge, K. (2000). Focal adhesions: a nexus for intracellular signaling and cytoskeletal dynamics. Exp Cell Res *261*, 25-36.

Satoh, A., Nakanishi, H., Obaishi, H., Wada, M., Takahashi, K., Satoh, K., Hirao, K., Nishioka, H., Hata, Y., Mizoguchi, A., and Takai, Y. (1998). Neurabin-II/spinophilin. An actin filament-binding protein with one pdz domain localized at cadherin-based cell-cell adhesion sites. J Biol Chem *273*, 3470-3475.

Schindelholz, B., Knirr, M., Warrior, R., and Zinn, K. (2001). Regulation of CNS and motor axon guidance in Drosophila by the receptor tyrosine phosphatase DPTP52F. In Development, pp. 4371-4382.

Schmucker, D., and Zipursky, S. L. (2001). Signaling downstream of Eph receptors and ephrin ligands. In Cell, pp. 701-704.

Seeger, M., Tear, G., Ferres-Marco, D., and Goodman, C. S. (1993). Mutations affecting growth cone guidance in Drosophila: genes necessary for guidance toward or away from the midline. Neuron *10*, 409-426.

Selleck, S. B., and Steller, H. (1991). The influence of retinal innervation on neurogenesis in the first optic ganglion of Drosophila. Neuron *6*, 83-99.

Senti, K., Keleman, K., Eisenhaber, F., and Dickson, B. J. (2000). brakeless is required for lamina targeting of R1-R6 axons in the Drosophila visual system. Development *127*, 2291-2301.

Shenolikar, S. (1994). Protein serine/threonine phosphatases--new avenues for cell regulation. In Annu Rev Cell Biol, pp. 55-86.

Shiraishi, Y., Mizutani, A., Bito, H., Fujisawa, K., Narumiya, S., Mikoshiba, K., and Furuichi, T. (1999). Cupidin, an isoform of Homer/Vesl, interacts with the actin cytoskeleton and activated rho family small GTPases and is expressed in developing mouse cerebellar granule cells. J Neurosci *19*, 8389-8400.

Sisson, J. C., Field, C., Ventura, R., Royou, A., and Sullivan, W. (2000). Lava lamp, a novel peripheral golgi protein, is required for Drosophila melanogaster cellularization. J Cell Biol *151*, 905-918.

Song, H., Ming, G., He, Z., Lehmann, M., McKerracher, L., Tessier-Lavigne, M., and Poo, M. (1998). Conversion of neuronal growth cone responses from repulsion to attraction by cyclic nucleotides. Science *281*, 1515-1518.

Song, H. J., and Poo, M. M. (1999). Signal transduction underlying growth cone guidance by diffusible factors. Curr Opin Neurobiol *9*, 355-363.

Spector, I., Shochet, N. R., Blasberger, D., and Kashman, Y. (1989). Latrunculins--novel marine macrolides that disrupt microfilament organization and affect cell growth: I. Comparison with cytochalasin D. Cell Motil Cytoskeleton *13*, 127-144.

Spector, I., Shochet, N. R., Kashman, Y., and Groweiss, A. (1983). Latrunculins: novel marine toxins that disrupt microfilament organization in cultured cells. Science *219*, 493-495.

Spradling, A. C. (1993). Developmental Genetics of Oogenesis. In The Development of Drosophila melanogaster, B. a. Martinez-Arias, ed. (Cold Spring Harbour Laboratory Press).

St Johnston, D. (1993). Pole Plasm and the Posterior Group Genes. In The Development of Drosophila melanogaster, M. B. a. Martinez-Arias, ed. (Cold spring Harbour Laboratory Press).

St Johnston, D., Beuchle, D., and Nusslein-Volhard, C. (1991). Staufen, a gene required to localize maternal RNAs in the Drosophila egg. Cell *66*, 51-63.

Sun, Q., Bahri, S., Schmid, A., Chia, W., and Zinn, K. (2000). Receptor tyrosine phosphatases regulate axon guidance across the midline of the Drosophila embryo. Development *127*, 801-812.

Suter, D. M., and Forscher, P. (1998). An emerging link between cytoskeletal dynamics and cell adhesion molecules in growth cone guidance. Curr Opin Neurobiol *8*, 106-116.

Tan, J. L., Ravid, S., and Spudich, J. A. (1992). Control of nonmuscle myosins by phosphorylation. Annu Rev Biochem *61*, 721-759.

Tanaka, J., Ito, M., Feng, J., Ichikawa, K., Hamaguchi, T., Nakamura, M., Hartshorne, D. J., and Nakano, T. (1998). Interaction of myosin phosphatase target subunit 1 with the catalytic subunit of type 1 protein phosphatase. Biochemistry *37*, 16697-16703.

Tear, G., Harris, R., Sutaria, S., Kilomanski, K., Goodman, C. S., and Seeger, M. A. (1996). commissureless controls growth cone guidance across the CNS midline in Drosophila and encodes a novel membrane protein. Neuron *16*, 501-514.

Terry-Lorenzo, R. T., Carmody, L. C., Voltz, J. W., Connor, J. H., Li, S., Smith, F. D., Milgram, S. L., Colbran, R. J., and Shenolikar, S. (2002). The neuronal actin-binding proteins, neurabin I and neurabin II, recruit specific isoforms of protein phosphatase-1 catalytic subunits. In J Biol Chem, pp. 27716-27724.

Tessier-Lavigne, M., and Goodman, C. S. (1996). The molecular biology of axon guidance. Science *274*, 1123-1133.

Tetzlaff, M. T., Jackle, H., and Pankratz, M. J. (1996). Lack of Drosophila cytoskeletal tropomyosin affects head morphogenesis and the accumulation of oskar mRNA required for germ cell formation. Embo J *15*, 1247-1254.

Theurkauf, W. E., Smiley, S., Wong, M. L., and Alberts, B. M. (1992). Reorganization of the cytoskeleton during Drosophila oogenesis: implications for axis specification and intercellular transport. Development *115*, 923-936.

Tomancak, P., Piano, F., Riechmann, V., Gunsalus, K. C., Kemphues, K. J., and Ephrussi, A. (2000). A Drosophila melanogaster homologue of Caenorhabditis elegans par-1 acts at an early step in embryonic-axis formation. Nat Cell Biol *2*, 458-460.

Tomarev, S. I., Callaerts, P., Kos, L., Zinovieva, R., Halder, G., Gehring, W., and Piatigorsky, J. (1997). Squid Pax-6 and eye development. Proc Natl Acad Sci U S A *94*, 2421-2426.

Tomlinson, A., and Ready, D. (1987). Cell Fate in the Drosophila Ommatidium. Dev Biol *123*, 264-275.

Van Eynde, A., Wera, S., Beullens, M., Torrekens, S., Van Leuven, F., Stalmans, W., and Bollen, M. (1995). Molecular cloning of NIPP-1, a nuclear inhibitor of protein phosphatase-1, reveals homology with polypeptides involved in RNA processing. In J Biol Chem, pp. 28068-28074.

Van Vactor, D., Jr., Krantz, D. E., Reinke, R., and Zipursky, S. L. (1988). Analysis of mutants in chaoptin, a photoreceptor cell-specific glycoprotein in Drosophila, reveals its role in cellular morphogenesis. Cell *52*, 281-290.

Vanzo, N. F., and Ephrussi, A. (2002). Oskar anchoring restricts pole plasm formation to the posterior of the Drosophila oocyte. Development *129*, 3705-3714.

Waddington, C. a. P., MM (1960). The ultra-srtucture of the developing eye. Drosophila Proc Roy Soc Lond B *153*, 155-178.

Walther, C., and Gruss, P. (1991). Pax-6, a murine paired box gene, is expressed in the developing CNS. Development *113*, 1435-1449.

Wawersik, S., and Maas, R. L. (2000). Vertebrate eye development as modeled in Drosophila. Hum Mol Genet *9*, 917-925.

Wera, S., and Hemmings, B. A. (1995). Serine/threonine protein phosphatases. In Biochem J, pp. 17-29.

Westphal, R. S., Tavalin, S. J., Lin, J. W., Alto, N. M., Fraser, I. D., Langeberg, L. K., Sheng, M., and Scott, J. D. (1999). Regulation of NMDA receptors by an associated phosphatase-kinase signaling complex. In Science, pp. 93-96.

Winberg, M. L., Perez, S. E., and Steller, H. (1992). Generation and early differentiation of glial cells in the first optic ganglion of Drosophila melanogaster. Development *115*, 903-911.

Wolff, T., and Ready, D. F. (1991). The beginning of pattern formation in the Drosophila compound eye: the morphogenetic furrow and the second mitotic wave. Development *113*, 841-850.

Wolff, T. a. R. D. (1993). Pattern Formation in the Drosophila Retina. In The Development of Drosophila melanogaster, M. B. a. Martinez-Arias, ed. (Cold spring Harbour Laboratory Press).

Wong, K., Park, H. T., Wu, J. Y., and Rao, Y. (2002). Slit proteins: molecular guidance cues for cells ranging from neurons to leukocytes. Curr Opin Genet Dev *12*, 583-591.

Xu, P. X., Woo, I., Her, H., Beier, D. R., and Maas, R. L. (1997). Mouse Eya homologues of the Drosophila eyes absent gene require Pax6 for expression in lens and nasal placode. Development *124*, 219-231.

Yu, T. W., and Bargmann, C. I. (2001). Dynamic regulation of axon guidance. Nat Neurosci *4 Suppl*, 1169-1176.

Zhao, S., and Lee, E. Y. (1997). A protein phosphatase-1-binding motif identified by the panning of a random peptide display library. In J Biol Chem, pp. 28368-28372.

Zipursky, S. L., Venkatesh, T. R., Teplow, D. B., and Benzer, S. (1984). Neuronal development in the Drosophila retina: monoclonal antibodies as molecular probes. Cell *36*, 15-26.

PUBLICATIONS

Helps NR*, Cohen PTW, Bahri SM, Chia W and **Babu K***.

Interaction with protein phosphatase 1 is essential for bifocal function during the morphogenesis of the *Drosophila* compound eye. Mol Cell Biol**.,** 2001: 2154-2164.

*Equal Contribution.

Babu K, Cai Y, Bahri S, Yang X and Chia W.

Roles of Bifocal, Homer and F-actin in anchoring Oskar to the posterior cortex of *Drosophila* oocytes. Genes and Development, 2004: 138-143.

Babu K, Bahri S and Chia W.

Role of Bifocal and protein phosphatase 1 in photoreceptor axon guidance.

Manuscript in preparation.